2011

Timing, Distribution, Amount, and Style of Cenozoic Extension in the Northern Great Basin

Christopher D. Henry
University of Nevada, Reno

Allen J. McGrew
University of Dayton, amcgrew1@udayton.edu

Joseph P. Colgan
U.S. Geological Survey

Arthur W. Snoke
University of Wyoming

Matthew E. Brueseke
Kansas State University

The Geological Society of America
Field Guide 21
2011

Timing, distribution, amount, and style of Cenozoic extension in the northern Great Basin

Christopher D. Henry*
Nevada Bureau of Mines and Geology, University of Nevada, Reno, Nevada 89557-0178, USA

Allen J. McGrew*
Department of Geology, University of Dayton, Dayton, Ohio 45469-2364, USA

Joseph P. Colgan*
U.S. Geological Survey, Menlo Park, California 94025, USA

Arthur W. Snoke*
Department of Geology and Geophysics, University of Wyoming, Laramie, Wyoming 82071-2000, USA

Matthew E. Brueseke*
Department of Geology, Kansas State University, Manhattan, Kansas 66506, USA

ABSTRACT

This field trip examines contrasting lines of evidence bearing on the timing and structural style of Cenozoic (and perhaps late Mesozoic) extensional deformation in northeastern Nevada. Studies of metamorphic core complexes in this region report extension beginning in the early Cenozoic or even Late Cretaceous, peaking in the Eocene and Oligocene, and being largely over before the onset of "modern" Basin and Range extension in the middle Miocene. In contrast, studies based on low-temperature thermochronology and geologic mapping of Eocene and Miocene volcanic and sedimentary deposits report only minor, localized extension in the Eocene, no extension at all in the Oligocene and early Miocene, and major, regional extension in the middle Miocene.

A wealth of thermochronologic and thermobarometric data indicate that the Ruby Mountains–East Humboldt Range metamorphic core complex (RMEH) underwent ~170 °C of cooling and 4 kbar of decompression between ca. 85 and ca. 50 Ma, and another 450 °C cooling and 4–5 kbar decompression between ca. 50 and ca. 21 Ma. These data require ~30 km of exhumation in at least two episodes, accommodated at least in part by Eocene to early Miocene displacement on the major west-dipping mylonitic zone and detachment fault bounding the RMEH on the west (the mylonitic zone may also have been active during an earlier phase of crustal extension). Meanwhile, Eocene paleovalleys containing 45–40 Ma ash-flow tuffs drained eastward from

*chenry@unr.edu; allen.mcgrew@notes.udayton.edu; jcolgan@usgs.gov; snoke@uwyo.edu; brueseke@ksu.edu.

Henry, C.D., McGrew, A.J., Colgan, J.P., Snoke, A.W., and Brueseke, M.E., 2011, Timing, distribution, amount, and style of Cenozoic extension in the northern Great Basin, *in* Lee, J., and Evans, J.P., eds., Geologic Field Trips to the Basin and Range, Rocky Mountains, Snake River Plain, and Terranes of the U.S. Cordillera: Geological Society of America Field Guide 21, p. 27–66, doi: 10.1130/2011.0021(02).

northern Nevada to the Uinta Basin in Utah, and continuity of these paleovalleys and infilling tuffs across the region indicate little, if any deformation by faults during their deposition. Pre–45 Ma deformation is less constrained, but the absence of Cenozoic sedimentary deposits and mappable normal faults older than 45 Ma is also consistent with only minor (if any) brittle deformation. The presence of ≤1 km of late Eocene sedimentary—especially lacustrine—deposits and a low-angle angular unconformity between ca. 40 and 38 Ma rocks attest to an episode of normal faulting at ca. 40 Ma.

Arguably the greatest conundrum is how much extension occurred between ca. 35 and 17 Ma. Major exhumation of the RMEH is interpreted to have taken place in the late Oligocene and early Miocene, but rocks of any kind deposited during this interval are scarce in northeastern Nevada and absent in the vicinity of the RMEH itself. In most places, no angular unconformity is present between late Eocene and middle Miocene rocks, indicating little or no tilting between the late Eocene and middle Miocene. Opinions among authors of this report differ, however, as to whether this indicates no extension during the same time interval. The one locality where Oligocene deposits have been documented is Copper Basin, where Oligocene (32.5–29.5 Ma) conglomerates are ~500 m thick. The contact between Oligocene and Eocene rocks in Copper Basin is conformable, and the rocks are uniformly tilted ~25° NW, opposite to a normal fault system dipping ~35° SE. Middle Miocene rhyolite (ca. 16 Ma) rests nonconformably on the metamorphosed lower plate of this fault system and appears to rest on the tilted upper-plate rocks with angular unconformity, but the contact is not physically exposed. Different authors of this report interpret geologic relations in Copper Basin to indicate either (1) significant episodes of extension in the Eocene, Oligocene, and middle Miocene or (2) minor extension in the Eocene, uncertainty about the Oligocene, and major extension in the middle Miocene.

An episode of major middle Miocene extension beginning at ca. 16–17 Ma is indicated by thick (up to 5 km) accumulations of sedimentary deposits in half-graben basins over most of northern Nevada, tilting and fanning of dips in the synextensional sedimentary deposits, and apatite fission-track and (U-Th)/He data from the southern Ruby Mountains and other ranges that indicate rapid middle Miocene cooling through near-surface temperatures (~120–40 °C). Opinions among authors of this report differ as to whether this period of extension was merely the last step in a long history of extensional faulting dating back at least to the Eocene, or whether it accounts for most of the Cenozoic deformation in northeastern Nevada. Since 10–12 Ma, extension appears to have slowed greatly and been accommodated by high-angle, relatively wide-spaced normal faults that give topographic form to the modern ranges. Despite the low present-day rate of extension, normal faults are active and have generated damaging earthquakes as recently as 2008.

INTRODUCTION

Although crustal extension in the North American Cordillera has been studied for nearly 100 years, many aspects of it—spatial distribution, timing, amount, structural style, and causes—remain controversial (Wernicke, 1992; Dickinson, 2002). These controversies are exemplified by the area of the northern Great Basin surrounding the Ruby Mountains–East Humboldt Range metamorphic core complex (RMEH) in northeastern Nevada (Fig. 1). This region underwent a series of Paleozoic to Mesozoic contractional episodes that significantly thickened the crust and probably raised its elevation, followed by moderate to large-magnitude extension in the Cenozoic. Thermochronologic and thermobarometric studies of the metamorphic rocks in the RMEH and analysis of some Cretaceous and Paleogene strata are interpreted to indicate that major cooling, exhumation, and extension began in the Eocene or even Late Cretaceous, soon after—or even during—contraction, and continued through the middle Cenozoic (e.g., Hodges and Walker, 1992; McGrew and Snee, 1994; Camilleri and Chamberlain, 1997; Snoke et al., 1997; McGrew et al., 2000; Wells and Hoisch, 2008; Druschke et al., 2009a, 2009b). In contrast, geologic mapping and dating of Eocene to Miocene sedimentary and volcanic rocks and more recent low-temperature thermochronology studies are interpreted to indicate

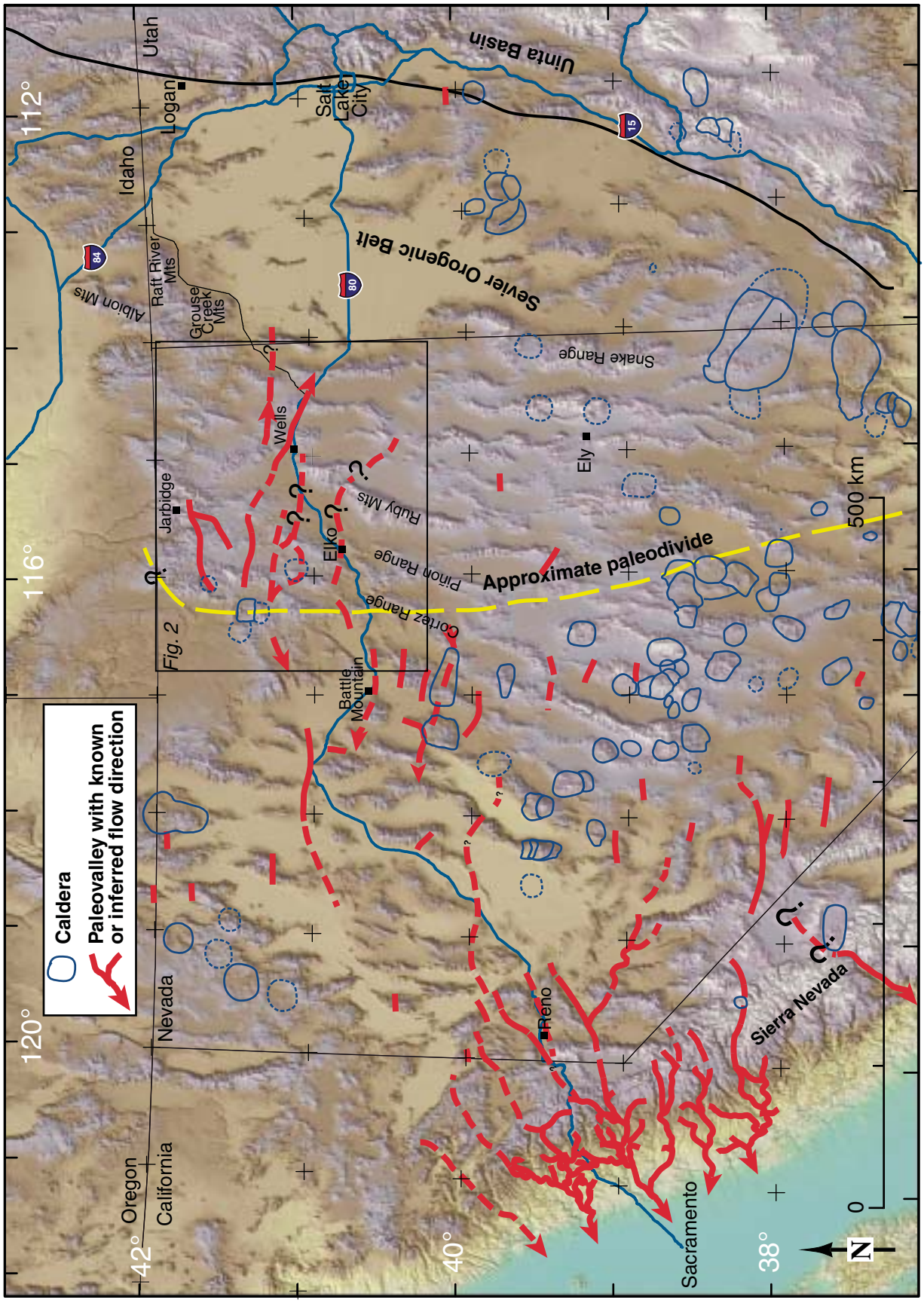

Figure 1. Digital elevation map of the Great Basin showing the region of the field trip centered around Wells in northeastern Nevada. The Ruby Mountains, Albion–Raft River Mountains, and Snake Range are major core complexes. Northeastern Nevada in the Eocene was part of the "Nevadaplano," a high area probably resulting from crustal thickening during Mesozoic contraction (DeCelles, 2004). Major rivers drained eastward to the Uinta basin and westward to the Pacific Ocean, which was in the Great Valley of California at the time. Paleovalleys and a proposed Eocene paleodivide from Henry (2008) based on data from Lindgren (1911), Faulds et al. (2005), Garside et al. (2005), and Henry and Faulds (2010).

that early to middle Cenozoic extension was relatively minor and that major extension took place in the middle Miocene (Henry, 2008; Wallace et al., 2008; Colgan and Henry, 2009; Colgan et al., 2010). The influence on extension of gravitational collapse of thickened crust, magmatic heating and weakening of the lithosphere, and changes in boundary conditions are similarly debated (Sonder and Jones, 1999; Rahl et al., 2002; Henry, 2008; Colgan and Henry, 2009). The characteristics of extension are significant not only for scientific reasons but are important to the formation and exploration for ore deposits and for hazards (Seedorff, 1991; Muntean et al., 2004; Cline et al., 2005; dePolo et al., 2011).

This field trip examines the evidence for the timing of extension and uplift, emphasizing three different aspects of the regional geology: (1) the deeply exhumed metamorphic rocks and structures of the East Humboldt Range and evidence for their P-T-t paths; (2) Eocene and Miocene sedimentary deposits at Clover Hill (East Humboldt Range) that record the unroofing of the core complex; and (3) Eocene, rare Oligocene, and Miocene volcanic and sedimentary rocks that record the regional paleogeographic and tectonic evolution of northeastern Nevada at sites including the Copper Mountains area of northern Elko County and the northern Pequop Mountains east of the RMEH–Wood Hills metamorphic terrain (Figs. 2, 3, 4). Fault and tilt relationships between Cenozoic rocks are examined at several locations, especially in two ash-flow tuff- and sediment-filled paleovalleys that cross the extended region. The authors and field trip leaders represent the spectrum of interpretations about Cenozoic extension.

STRATIGRAPHY AND ROCK UNITS

Precambrian

Though the presence of early Precambrian rocks in the deep subsurface of northeastern Nevada has long been inferred on the basis of the isotope geochemistry of younger plutonic rocks (Farmer and DePaolo, 1983; Wooden et al., 1997; Wright and Wooden, 1991), the gneiss complex of Angel Lake in the northern part of the East Humboldt Range provides the only reported exposures of Precambrian rocks predating the Neoproterozoic McCoy Creek Group (Lush et al., 1988). Although the age and petrogenesis of these polymetamorphic, migmatitic rocks has recently emerged as a matter of debate (Premo et al., 2008; McGrew and Snoke, 2010; Premo et al., 2010), new mapping by McGrew in the summer of 2009 coordinated with new U-Pb SHRIMP zircon geochronology by Premo sheds light on this controversy as briefly summarized below.

The gneiss complex of Angel Lake consists of an orthogneiss unit and two paragneiss units occupying the core of the Winchell Lake fold-nappe, a map-scale, southward-closing recumbent fold with a WNW-trending hingeline (Figs. 5A, 5B). The core of the Winchell Lake fold is occupied by a newly mapped unit of strongly migmatitic biotite schist and impure metapsammittic rock yielding a suite of Archean detrital zircons suggesting a latest Archean or Paleoproterozoic protolith age overprinted by a previously unrecognized metamorphic event at ca. 1.7 Ga (Fig. 5C) (W.R. Premo, 2010, personal commun.). Folded around this "core paragneiss" is the migmatitic orthogneiss of Angel Lake, a distinctively striped biotite monzogranitic orthogneiss with an Early Proterozoic age of 2450 ± 5 Ma based on a newly collected, minimally migmatized sample (Fig. 5B) (W.R. Premo, 2010, personal commun.). Folded around both the core paragneiss and the orthogneiss is an outer quartzite-pelitic schist unit that yields a detrital zircon suite with a strong Grenville-age spike, indicating a Neoproterozoic or younger depositional age and a probable correlation with the McCoy Creek Group of the northeastern Great Basin (W.R. Premo, 2010, personal commun.). All three units also host widespread amphibolite and garnet amphibolite sheets interpreted as metamorphosed mafic dikes and sills (Fig. 5B). Original contact relationships between these units are obscured by younger metamorphic and deformational overprints, and integrated geochemical, geochronologic and field-based studies are continuing in an effort to unravel the protracted history of these important exposures, which provide a unique opportunity to investigate and constrain the Precambrian history of continent formation as well as the subsequent polyphase tectonic history. These rocks are the focus of Stop 1-3.

Paleozoic to Early Mesozoic

Pre-Mississippian strata in northeastern Nevada are traditionally divided into a western facies assemblage consisting mostly of deepwater argillite and chert with associated dark quartzite, greenstone and limestone (Ordovician to Devonian Valmy, Vinini, and Woodruff Formations) and an eastern facies assemblage consisting of a thick sequence of Neoproterozoic to Cambrian clastic strata overlain by 5–7 km of lower Paleozoic shelf carbonates terminating in uppermost Devonian to Lower Mississippian shale (Figs. 3, 4). The eastern facies is inferred to have been deposited on cratonic North American basement, but this contact is not exposed in northeastern Nevada, with the possible exception of an outcrop of gneiss in the core of the Winchell Lake fold near Angel Lake in the East Humboldt Range (Stop 1-3).

Both the eastern and western assemblages are overlapped by a Mississippian clastic sequence and then a return to shelf-carbonate deposition extending into the Lower Triassic. The western facies was thrust eastward over the eastern facies initially during the Late Devonian to Mississippian Antler orogeny along the regional Roberts Mountains thrust (Roberts, 1964; Smith and Ketner, 1977). Locally, however, the basal thrust cuts and therefore post-dates strata as young as Triassic (Coats and Riva, 1983).

Jurassic and Cretaceous Plutons and Sedimentary Rocks

Jurassic and Cretaceous plutons are scattered through northeastern Nevada (Coats, 1987; Wright and Snoke, 1993; Barton, 1996; Mortensen et al., 2000). They are relatively localized near the surface but presumably are more abundant at depth,

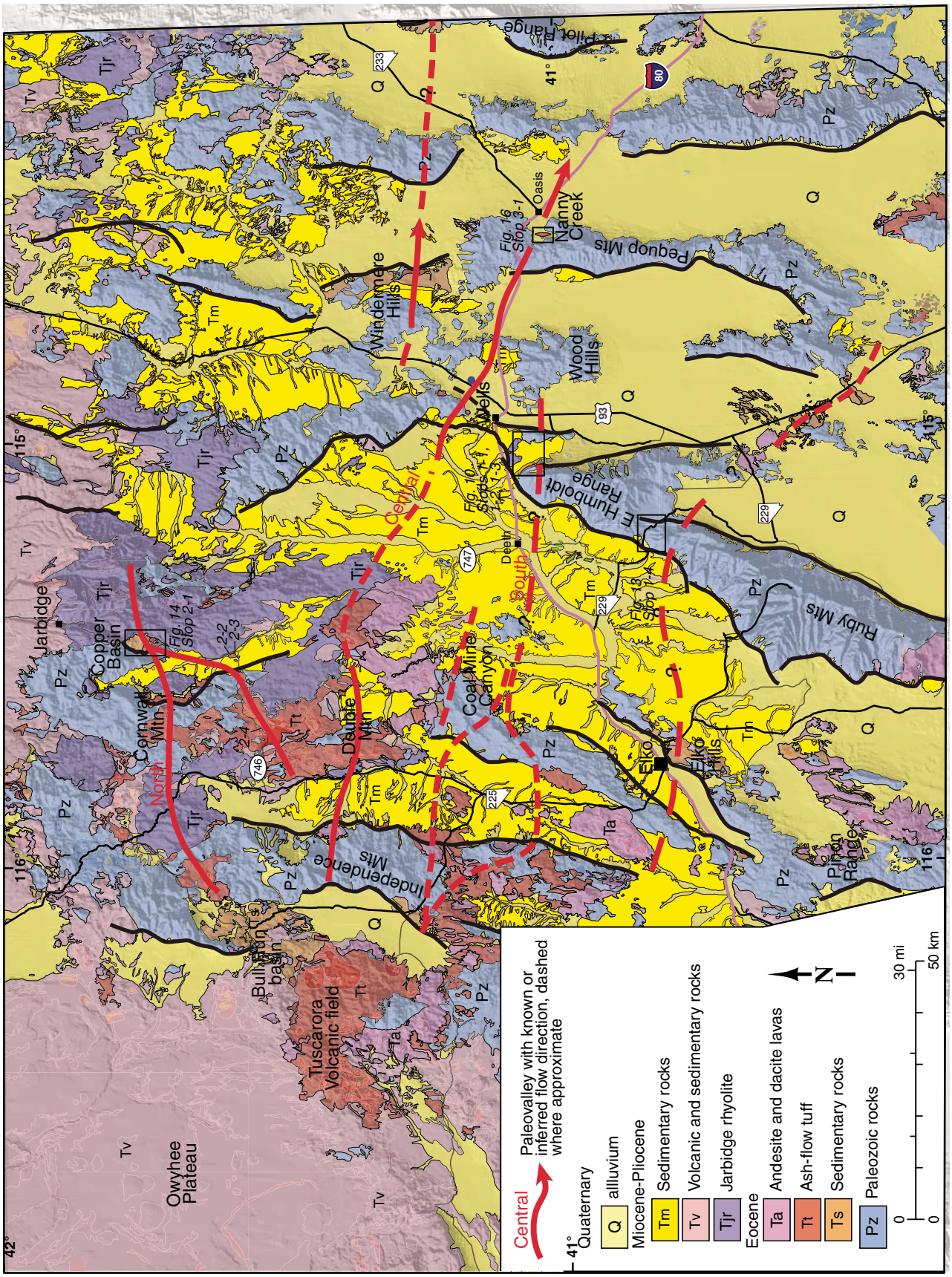

Figure 2. Geologic map of northeastern Nevada (simplified from Coats, 1987), showing locations of more detailed maps around major stops. Blue dot near Wells is epicenter of 21 February 2008 M_w 6.0 earthquake, which resulted from northwest-oriented extension on a 40°-striking, 55° southeast-dipping normal fault (dePolo et al., 2011).

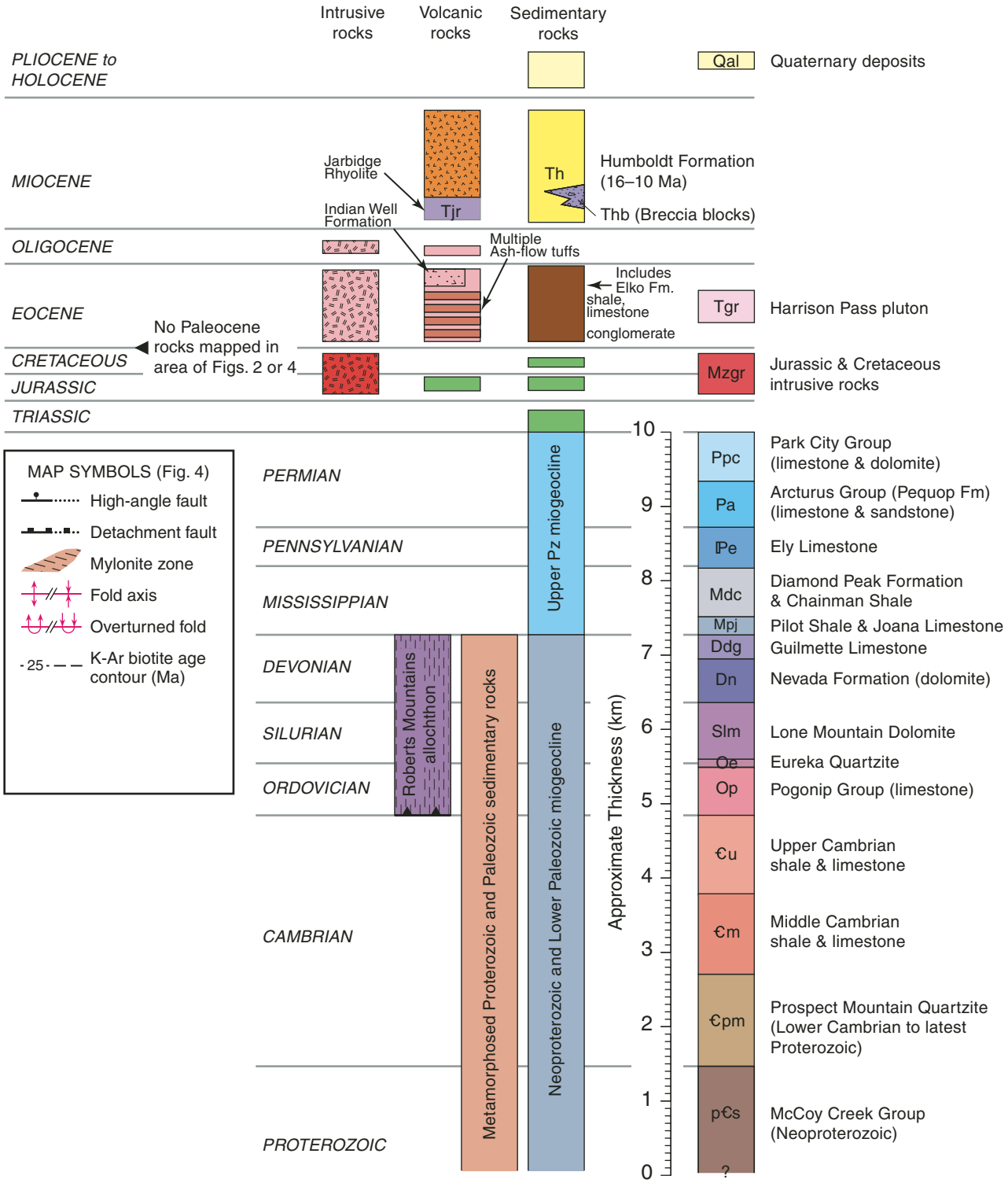

Figure 3. Guide to stratigraphic units in the Ruby Mountains area of northeastern Nevada and explanation for Figure 4 (modified from Colgan et al., 2010). Right column is scaled to approximate thickness of Paleozoic to Triassic shelf sequence in the Ruby Mountains. Many Paleozoic units have different names in different mountain ranges.

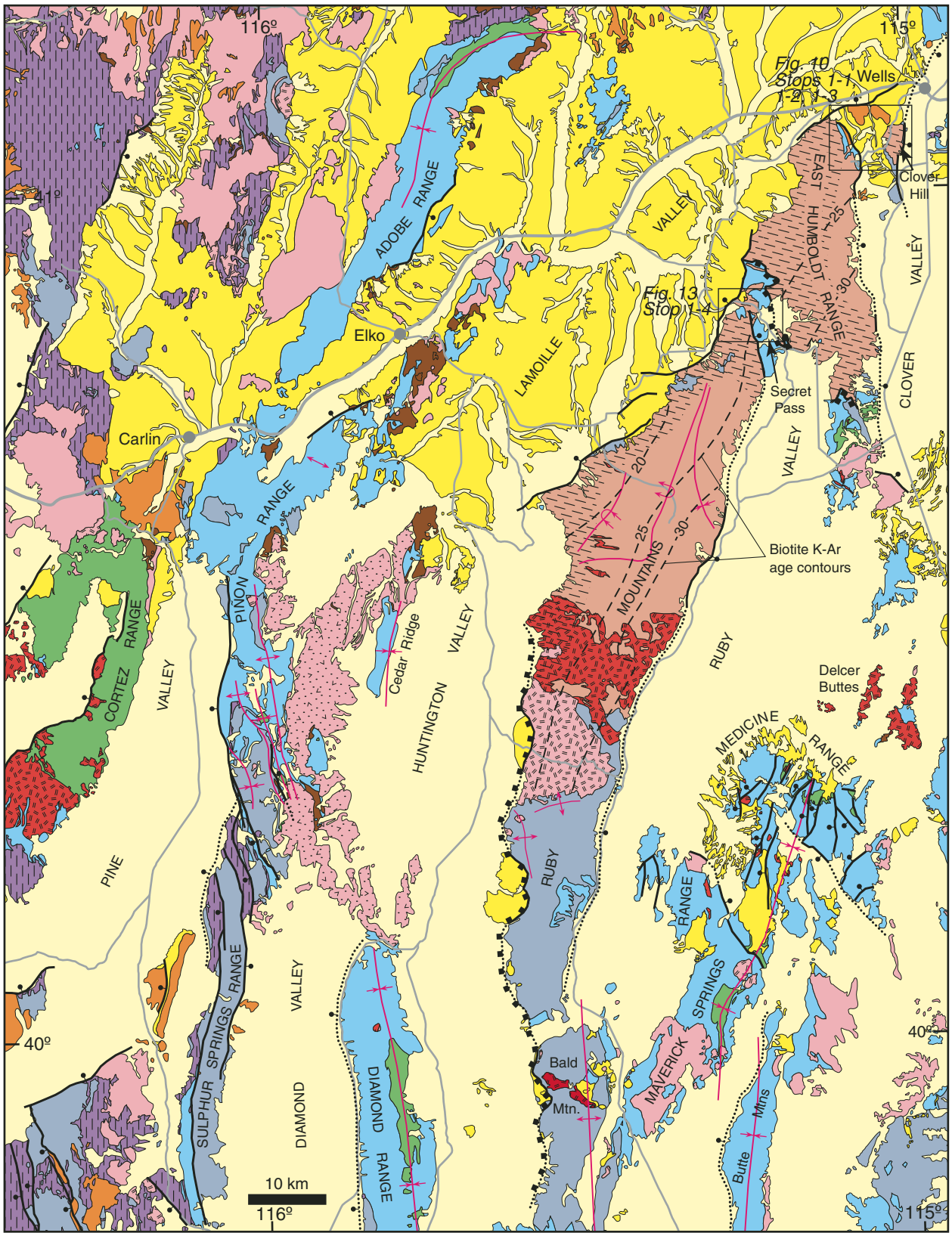

Figure 4. Geologic map of the Ruby Mountains area (from Crafford, 2007, and Colgan et al., 2010). Day 1 of field trip focuses on geology of the Ruby Mountains–East Humboldt Range metamorphic core complex around Clover Hill, the East Humboldt Range, and Secret Pass.

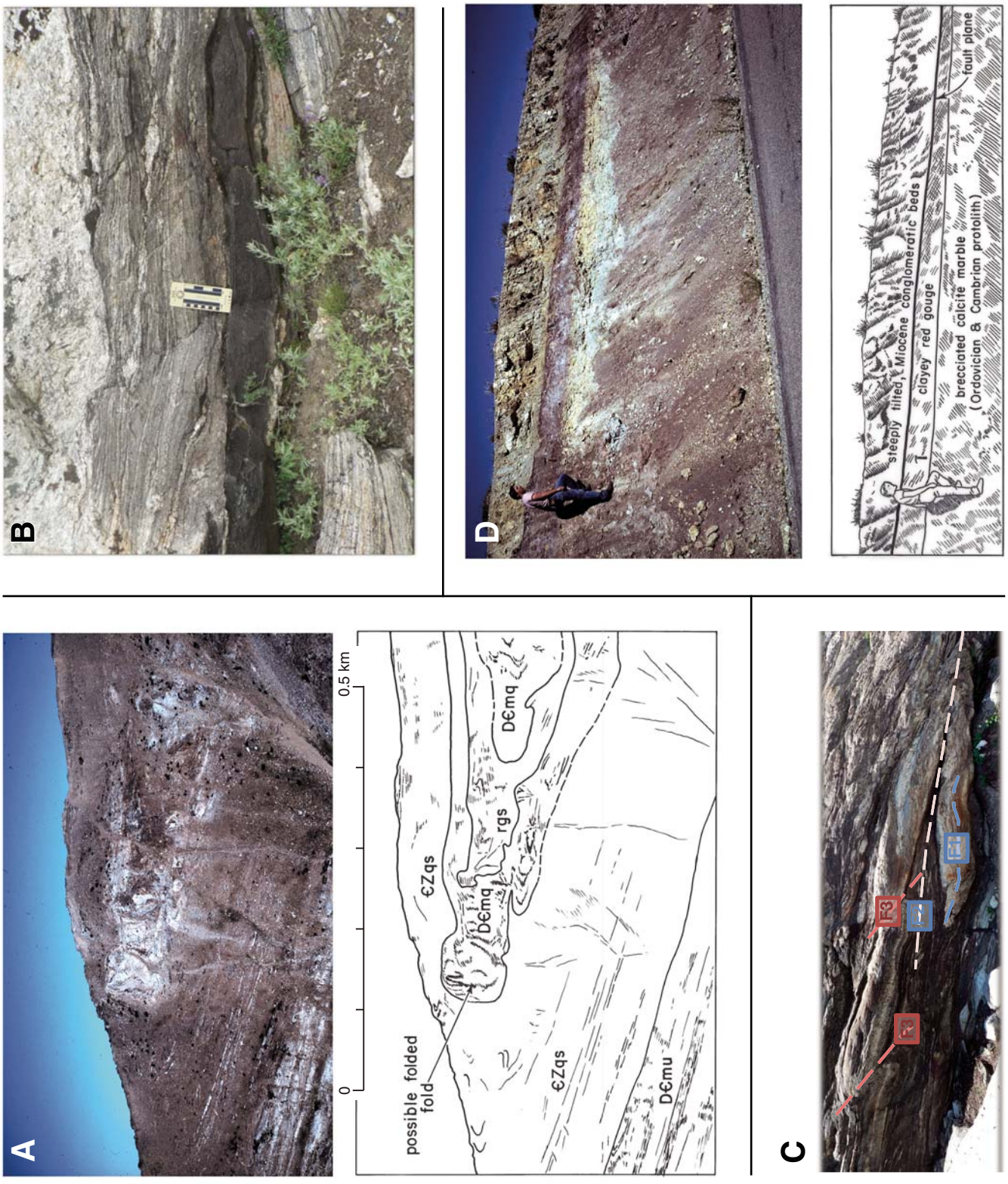
A
0
0.5 km
possible folded fold
€Zqs
D€mq
rgs
D€mq
€Zqs
D€mu
B
C
D
steeply tilted, Miocene conglomeratic beds
clayey red gouge
brecciated calcite marble
(Ordovician & Cambrian protolith)
fault plane

as indicated by the abundance of granitic rocks in the RMEH (Snoke et al., 1997; McGrew et al., 2000; Howard, 2003; Lee et al., 2003). Late Cretaceous peraluminous granites formed by crustal anatexis in thickened crust are common (Miller et al., 1990; Lee et al., 2003), and exposures of Late Cretaceous migmatites in the deep-crustal rocks of the northern East Humboldt Range provide insight into how those granites may have formed (McGrew et al., 2000; Premo et al., 2008; McGrew and Snoke, 2010; Premo et al., 2010; Hallett and Spear, 2010).

Cretaceous clastic rocks have been mapped in the eastern Cortez Range and at scattered localities throughout the Piñon Range (Fig. 3; Smith and Ketner, 1978). The only directly dated Cretaceous section, however, is the ~600-m-thick Newark Canyon Formation in the Cortez Range, known to be Early Cretaceous from fossils (Smith and Ketner, 1978) and a recent U-Pb zircon date of 116 ± 3 Ma on an interbedded tuff (Druschke et al., 2008).

Eocene Sedimentary and Volcanic Rocks

Two major sequences of volcanic and sedimentary rocks dominate the Cenozoic section of northeastern Nevada, Eocene and middle Miocene (Figs. 2, 3, 4). One area of Oligocene sedimentary rocks is known and may be particularly critical to understanding extension. The Eocene sequence includes conglomerate, sandstone, limestone, shale, andesite-dacite lava (and intrusive equivalents), and rhyolite to dacite ash-flow tuff (Ressel and Henry, 2006; Henry, 2008; Cook and Brueseke, 2010). The sedimentary rocks are exposed in small, widely scattered outcrops that are generally termed the Elko Formation because the largest and thickest exposures occur in the Elko Hills (Smith and Ketner, 1978). The Elko Formation in the Elko Hills consists of ~200 m of basal conglomerate and conglomeratic sandstone overlain by ~600 m of lacustrine shale, oil shale, claystone, siltstone, and minor water-laid tuff (Solomon et al., 1979; Ketner and Alpha, 1992; Haynes, 2003). Zircon U-Pb ages on water-laid tuffs in the basal conglomerate and near the top of the lacustrine sequence are 46.1 ± 0.2 Ma and 38.9 ± 0.3 Ma, respectively (Haynes et al., 2002; Haynes, 2003). Sequences in other areas are lithologically similar but thinner (Henry, 2008). The Elko Formation is generally interpreted to have accumulated in an extensional basin or basins formed during Eocene extension, including slip on the detachment fault bounding the west side of the Ruby Mountains (Solomon et al., 1979; Mueller and Snoke, 1993a; Satarugsa and Johnson, 2000; Haynes et al., 2002; Haynes, 2003). However, Henry (2008) interpreted that most Eocene sedimentary rocks accumulated in paleovalleys, probably where minor extension generated small half-graben basins.

Cenozoic magmatism began at ca. 45 Ma in northeastern Nevada, generally post-dating the oldest sedimentary deposits (whose age is constrained to post-Paleozoic, and locally post-Triassic), and was part of a southward-migrating belt that swept from Washington and Idaho, through northeastern Nevada and northwestern Utah, and into central Nevada in the Oligocene (Best and Christiansen, 1991; Christiansen and Yeats, 1992; Brooks et al., 1995a, 1995b; Humphreys, 1995; Henry and Ressel, 2000). Eocene magmatism in northeastern Nevada was dominated by andesitic to dacitic lavas and compositionally similar intrusions in numerous centers. The lavas are only locally interbedded with sedimentary deposits in paleovalleys.

Major ash-flow tuffs to be examined on this field trip are the "45 Ma tuff," one or more ca. 41–43 Ma plagioclase-biotite tuffs, the ca. 41.0 Ma tuff of Coal Mine Canyon, and the 40.0 Ma tuff of Big Cottonwood Canyon (Henry, 2008). The tuff of Big Cottonwood Canyon erupted from a caldera in the Tuscarora volcanic field (Fig. 2; Henry et al., 1999; Henry, 2008). Source calderas for the other tuffs were probably also in the Tuscarora and Bull Run basin areas, where the tuffs are thickest and most widely distributed, but have not been positively identified. Within ~20 km of known or probable sources, the tuffs apparently blanketed the area. At greater distances, the tuffs largely flowed through and were deposited in paleovalleys (Fig. 2).

Volcanism largely ceased in Elko County between ca. 35 and 16 Ma. Abundant silicic intrusions in the Ruby Mountains and East Humboldt Range are as young as 29 Ma, however, indicating that magmatism continued in the subsurface (Wright and Snoke, 1993; MacCready et al., 1997; Howard, 2000; Miller and Snoke, 2009). The only known locally derived volcanic rock between those times is an apparently minor 31 Ma ash-flow tuff in the Piñon Range west of the Ruby Mountains. Oligocene, probably

Figure 5. Photographs of key rock types and field relationships in the northern East Humboldt Range. (A) Photograph, view to northwest, and sketch of the hinge zone of the Winchell Lake fold-nappe as exposed along the back wall of Winchell Lake cirque on the eastern face of the northern East Humboldt Range (Snoke et al., 1997). The core of the fold at this locality consists of dark outcrops of rusty-weathering graphitic paragneiss (rgs) surrounded by white-weathering Cambrian and Ordovician marble (DCmu) and Ordovician metaquartzite (DCmq). Enveloping the fold is a thick sequence of Neoproterozoic and Lower Cambrian flaggy quartzite and schist (CZqs). These metasedimentary rocks, particularly the metaclastic units, contain abundant sheet-like bodies of leucogranite orthogneiss. The hinge zone of this major structure trends west-northwest, approximately parallel to mineral elongation lineations in the deformed rocks. Closure is to the south. To the north, the fold is cored by near-Archean orthogneiss (Angel Lake orthogneiss) and associated paragneiss. A pre-folding, low-angle fault is inferred to separate the metasedimentary rocks in this photograph from the basement complex enclosed in the core of the fold. Scale is approximate. (B) Striped gray biotite monzogranitic orthogneiss of Angel Lake (Neoarchean(?) to earliest Paleoproterozoic) intruded by an orthoamphibolite sheet of probable Proterozoic age and by millimeter-scale to meter-scale seams, veins, and lenses of probable Late Cretaceous leucogranite as discussed in text. View to northwest. (C) Refolded fold developed in intricately interdigitated Neoarchean(?) orthogneiss and migmatitic Paleoproterozoic paragneiss. Note that three overprinted fold phases are indicated. View is ~2.5 m wide. (D) Photograph, view to west, and sketch of road-cut exposure of a low-angle normal fault exposed on the west flank of Clover Hill separating steeply dipping fanglomerate of the Miocene Humboldt Formation from a footwall of brecciated, strongly foliated calcite marble. A distinct red gouge lies along the fault (Mueller and Snoke, 1993a).

distal pyroclastic-fall tuffs are present in Copper Basin (Day 2; Table 1; McGrew and Foland, 2004).

Miocene and Younger Sedimentary and Volcanic Rocks

Miocene and younger clastic sedimentary rocks are abundant throughout northeastern Nevada. In the Elko area, the Miocene rocks are called the Humboldt Formation, which was originally defined by Sharp (1939) to include Eocene rocks, and later restricted to the Miocene deposits by Smith and Ketner (1976, 1978). The Humboldt Formation and age-equivalent units range from ca. 16.5 to 10 Ma everywhere they have been dated by $^{40}Ar/^{39}Ar$ and tephrachronology (John et al., 2000; Wallace et al., 2008; Colgan et al., 2008; Colgan et al., 2010). These deposits include fine-grained fluvial and lacustrine deposits, primary and reworked tephra beds up to several meters thick, conglomerate whose clast composition depends on the local basement lithology, and very large (10s of meters) breccia blocks most often consisting of Paleozoic carbonate. Rhyolite lava flows are locally interbedded with the Humboldt Formation, although they are not considered part of the unit as typically defined. The Humboldt Formation at Stops 1-1 and 1-2 exhibits the types of deposits common to the unit. The Humboldt Formation was deposited in the hanging-wall basins of major Miocene normal faults during an episode of regional Basin and Range extension in the middle Miocene (Sharp, 1939; Smith and Ketner, 1978; John et al., 2000; Wallace et al., 2008; Colgan and Henry, 2009; Colgan et al., 2010). Late Miocene and younger (mostly Pliocene) deposits are rarely exposed but have been intercepted by drill holes in the deeper valleys and are lithologically similar to the Humboldt Formation.

Volcanism resumed in northeastern Nevada ca. 16.5 Ma, coincident with major extension, and was primarily bimodal, basalt and rhyolite (Zoback et al., 1994; John et al., 2000; Colgan and Henry, 2009). The oldest rocks are minor basalt with Steens-type petrographic (abundant plagioclase phenocrysts to 5 cm long) and chemical characteristics near Copper Basin dated at 16.5 Ma (Rahl et al., 2002; Coats, 1964). Mafic rocks make up most of the Tv unit in the western and northern part of Figure 2 (Owyhee Plateau); published K-Ar ages range from ca. 16 to 8 Ma. Recent mapping, geochemistry, and $^{40}Ar/^{39}Ar$ geochronology indicates that most, if not all, of the basalt flows and shield volcanoes exposed on the Owyhee Plateau are younger than 11 Ma and are more primitive than the mid-Miocene flood-basalt related lava flows (e.g., they are high-alumina olivine tholeiite, Snake River olivine tholeiite, and transitional; Shoemaker, 2004). A voluminous group of distinctive, coarsely porphyritic rhyolite lavas, the Jarbidge Rhyolite, is widespread across northern Elko County (Fig. 2), but a few flows are also present northeast and southwest of Wells. The oldest dates from Jarbidge Rhyolite are 16.3 ± 0.03 Ma on a lava dome west of Copper Basin (M.E. Brueseke, unpublished $^{40}Ar/^{39}Ar$ data) and 16.15 ± 0.02 Ma on a flow south of Bull Run basin (C.D. Henry, unpublished $^{40}Ar/^{39}Ar$ data). Jarbidge Rhyolite lava flows just north of Copper Basin are as young as 15.8 ± 0.06 Ma (M.E. Brueseke, unpublished $^{40}Ar/^{39}Ar$ data). Jarbidge-type rhyolites in the northeastern East Humboldt Range are referred to as the Willow Creek rhyolite complex, which yielded K-Ar (sanidine) ages in the interval 14.8–13.4 Ma (Mueller and Snoke, 1993b). The oldest Willow Creek rhyolite forms a sequence of flows. Rhyolite porphyry (13.8 ± 0.5 Ma) intruded the flows, and even younger "purple rhyolite" (13.4 ± 0.5 Ma) overlies volcaniclastic breccia in one fault-bounded block near the front of the range (Willow Creek rocks can be viewed on the way to Stop 1-1).

STRUCTURAL-TECTONIC-TOPOGRAPHIC EVOLUTION

Paleozoic-Mesozoic Contraction and Crustal Thickening and Paleogene Erosion

Northeastern Nevada underwent multiple episodes of contraction from the Late Devonian–Early Mississippian Antler orogeny through the Late Cretaceous Sevier orogeny (Roberts et al., 1958; Armstrong, 1968; Thorman, 1970; Miller et al., 1992; Poole et al., 1992; Camilleri et al., 1997; Taylor et al., 2000; DeCelles, 2004; Dickinson, 2006). Eastern Nevada lay in the hinterland of the Sevier orogenic belt (Armstrong, 1968; Miller and Gans, 1989; Camilleri et al., 1997; Vandervoort and Schmitt, 1990; Wright and Snoke, 1993; Howard, 2003; DeCelles, 2004), where the crust was inferred to have reached a thickness of 50–60 km by end of the Cretaceous, based on restoration of Tertiary extension (Coney and Harms, 1984; Gans, 1987; DeCelles, 2004; DeCelles and Coogan, 2006), estimates of shortening in the overthrust belt (Thorman et al., 1991; Camilleri et al., 1997), and metamorphic mineral assemblages (Camilleri et al., 1997; McGrew et al., 2000; Lee et al., 2003).

Northeastern Nevada was an eroding highland (Nevadaplano) at the beginning of the Cenozoic (Armstrong, 1968; Coney and Harms, 1984; Christiansen and Yeats, 1992; Dilek and Moores, 1999; DeCelles, 2004; Best et al., 2009), from which sediments were most likely carried eastward to the Uinta and Green River Basins (Baars et al., 1988; Hintze, 1993; Goldstrand, 1994; Davis et al., 2009), although there is little sedimentary record in Nevada until the Eocene (Fouch et al., 1979; Solomon et al., 1979; Vandervoort and Schmitt, 1990). Interpretations of the absolute surface elevation, timing of surface uplift, and paleotopography of northeastern Nevada during the Paleocene and Eocene vary widely, however. Coney and Harms (1984), Dilek and Moores (1999), DeCelles (2004), DeCelles and Coogan (2006), Best et al. (2009), and Cassel et al. (2010)—drawing analogies to present-day Tibet and the Andean Plateau—inferred surface elevations of >3 km, probably as a result of crustal thickening during the Cretaceous Sevier orogeny. Absolute Eocene elevations interpreted from fossil leaves in Copper Basin (Stop 2-1; present-day elevation 2.2 km) vary from 1.1 km (Axelrod, 1966a, 1966b), to 2.0 ± 0.2 km (Wolfe et al., 1998), to 1.6 ± 1.6 km or 2.8 ± 1.8 km (Chase et al., 1998). Mix et al. (2011)

TABLE 1. $^{40}Ar/^{39}Ar$ AGES, COPPER BASIN AND WINDERMERE HILLS, NEVADA

Sample	Mineral	Rock type and part of unit	Easting or longitude	Northing or latitude	Ages (Ma)					Reference
					Weighted mean	Integrated	Plateau	Isochron	$^{40}Ar/^{36}Ari$	
Copper Basin										
990704-1	Plagioclase	Plagioclase-phyric, 76 Creek Basalt (Steens-type)	628060	4623835		16.3	16.5 ± 0.2	16.3 ± 0.1	298 ± 2	Rahl et al. (2002)
Meadow Fork Formation										
010801-5	Hornblende	Pyroclastic-fall tuff	625425	4624225		28.3	29.2 ± 0.2	29.4 ± 0.4	293 ± 2	McGrew and Foland (unpub.)
"	Hornblende	"	625425	4624225		28.2	29.7 ± 0.3	29.5 ± 0.4	294 ± 2	McGrew and Foland (unpub.)
"	Biotite	"	625425	4624225		27.0	29.3 ± 0.4	27.8 ± 1.0	302 ± 5	McGrew and Foland (unpub.)
"	Biotite	"	625425	4624225		28.6	31.4 ± 0.3	29.3 ± 1.3	304 ± 5	McGrew and Foland (unpub.)
050720-10	Biotite	Fine pyroclastic-fall tuff, lower	625629	4624013		31.0	32.5 ± 0.2	33.7 ± 0.3	271 ± 4	McGrew and Foland (unpub.)
050720-9C	Biotite	Very fine pyroclastic-fall tuff, basal	625654	4623690		31.8				McGrew and Foland (unpub.)
Dead Horse Formation										
970728-3	Sanidine	Fine, white, pyroclastic-fall tuff, uppermost	627290	4624760		37.9	37.4 ± 0.2	37.8 ± 0.2	284 ± 10	Rahl et al. (2002)
050720-3B	Biotite	White, pyroclastic-fall tuff, directly beneath flora locality	626511	4623195		39.6	39.8 ± 0.2	39.6 ± 0.2	305 ± 6	McGrew and Foland (unpub.)
050721-11	Biotite	White, biotite-rich, pumiceous pyroclastic-fall tuff	627385	4624325		38.2	41.5 ± 0.2	40.0 ± 1.3	303 ± 5	McGrew and Foland (unpub.)
960702-1A	Biotite	Ash-flow tuff	626216	4621502		40.0	41.3 ± 0.1	40.9 ± 0.2	302 ± 3	Rahl et al. (2002)
050719-4	Biotite	Andesite, lower	625235	4621654		42.7	42.7 ± 0.1	42.5 ± 0.2	309 ± 9	McGrew and Foland (unpub.)
050727-1	Biotite	White pumiceous tuff, lower	626514	4621344		42.1		42.0 ± 1.7	258 ± 5	McGrew and Foland (unpub.)
"	"	"	626514	4621344		43.4		43.8 ± 0.9	255 ± 3	McGrew and Foland (unpub.)
050721-13	Biotite	White, biotite-rich, pumiceous pyroclastic-fall tuff, lower	627724	4623975		42.6	47.3 ± 0.2	46.3 ± 1.0	302 ± 6	McGrew and Foland (unpub.)
H06-121	Sanidine	Tuff of Big Cottonwood Canyon	–115.49297	41.74840	40.02 ± 0.10					Henry (2008)
H06-123	Sanidine	45 Ma tuff	–115.48560	41.74391	44.90 ± 0.07					Henry (2008)
Windermere Hills										
H06-108	Sanidine	Reworked tuff (same as WC-15, Mueller et al., 1999)	–114.64339	41.25447	34.75 ± 0.12					C.D. Henry (unpublished)

interpreted stable-isotope data to indicate uplift migrated southward through western North America during the early Cenozoic and Eocene elevations of ~3.4 km in the Elko and Copper basins.

Major Eocene and older(?) paleovalley systems that drained eastward across northeastern Nevada record erosion of the Nevadaplano (Figs. 1, 2; Henry, 2008). Paleovalleys are discontinuously exposed across a series of ranges that formed predominantly during middle Miocene or later Basin and Range extension. Recognition and correlation of paleovalleys is based on (1) paleovalley geometry where ash-flow tuffs and sedimentary rocks crop out within valleys incised into Paleozoic rocks, (2) recognition of depositional contacts of paleovalley fill against walls, (3) wedging out of paleovalley fill against paleovalley walls, (4) continuity of individual tuffs and distinctive groups of tuffs along the paleovalleys, and (5) the considerable thicknesses and dense welding of tuffs far from their source.

The north paleovalley can be traced from the Bull Run basin through Cornwall Mountain to Copper Basin, where it is joined by a probable tributary from the southwest and becomes buried eastward beneath Jarbidge Rhyolite (Fig. 2; Henry, 2008; McGrew and Vance, 2008; Cook and Brueseke, 2010). Insufficient data are available to follow the paleovalley farther east. The "45 Ma tuff" crops out all along this paleovalley and may have erupted from a caldera at the western end north of Bull Run basin. A plagioclase-biotite tuff, tuff of Coal Mine Canyon, tuff of Big Cottonwood Canyon, and a moderately thick section of conglomerate, tuffaceous sandstone, and shale overlie the 45 Ma tuff in Copper Basin (Stop 2-1).

The central paleovalley can be traced ~150 km from near the Tuscarora volcanic field eastward over the Independence Mountains as far as Nanny Creek (Stop 3-1; Pequop Mountains; Fig. 2). Although gaps exist across several modern basins, continuity is inferred based on proximity and trend of individual segments and similar stratigraphy within them, especially the presence of the tuff of Big Cottonwood Canyon. The tuff of Big Cottonwood Canyon was able to flow 150 km (present day) from Tuscarora to Nanny Creek. The amount of post–40 Ma extension across that distance is unknown, but, even if it was 100%, the tuff must have flowed 75 km.

What may be a branch of the central paleovalley passes through the Windermere Hills, where Mueller et al. (1999) interpreted Eocene sedimentary rocks to fill a half-graben above an east-rooted, Eocene low-angle detachment fault. Henry (2008) interpreted the same deposits to fill an east-draining paleovalley, consistent with cobble imbrications found by Mueller (1992), but probably dammed during small-magnitude Eocene extension. Eocene volcanic rocks, the sedimentary section, and overlying middle Miocene deposits are all tilted the same amount, which suggests major extension was middle Miocene or younger. Eocene (and Oligocene?) deposits on both west and east sides of the Pilot Range form a thick section of tuffaceous sedimentary rocks, possibly some primary ash-flow tuff, and coarse conglomerate (Miller, 1985; Miller et al., 1993; this study) that may be in the eastern continuation of this paleovalley.

A south paleovalley extends from the southern Independence Mountains through Coal Mine Canyon and may connect eastward across the northern East Humboldt Range to Clover Hill, where a thick section of Eocene and Miocene sedimentary rocks is exposed. The relative proportions of each are uncertain, but a basal conglomerate and ash-flow tuff are almost certainly Eocene. A cobble in the basal conglomerate was dated at ca. 38 Ma (Brooks et al., 1995a, 1995b). The upper part of the section contains a ca. 15.5 Ma tephra that is overlain by Willow Creek rhyolite (Jarbidge Rhyolite; Snoke et al., 1997; J.P. Colgan, K.A. Howard, and C.D. Henry, unpublished data). Coarsely clastic and breccia-bearing sedimentary rocks make up most of the section. Stops 1-1 and 1-2 show the sedimentary section, structure of the Clover Hill area, and highly metamorphosed rocks of the adjacent RMEH.

Figure 2 shows a possible paleovalley crossing the Ruby Mountains, based on the thick section of Elko Formation in the Elko Hills, a thick section of Miocene or Eocene deposits identified by seismic-reflection methods in the valley west of the Ruby Mountains (Satarugsa and Johnson, 2000), and a thick section of dacitic and andesitic lavas with a basal coarse conglomerate in the southern East Humboldt Range (Brooks et al., 1995a, 1995b; this study). Satarugsa and Johnson (2000) interpreted the subsurface rocks to be middle Miocene, but distinguishing Eocene and Miocene rocks without drill hole data is uncertain.

Cenozoic Extension

Interpreted episodes of extension began with initial exhumation of the Ruby Mountains between the Late Cretaceous and Eocene (McGrew and Snee, 1994; Camilleri and Chamberlain, 1997; McGrew et al., 2000) and development of the Elko basin of the Elko Hills at ca. 46 Ma (Haynes et al., 2002; Cline et al., 2005; Hickey et al., 2005). A major episode of extension began in the middle Miocene throughout northern Nevada (Zoback et al., 1994; Miller et al., 1999; John et al., 2000; Wallace et al., 2008; Colgan and Henry, 2009; Colgan et al., 2010), and extension continues to today (e.g., 2008 M_w 6.0 Wells earthquake; Fig. 2). How much extension occurred at different times in the Cenozoic is the focus of this trip. The following four subsections discuss different approaches and perspectives.

Evidence from Thermochronology and Thermobarometry of the RMEH (A.J. McGrew)

Integrated thermobarometric and thermochronologic results indicate ~170 °C of cooling and 4 kbar of decompression of the RMEH between ca. 85 Ma and ca. 50 Ma (e.g., Dallmeyer et al., 1986; Dokka et al., 1986; Hurlow et al., 1991, Hodges et al., 1992; McGrew and Snee, 1994; McGrew et al., 2000; Hallett and Spear, 2010) (Fig. 6). However, maximum tectonic burial of the RMEH occurred before 85 Ma and is recorded by peak pressure conditions represented by a relict kyanite + staurolite assemblage that is preserved locally at high structural levels in the northern East Humboldt Range and better preserved at the still-higher

structural levels of nearby Clover Hill (Snoke, 1992). Based on Gibbs Method modeling of the Clover Hill assemblage, Hodges et al. (1992) interpreted isothermal decompression from 9–10 kbar to 5.0–6.4 kbar at temperatures of 550–630 °C before partial degassing inferred from an $^{40}Ar/^{39}Ar$ hornblende age spectrum in the mid-Cretaceous (Dallmeyer et al., 1986).

At the deeper structural levels of the northern East Humboldt Range, peak metamorphism recorded by growth of sillimanite occurred contemporaneously with in situ partial melting in the Late Cretaceous, resulting in re-equilibration of most mineral assemblages, although growth zoning has been preserved in some garnets at higher structural levels (Hallett and Spear, 2010; McGrew et al., 2000; McGrew and Snoke, 2010). McGrew et al. (2000) documented a major phase of leucogranite generation at 84.8 ± 2.8 Ma synkinematic with fold-nappe emplacement and metamorphism above the second sillimanite isograd. More recently, U-Pb SHRIMP analyses of zircon rims from the orthogneiss of Angel Lake confirm the presence of abundant Late Cretaceous melt (yielding a spectrum of essentially concordant ages from 72 to 91 Ma) (Premo, et al., 2008; McGrew et al., 2009).

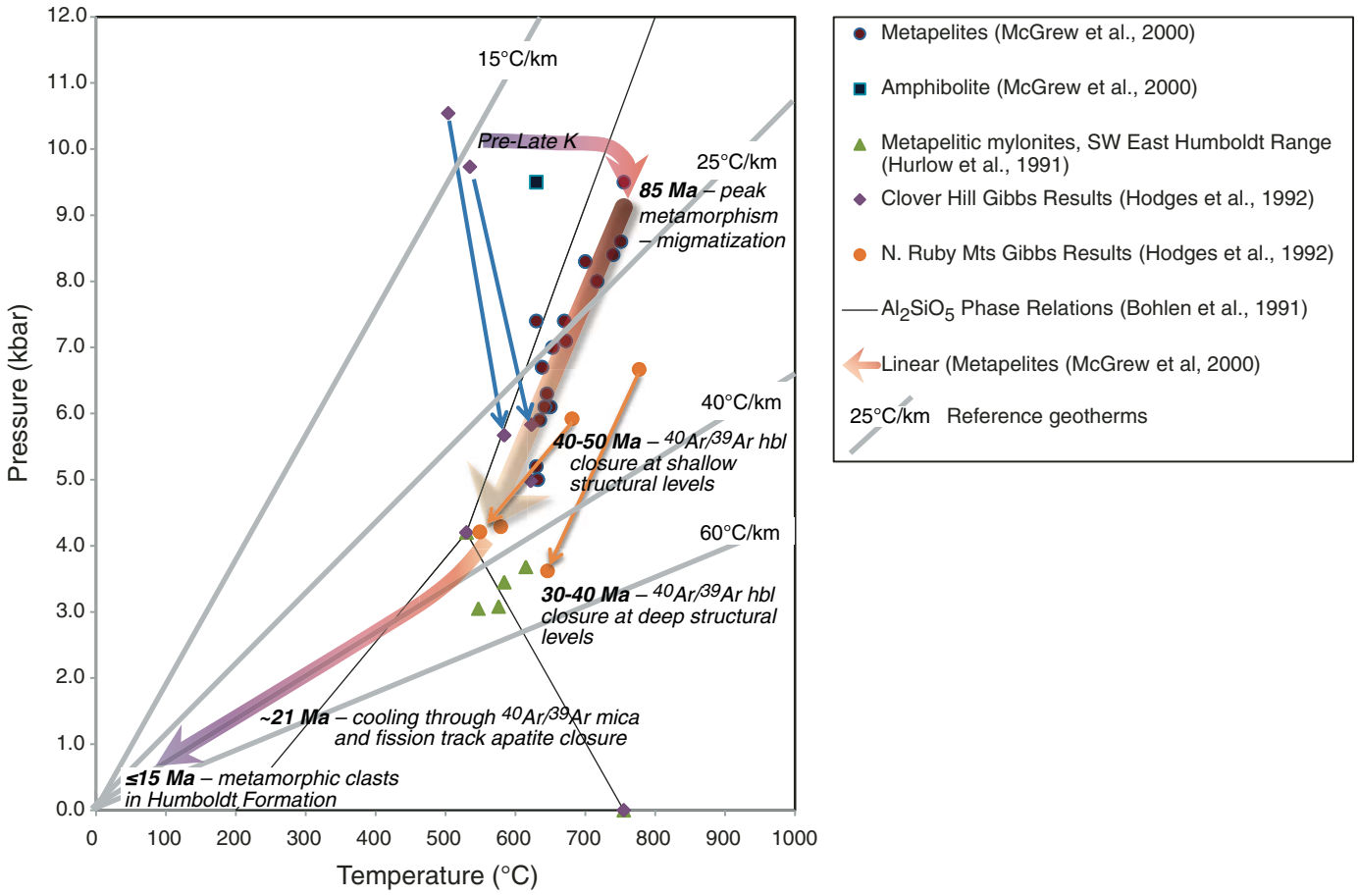

Figure 6. Interpretative diagram of P-T results from the Ruby Mountains–East Humboldt Range metamorphic core complex (RMEH) from McGrew et al. (2000) combined with previously published results from elsewhere in the RMEH (Hurlow et al., 1991; Hodges et al., 1992). Error ellipses have been left off to simplify viewing. The thick, colored arrows show the general P-T-t path inferred for the East Humboldt Range from late Mesozoic time to ca. 15 Ma based on the integration of P-T data with thermochronometric and other constraints. The earliest phase in the P-T-t path, illustrated by the upper arrow, records initial tectonic burial to kyanite-grade conditions before overprinting in the Late Cretaceous by peak metamorphism above the second sillimanite isograd and widespread migmatization. The second arrow represents a linear fit to the P-T results of McGrew et al. (2000) with a slope of 0.025 kbar/°C interpreted as a decompressional cooling path based on a variety of decompressional reaction textures. This segment is bracketed between 85 Ma and $^{40}Ar/^{39}Ar$ hornblende cooling ages of 40–50 Ma (at shallow structural levels) or 30–40 Ma (at deep structural levels). Thinner arrows represent net Gibbs model paths for samples from Clover Hill and the northern Ruby Mountains (Hodges et al., 1992). The lowermost heavy arrow illustrates inferred cooling based on late Oligocene to early Miocene $^{40}Ar/^{39}Ar$ muscovite and biotite and fission-track apatite cooling ages (Dallmeyer et al., 1986; Dokka et al., 1986; McGrew and Snee, 1994) combined with the constraint that metamorphosed footwall clasts do not appear until deposition of the middle Miocene Humboldt Formation. Additionally, ages of 11.6–13.8 Ma on authigenic illite from fault gouge in Secret Pass are interpreted to record last major activity of the RMEH detachment and associated faults (Haines and van der Pluijm, 2010). The modern-day geothermal gradient in the Basin and Range province is ~25 °C/km, whereas the Battle Mountain heat-flow high is characterized by geothermal gradients as high as 40–75 °C/km.

Collectively, P-T estimates based on mineral rim thermobarometry from the northern East Humboldt Range define a data array extending from 798 °C, 9.3 kbar to 630 °C, 5.2 kbar, inferred to represent equilibration at different points along a decompressional P-T-t path (Fig. 6) (McGrew et al., 2000). Including data interpreted to constrain the P-T conditions during mylonitization at higher structural levels in the southwestern part of the East Humboldt Range extends this trend down to ~550 °C, 3–5 kbar (Hurlow et al., 1991).

$^{40}Ar/^{39}Ar$ hornblende isochron ages ranging from 50 to 63 Ma at higher structural levels in the East Humboldt Range imply that much if not all of this decompressional P-T-t path occurred between the Late Cretaceous and early Eocene, although the lowest P-T results, inferred to represent conditions during extensional mylonitic deformation, may have equilibrated in the late Eocene (Fig. 6; Hurlow et al., 1991; McGrew et al., 2000). Aluminum-in-hornblende barometry on late Eocene (40–36 Ma) quartz diorites exposed in the RMEH further supports this interpretation, indicating that these granitic rocks intruded at mid-crustal levels and pressures of ~5.5 kbar, near the base of the P-T trend described above and illustrated in Figures 6 and 7 (Snoke et al., 2004).

Evidence of extension at upper crustal levels during the Late Cretaceous to the Eocene (ca. 46 Ma) in the RMEH environs is scant, although Camilleri and Chamberlain (1997) interpret a major normal fault, the Pequop Fault, that they bracket within this time frame. However, deep-crustal spreading or diapiric upwelling triggered by partial melting of a buoyant, thermally weakened lower-crustal root could have transferred this terrain from deep-crustal to mid-crustal levels without greatly extending the overlying rigid upper crustal layer (e.g., Wernicke and Getty, 1997; McGrew, 2002; Hodges, 2006). MacCready et al. (1997) provided evidence of such channel flow from the northern Ruby Mountains. However, to maintain crustal-scale strain compatibility, any such model would require a decoupling zone at mid-crustal levels separating the ductilely flowing deeper crustal layer from the overlying, more rigid upper crust. In this context,

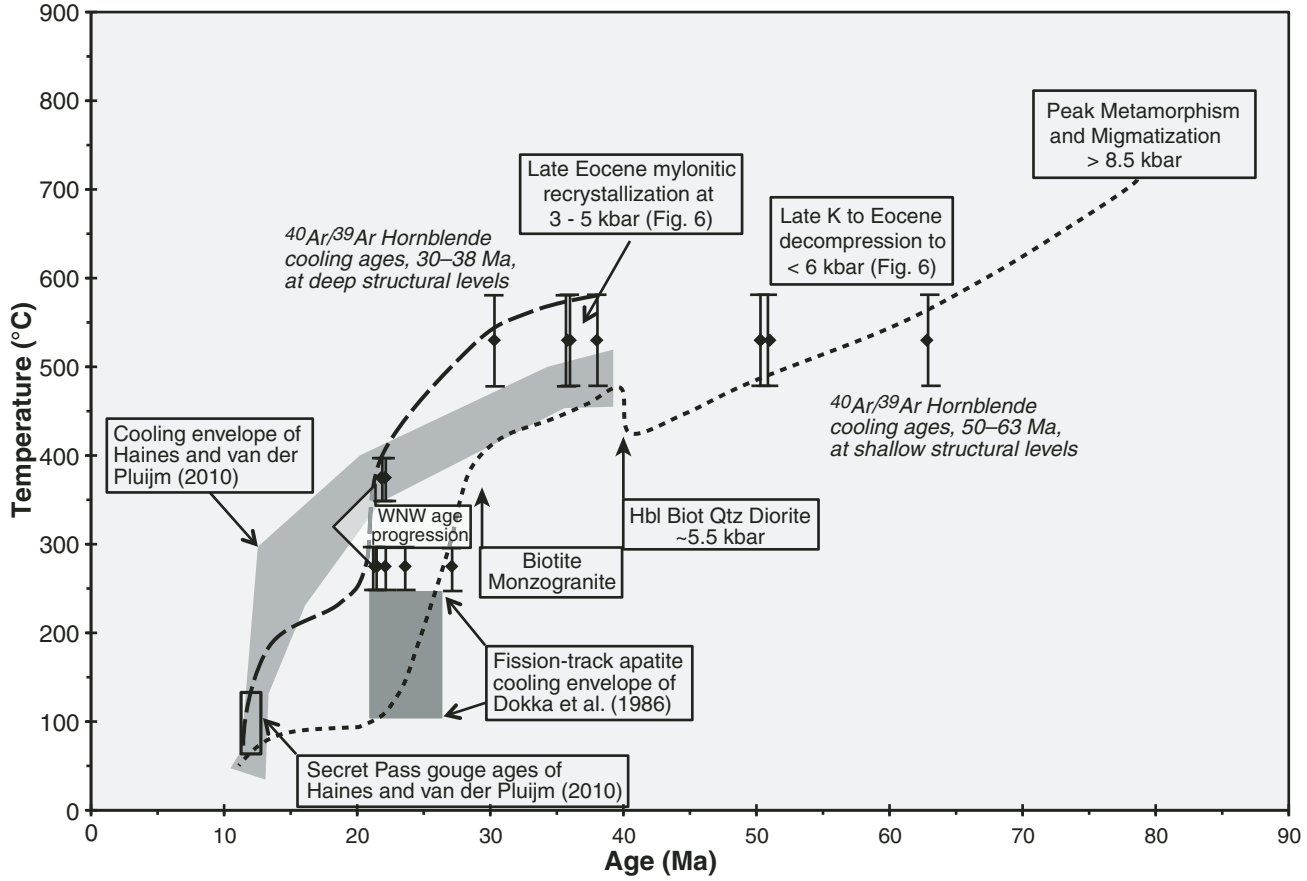

Figure 7. Generalized time-temperature curve for the northern East Humboldt Range synthesizing results modified from McGrew and Snee (1994), and summarizing results from other studies (Dallmeyer et al., 1986; Dokka et al., 1986; Haines and van der Pluijm, 2010). Vertical black bars represent the inferred closure temperature ranges for hornblende (480–580 °C), muscovite (350–400 °C), and biotite (250–300 °C), respectively. Pressure estimates for metamorphism above hornblende closure temperatures derive from thermobarometric studies summarized in Figure 6. Short-dash line is a lower bound for relatively shallow structural levels, and long-dash line is an upper bound for deeper structural levels. Important magmatic events are the intrusion of a thick sheet of hornblende biotite quartz diorite at 40 ± 3 Ma and injection of widespread biotite monzogranitic sheets at 29 ± 0.5 Ma (Wright and Snoke, 1993).

large-scale fold-nappes such as the Winchell Lake fold-nappe in the East Humboldt Range or the Soldier Peak or Lamoille Canyon fold-nappes in the Ruby Mountains could be manifestations characteristic of the "roof zone" of a laterally spreading and upwelling deep-crustal migmatite complex as presaged by Howard (1980). In this light, it is interesting that the Winchell Lake fold-nappe is both temporally and spatially associated with the "roof" of the migmatite complex in the very zone where the rheologically critical melt percentage is likely to have been achieved (Vanderhaeghe et al., 2001).

Regardless of the pre-Eocene history of the RMEH, a variety of lines of evidence indicate that it remained at mid-crustal depths and elevated temperatures at least into the Oligocene:

(1) Aluminum-in-hornblende barometry on 40–36 Ma quartz diorites indicates that they were intruded at mid-crustal depths, ~5.5 kbar (Snoke et al., 2004).

(2) Both the 36–40 Ma intrusive suite and a younger, 29 Ma biotite monzogranitic intrusive suite were foliated, mylonitized, and locally complexly folded after emplacement. Moreover, petrographic relationships such as dynamic recrystallization of biotite along shear bands and crystal-plastic deformation of feldspars in these rocks indicates that the plastic deformation occurred at elevated temperatures (probably at least 450 °C).

(3) Hurlow et al. (1991) and Hodges et al. (1992) document P-T conditions of 550–650 °C, 3.0–4.3 kbar based on thermobarometry of syn-mylonitic mineral assemblages in pelitic schist from the RMEH mylonitic shear zone in the southwestern East Humboldt Range (Fig. 6).

(4) Quartz crystallographic preferred orientations (CPOs) are interpreted to record WNW- or ESE-directed shearing within and beneath the mylonitic zone, and show the hallmarks of recrystallization at temperatures as high as 600–700 °C (e.g., strong c-axis maxima parallel to the Y-strain axis and/or crossed girdle fabrics with a 90° opening angle at deeper structural levels, resembling relationships in the Saxony granulite terrain) (McGrew and Casey, 1993; MacCready, 1996; Law et al., 2004).

(5) Deep structural levels of the RMEH last cooled through $^{40}Ar/^{39}Ar$ hornblende closure temperatures during the late Eocene to the Oligocene (25–36 Ma) (Figs. 6, 7) (Dallmeyer et al., 1986; McGrew and Snee, 1994).

Cooling through $^{40}Ar/^{39}Ar$ biotite closure temperatures (250–300 °C) occurred diachronously across the RMEH from ESE to WNW over the interval ca. 36–21 Ma, giving rise to an asymmetrical, WNW-younging cooling age "chrontour" pattern across the core complex (Kistler et al., 1981; Dallmeyer et al., 1986; McGrew and Snee, 1994) (Figs. 4, 7). The cooling age chrontours are perpendicular to mylonitic stretching lineation associated with numerous WNW-directed normal-sense kinematic indicators, leading to the common interpretation that the chrontour pattern tracks the unroofing history of the lower plate as the mylonitic shear zone progressively translated the upper plate to the WNW. However, the pattern could alternatively be interpreted as a transect through an exhumed, ESE-rotated partial retention zone (e.g., Colgan et al., 2010).

Finally, based on apatite, zircon, and sphene fission-track results from the RMEH, Dokka et al. (1986) interpreted rapid cooling between ~285 °C and ~70 °C between ca. 25 and 23 Ma, which suggests that exhumation was largely complete by the early Miocene. Early Miocene cooling of the RMEH is also constrained by the fact that metamorphic foliations in both the mylonitic zone and the underlying infrastructure are cut by unmetamorphosed and undeformed amygdaloidal basaltic dikes with chilled margins dated ca. 17–15 Ma (Snoke, 1980; Hudec, 1992). Consequently, it would appear that mylonitization had ceased and the RMEH had cooled to temperatures below ~120 °C, corresponding to paleodepths less than 4–6 km depending on the geothermal gradient assumed, by the early Miocene. While internally consistent, this cooling history contrasts with a recently documented cooling history for the Secret Pass area and continued slip on the RMEH detachment fault to ca. 12 Ma (Figs. 6, 7) (Haines and van der Pluijm, 2010). In addition, the accumulation of up to 5 km of middle Miocene fill in the adjoining basins to the west and evidence for rapid middle Miocene extension and exhumation in the southern Ruby Mountains pose a further challenge to the idea that most extension was completed by ca. 20 Ma (see "Miocene Basins and Thermochronology" section) (Satarugsa and Johnson, 2000; Colgan et al., 2010).

Evidence from Eocene Paleovalleys and Ash-Flow Tuffs (C.D. Henry)

The (1) continuity of paleovalleys across northeastern Nevada in the Eocene (Figs. 1, 2), (2) ability of Eocene ash-flow tuffs to flow long distances in the paleovalleys, (3) presence of relatively thin (<1 km) Eocene (≥41 Ma and ca. 38–35 Ma) sedimentary/lacustrine deposits, and (4) mostly concordant contacts between Eocene and middle Miocene deposits suggest one or two episodes of minor Eocene extension and little if any extension between the Eocene and middle Miocene (Henry, 2008; Colgan and Henry, 2009). A fundamental assumption is that tilting is a proxy for extension.

The first two observations preclude northeastern Nevada being either a series of north-striking basins and ranges similar to the present topography or a single large basin having overall low relief. The tuff of Big Cottonwood Canyon flowed at least 75 km from source to its most distal known outcrop (Nanny Creek, Stop 3-1; original, pre-extension distance), and the tuff's thickness and dense welding there suggest that it traveled significantly farther. Ash-flow tuffs erupted onto any low-relief surface would have spread radially and dispersed, and therefore would not show the linear distribution that they do or traveled very far. If erupted into a lake, these tuffs would have formed water-laid tuffs instead of thick, densely welded deposits. Tuffs erupted into basin-and-range topography like today also would have been channelized, but into wide north-trending paleovalleys, and would not have been able to reach distant locations to the east. Although low-density pyroclastic flows can surmount major ridges far from source, such flows are so dilute that they do not generate thick, densely welded deposits (Woods et al., 1998).

Continuous paleovalleys had been eroded to their full depth by 45–40 Ma—the age range of ash-flow tuffs found in them—but may have formed much earlier. The paleovalleys are deep (possibly up to 1.6 km) but wide (6–8 km) and had low-relief interfluves, which seem characteristic of relatively deeply eroded topography. Formation of the paleovalleys during regional surface uplift related to the Late Cretaceous Sevier orogeny is therefore plausible.

The third and fourth observations support possibly two episodes of low-magnitude extension, one before ca. 41 Ma and possibly as old as 46 Ma and a second between ca. 40 and 38 Ma. The Eocene sedimentary—especially lacustrine—deposits seem to require deposition in extensional basins, not only along paleovalleys. The deposits are widespread over northeastern Nevada but as small, discontinuous packages. Lacustrine deposits fall into two age groups: older than ca. 40 Ma in the Elko Hills and at Double Mountain, Coal Mine Canyon, and Copper Basin (Haynes et al., 2002; Rahl et al., 2002; Haynes, 2003; Henry, 2008; this report) and ≤38–35 Ma in the Windermere Hills (Mueller et al., 1999). These deposits are ~600 m thick in the Elko Hills and a few hundreds of meters thick elsewhere (Solomon et al., 1979; Mueller et al., 1999; Haynes, 2003; Henry, 2008).

The only definite angular unconformity between rocks in the age range 45–16 Ma in most of northeastern Nevada is a ≤15° unconformity between the Elko Formation and 38 Ma volcanic rocks (Smith and Ketner, 1976; Solomon et al., 1979; Brooks et al., 1995a; Henry and Faulds, 1999; Haynes, 2003; Cline et al., 2005), immediately preceding the second episode of Eocene deposition. Where adequately studied, sub-unconformity rocks were tilted to the southeast. Southeast-tilted, pre–38 Ma rocks are present elsewhere but not overlain by younger rocks. For example, 41–40 Ma volcanic rocks in the Independence Mountains were also tilted to the southeast, but younger Eocene rocks are absent there (Muntean and Henry, 2007; Henry, 2008). The 46–39 Ma Elko Formation in the Elko Hills shows no fanning of dips (Haynes, 2003), which indicates no tilting and probably relatively little extension during its deposition. Similarly, Eocene and Miocene deposits are concordant in most areas of northeastern Nevada (Best and Christiansen, 1991; Thorman et al., 1991; Mueller, 1993; Brooks et al., 1995a; Mueller et al., 1999; Henry, 2008), which precludes significant tilting and extension.

The distribution, characteristics, and timing of Eocene sedimentary and lacustrine deposits are consistent with their deposition in small depocenters along paleovalleys where they were intersected by Eocene high-angle normal faults. An ~65°-dipping normal fault with ~1 km of slip could form a half-graben basin along a paleovalley that would accumulate ~1 km of sediment. However, the thinness of Eocene deposits (≤1 km compared to as much as 5 km of middle Miocene and younger basin fill; Satarugsa and Johnson, 2000) and the small degree of angular unconformity imply small-magnitude extension in the Eocene.

The absence of sedimentary deposits between ca. 38 and 16 Ma over most of northeastern Nevada, with the significant exception of Copper Basin, indicates no depocenters existed to accumulate sediments. This observation implies little or no tilting and formation of half-graben basins, which suggests little if any extension in the upper crust. Whether or not the paleovalleys continued to be active drainages is uncertain, because no deposits of this age range are found in them. However, deposition continued throughout the Oligocene in the Uinta, Flagstaff, and Claron Basins in Utah (Baars et al., 1988; Hintze, 1993; Bryant et al., 1989; Davis et al., 2009), although whether northeastern Nevada was a source area is unknown.

Eocene and Oligocene Extension: Copper Basin (A.J. McGrew)

The Copper Mountains and adjacent Copper Basin uniquely preserve one of the earliest and most sustained records of coevolving extension and volcanism in northeastern Nevada and are the only areas where significant Oligocene extension is reported to affect upper crustal rocks (Figs. 8, 9; Rahl et al., 2002). However, interpretations of the origin of Copper Basin continue to evolve. The Copper Mountains expose a Late Cretaceous greenschist to amphibolite facies terrain intruded by a large, ca. 110 Ma quartz monzonitic stock and bounded to the east by two normal faults that juxtapose the footwall against a 1.5-km-thick sequence of volcanic and sedimentary rock in adjacent Copper Basin. $^{40}Ar/^{39}Ar$ dates on volcanic rocks from the Eocene Dead Horse Formation range from 46.3 ± 1 Ma to 37.4 ± 0.23 Ma near the base and top of the sequence, respectively (Table 1). Locally, the Dead Horse Formation includes exposures of channel-filling conglomerate, and the similarity in tephro-stratigraphic sequence with paleovalley fills farther south and west led Henry (2008) to hypothesize that Copper Basin initiated as a paleovalley that was subsequently dammed due to the onset of late Eocene extension. Therefore, lacustrine deposition in the late Eocene may record the onset of basin subsidence associated with initiation of the Copper Creek normal fault (Figs. 9A–9C).

Despite the evidence for an Eocene onset of extension, footwall-derived detritus did not appear until deposition of the overlying Oligocene Meadow Fork Formation (Fig. 9D). Coats (1964) interpreted the Meadow Fork Formation to have

Figure 8. Retrodeformed cross-section sequence for the Copper Basin fault system (from Rahl et al., 2002). (A) Initial state immediately before the onset of extension at ca. 42 Ma. Due to extensive cover and poorly known or ambiguous contact relationships, structural levels above the Tennessee Mountain Formation are illustrated schematically. However, unit thicknesses and structural relationships are consistent with relationships in adjoining areas (e.g., Coats, 1964, 1987; Bushnell, 1967; Coash, 1967; Ketner et al., 1993, 1995). All units above the modern erosional surface are shaded. (B) Cross section after displacement on the Copper Creek and Meadow Fork normal faults but immediately before activity on the Bruneau Valley normal fault. Levels above the restored position of the modern erosional surface are again shaded. (C) Modern cross section established after eruption of the Jarbidge Rhyolite and down-faulting of the western fault block on the Bruneau Valley normal fault.

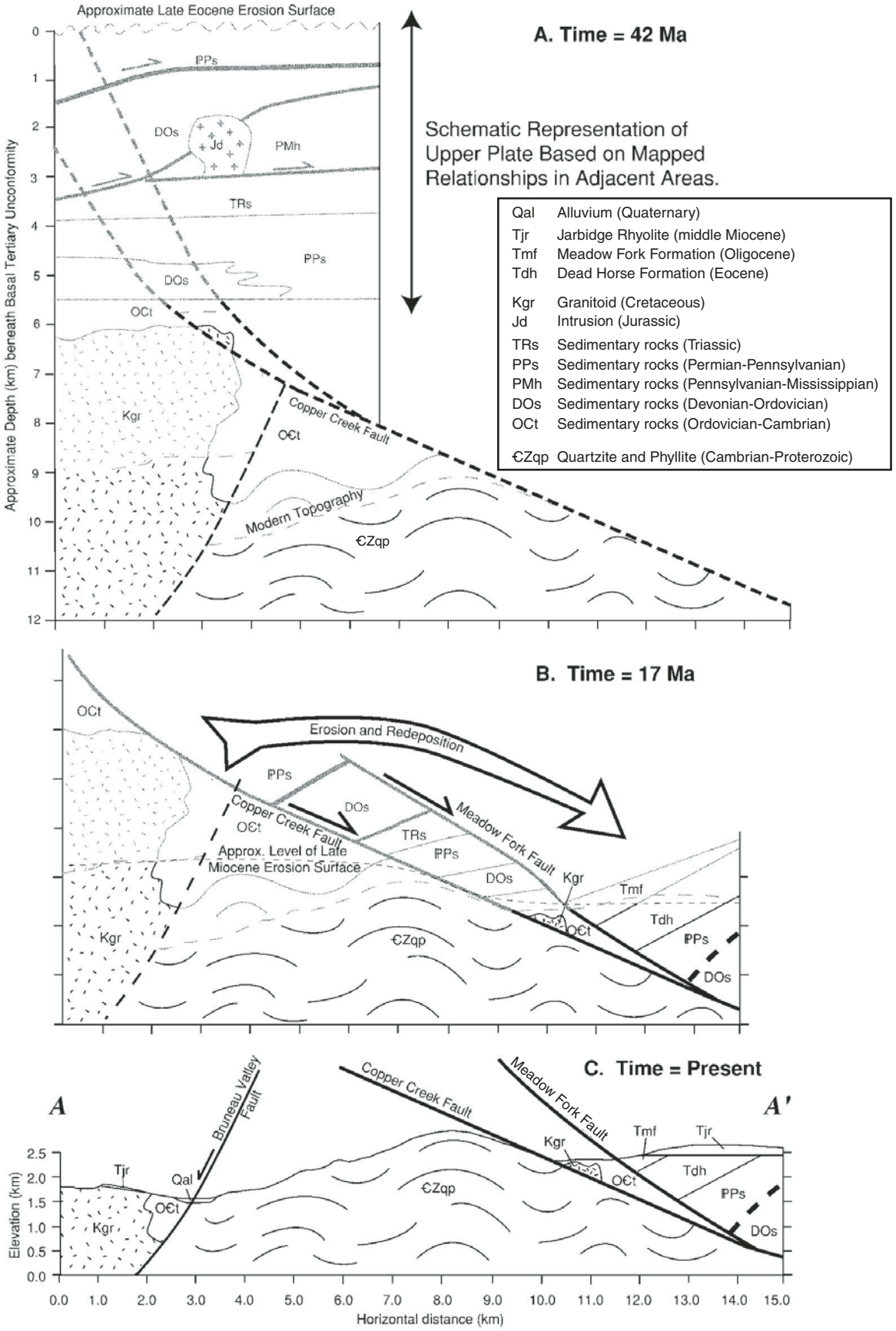
A. Time = 42 Ma
Approximate Late Eocene Erosion Surface
Approximate Depth (km) beneath Basal Tertiary Unconformity
Schematic Representation of Upper Plate Based on Mapped Relationships in Adjacent Areas.
Qal Alluvium (Quaternary)
Tjr Jarbidge Rhyolite (middle Miocene)
Tmf Meadow Fork Formation (Oligocene)
Tdh Dead Horse Formation (Eocene)
Kgr Granitoid (Cretaceous)
Jd Intrusion (Jurassic)
TRs Sedimentary rocks (Triassic)
PPs Sedimentary rocks (Permian-Pennsylvanian)
PMh Sedimentary rocks (Pennsylvanian-Mississippian)
DOs Sedimentary rocks (Devonian-Ordovician)
OCt Sedimentary rocks (Ordovician-Cambrian)
€Zqp Quartzite and Phyllite (Cambrian-Proterozoic)
Copper Creek Fault
Modern Topography
B. Time = 17 Ma
Erosion and Redeposition
Meadow Fork Fault
Approx. Level of Late Miocene Erosion Surface
C. Time = Present
A
A'
Bruneau Valley Fault
Elevation (km)
Horizontal distance (km)

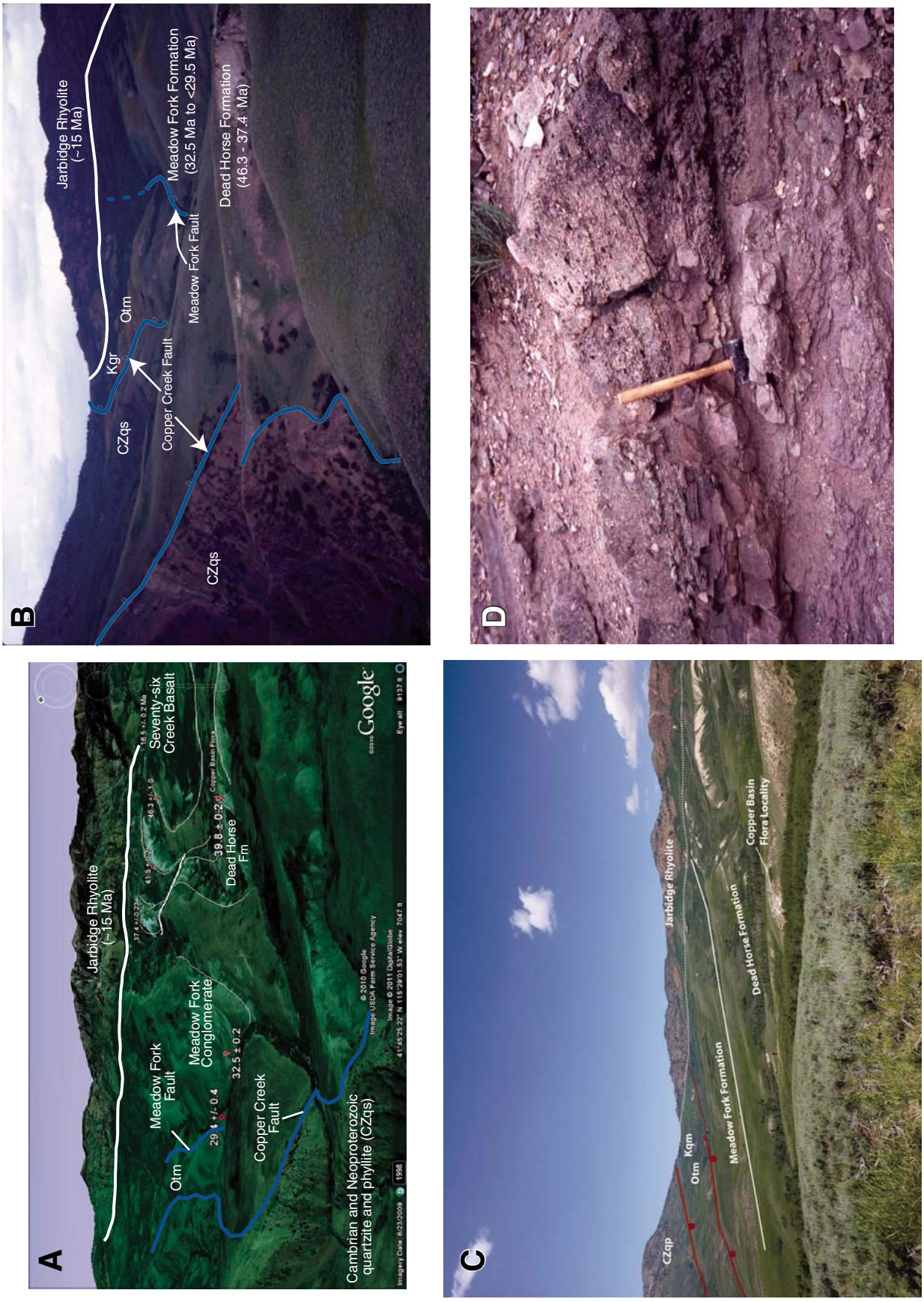
A
Jarbidge Rhyolite (~15 Ma)
Meadow Fork Fault
Meadow Fork Conglomerate
Otm
29.4 +/- 0.4
32.5 ± 0.2
Copper Creek Fault
Cambrian and Neoproterozoic quartzite and phyllite (CZqs)
39.8 ± 0.2
Dead Horse Fm
Seventy-six Creek Basalt
Google
B
Jarbidge Rhyolite (~15 Ma)
Kgr
Otm
CZqs
Copper Creek Fault
Meadow Fork Fault
Meadow Fork Formation (32.5 Ma to <29.5 Ma)
Dead Horse Formation (46.3 - 37.4 Ma)
CZqs
C
Jarbidge Rhyolite
Copper Basin Flora Locality
Dead Horse Formation
Meadow Fork Formation
Kqm
Otm
CZqp
D

accumulated in a narrow, northeast-trending, fault-bounded basin because of its coarse clasts and the fact that both it and the Dead Horse Formation wedge out abruptly. This formation contains rare, probably distally sourced pyroclastic-fall tuffs dated at 32.5 ± 0.2 Ma and 29.4 ± 0.4 Ma near the base and in the middle of the sequence, respectively (Table 1). These dates indicate a ca. 5 Ma hiatus in basin filling and presumably in normal faulting (Fig. 9). Both formations were subsequently tilted ~25° toward 220°. The tilted strata are intruded by 16.5 Ma basalt, and the tilted strata, the basalt, and the bounding Meadow Fork fault to the west are overlain by ca. 16 Ma Jarbidge Rhyolite. Although buried by Quaternary landslide deposits, the contact between flat-lying rhyolite and tilted Eocene-Oligocene deposits and the change of underlying strata from Dead Horse Formation northward to Meadow Fork Formation leave little doubt that the contact is an angular unconformity. Moreover, the Jarbidge Rhyolite rests nonconformably on lower plate rocks of the Coffeepot stock north and west of Copper Basin, clearly implying that the rhyolite postdated the tectonic juxtaposition of hanging wall and footwall rocks.

Despite the above relationships, Eocene and middle Miocene strata in the Jarbidge Wilderness area farther east are broadly concordant. Thus the angular discordance between Eocene and Middle Miocene strata appears to be localized along the Copper Creek fault system. A steep, west-dipping normal fault in the Bruneau Valley west of Copper Mountain cuts and rotates the Jarbidge Rhyolite and other Miocene rocks and must be Miocene in age. Taken together, these relationships imply an extensional history resembling that illustrated in the retrodeformed cross sections shown in Figure 8.

$^{40}Ar/^{39}Ar$ K-feldspar and (U-Th)/He apatite ages from lower plate rocks further constrain the progression of extensional unroofing outlined above (McGrew et al., 2007). A boulder of quartz monzonite collected from the Meadow Fork Formation documents that the footwall clast cooled through (U-Th)/He apatite closure (nominally 70 °C) by 43.0 ± 2.1 Ma followed by exhumation to the surface, erosion and redeposition in the adjoining basin before 29.5 Ma. Similarly, granitoid samples from the structurally highest, western part of the lower plate yield (U-Th)/He apatite cooling ages of 40.9–42.1 Ma, consistent with Eocene unroofing of these rocks as illustrated in Figure 8A. In addition, the structurally deeper eastern part of the range yields (U-Th)/He zircon ages of 46.1 and 53.7 Ma, and K-feldspar multi-diffusion domain modeling suggests that final cooling began in the same 40–45 Ma time frame. Finally, granitic rocks from the intermediate fault slice between the Copper Creek and Meadow Fork faults yield a (U-Th)/He apatite cooling age of 32.6 ± 2 Ma. This suggests that cooling and exhumation of the fault slice immediately beneath the Meadow Fork fault probably did not occur until the Oligocene and was approximately synchronous with the second pulse of extension recorded by the deposition of the Meadow Fork Formation.

A potentially surprising aspect of the relationships at Copper Basin is the absence of a growth fault relationship, i.e., fanning of dips forming angular unconformities between the Eocene and Oligocene strata. However, the absence of such a relationship does not necessarily preclude syntectonic deposition. Rather, it could merely indicate that during the initial phases of extension the proximal part of the hanging wall immediately adjacent to the fault subsided with little or no rotation and hence without developing a growth faulting relationship. Instead, most of the rotation must have occurred during the closing phases of slip on the bounding normal fault. This progression would require that the initial fault geometry was relatively planar down to mid-crustal depths (6–10 km), at which depth the fault must have become increasingly listric. Under these conditions, rotation of the proximal part of the hanging wall would not be expected to occur until it was translated down against the lower-angle part of the listric fault surface.

Taken together, currently available evidence from Copper Basin indicates that extension on the adjacent fault systems must have initiated with an early pulse of normal faulting in the late Eocene, followed by a lull during the early Oligocene, and then a pulse of extension in the late Oligocene. Extension on the Copper Creek fault system must have been largely completed before the Miocene based on: (1) (U-Th)/He apatite cooling ages no younger than 27.0 Ma in the lower plate from the footwall of the fault, (2) appearance of footwall clasts in syntectonic fanglomerate deposits by 32.5 Ma, and (3) a probable angular unconformity

Figure 9. (A) Annotated oblique northeast Google Earth view of Copper Basin in north central Elko County. The basin is bounded to the west by two subparallel, SE-dipping normal faults, with Neoproterozoic to Lower Cambrian quartzite and phyllite in the footwall of the lower, Copper Creek fault, and inferred Middle Cambrian to Ordovician marble and calc-silicate rock (Tennessee Mountain Formation, Otm) in the aureole of a Late Cretaceous pluton between the Copper Creek and Meadow Fork faults. Overlying both faults is the Eocene Dead Horse Formation and conformably overlying Oligocene Meadow Fork Formation, both of which are equally tilted ~25° NW. Tuffs in the Dead Horse Formation are dated between 46.3 ± 1.0 Ma and 37.4 ± 0.2 Ma near the top of the sequence (Table 1). Lacustrine strata preserving mixed deciduous and coniferous leaf fossils lie immediately above a tuff with an age of 39.8 ± 0.2 Ma. The age of the overlying Meadow Fork Formation is constrained by ages of 32.5 ± 0.2 Ma and 29.3 ± 0.4 Ma on pyroclastic-fall tuffs near the base and middle of the sequence, respectively. The sequence is intruded by hypabyssal, plagioclase-phyric basalt with an age of 16.5 ± 0.2 Ma, and relatively flat-lying Jarbidge Rhyolite (ca. 15.5 Ma) appears to overlie the entire assemblage with angular unconformity. (B) View NNE along strike of the Copper Creek normal fault system. (C) View north of white Eocene pyroclastic-fall deposits (Dead Horse Formation, Tdh) forming NW-dipping beds below gently dipping middle Miocene Jarbidge Rhyolite (Tjr) in Copper Basin. Note the apparent angular unconformity between the Eocene and Miocene units, although the contact is covered by Quaternary landslide and colluvial deposit. (Photo by A.J. McGrew.) (D) Typical outcrop character of Meadow Fork conglomerate. The base of the Meadow Fork Formation is marked by the first appearance of abundant footwall clasts, including quartzite, calc-silicate rock, and granitic clasts that strongly resemble the Cretaceous Coffeepot quartz monzonite.

between west-tilted Oligocene rocks and overlying middle Miocene Jarbidge Rhyolite. Nevertheless, more widely distributed normal faults with substantial displacement (probably ≥1 km on the Bruneau Valley fault west of Copper Mountain) cut, offset and rotate the Jarbidge Rhyolite, documenting significant middle Miocene or later extension.

Evidence from Miocene Basins and Thermochronology (J.P. Colgan)

Based on a synthesis of new and existing data covering an area from the East Range to the Ruby Mountains, Colgan and Henry (2009) advanced the hypothesis that—rather than a quasi-continuous process from the Eocene to the present—Basin and Range extension in north-central Nevada took place primarily during a relatively brief interval in the Miocene that began ca. 17–16 Ma and was over by 12–10 Ma, following a period of quiescence from ca. 35–17 Ma during which little or no deformation, deposition, and volcanism took place.

Primary lines of evidence for this interpretation include: (1) the lack of Tertiary rocks dating from ca. 35 Ma to 17 Ma, which indicates a period of little or no surficial deformation and volcanism in the Oligocene and early Miocene; (2) the age, composition, and distribution of Miocene sedimentary rocks (Humboldt Formation and age-equivalent units), which were deposited over a very wide area beginning at essentially the same time (17–16 Ma) and consist of coarse material shed from rising, fault-bounded blocks into nearby basins; and (3) apatite fission-track and (U-Th)/He data from exhumed footwall blocks in several ranges, which document rapid cooling beginning ca. 17–15 Ma. Rapid extension during this specific time window has been documented across nearly the entire modern extent of the northern Basin and Range province and is thus a province-wide phenomenon not limited to northeastern Nevada.

In northeastern and north-central Nevada, normal faults and sedimentary basins formed during the middle Miocene are cross-cut by distinctly younger normal faults that are high-angle, much more widely spaced, and represent very minor horizontal extension. The major east-dipping normal faults that bound the east sides of the Ruby Mountains and East Humboldt Ranges (Day 1) are examples of this generation of structures. The onset of this faulting is younger than 10 Ma but otherwise poorly constrained. These high-angle faults have Quaternary slip and one, the "Clover Hill fault," observable along our route to Stop 1-4, slipped on 21 February 2008, yielding a M_w 6.0 earthquake, which did not break the surface but did significant damage to the town of Wells (dePolo et al., 2011).

Summary of Observations: Cenozoic Extension

All authors agree that:

(1) The record of deep-crustal cooling and decompression between the Late Cretaceous and early Miocene implies substantial, but incomplete unroofing of deep-crustal rocks exposed in the RMEH, but whether this unroofing was tied to simultaneous major extension at shallower crustal levels is uncertain.

(2) Extension occurred in the Eocene, but its distribution, amount, and style are uncertain. Eocene extension may have been widespread over northeastern Nevada or more narrowly focused on a few well-developed systems such as the RMEH. This episode produced small basins, thin sedimentary deposits, and mostly small stratal tilts. Whether these differences compared to Miocene extension reflect different magnitude or different style of extension is particularly uncertain.

(3) The record of Oligocene volcanism, sedimentation, and surficial extension is minimally preserved at best and may be restricted to just a few isolated localities such as Copper Basin. Whether this implies that Oligocene extension was largely absent, restricted to a particularly narrow region, or proceeded under a fundamentally different tectonic regime that may not have left a clear surficial record is unknown.

(4) Extension beginning in the middle Miocene was widespread throughout northeastern Nevada, and indeed, across the entire northern Basin and Range province. The magnitude of extension varied across the region, but, where large, this episode generally produced large basins, thick sedimentary deposits, and large stratal tilts.

FIELD TRIP GUIDE

Day 1. Northern East Humboldt Range and the Secret Creek Gorge Area, Northern Ruby Mountains, Nevada

Overview of the Ruby Mountains–East Humboldt Range (RMEH) Core Complex

The first part of this field excursion focuses on field relationships at a variety of structural levels in the core complex as exposed at its northern end in the East Humboldt Range (Fig. 10). The Tertiary extensional architecture of the RMEH consists of two structural tiers (Sullivan and Snoke, 2007). The upper tier consists of non-metamorphosed to weakly metamorphosed, brittlely attenuated stratified rocks. These rocks range in age from late Paleozoic to Miocene and lie above the frictional/brittle, normal-sense, Ruby–East Humboldt detachment fault. The uppermost part of the lower structural tier is a km-thick, west-rooted, Tertiary mylonitic shear zone that passes down into a "metamorphic infrastructure" (Armstrong and Hansen, 1966).

The evolution of the Ruby–East Humboldt detachment fault system and its relationship to the mid-Tertiary mylonitic shear zone of the lower structural tier have not been completely deciphered despite many detailed studies of this plastic-to-brittle fault/shear-zone system (Hacker et al., 1990; Hurlow et al., 1991; Mueller and Snoke, 1993b; MacCready, 1996; McGrew and Casey, 1993; Colgan et al., 2010; Haines and van der Pluijm, 2010). Virtually all of the brittle deformation associated with the exposed fault system overprints and therefore postdates the mid-Tertiary mylonitic shear zone. Thermobarometric data from mylonitic pelitic schists indicate a P-T of 3.1–3.7 kbar and 580–620 °C (Hurlow et al., 1991)—physical conditions well beyond the onset of quartz and feldspar plasticity (Scholz, 1990).

Thermochronological data indicate that mylonites were significantly cooler than 300 °C by the early Miocene (Dallmeyer et al., 1986; Dokka et al., 1986; McGrew and Snee, 1994), and middle to upper Miocene rocks locally occur in the hanging wall of the detachment system (Snoke et al., 1984; Mueller and Snoke, 1993b; Fig. 10). Finally, although the bulk of the thermochronologic and radiometric data suggest that mylonitization occurred in the time interval of ca. 29–21.5 Ma (Wright and Snoke, 1993), some thermochronological data and field relationships suggest that Eocene mylonitization may be related to an earlier movement history along the shear zone that was strongly overprinted by late Oligocene mylonitization (Mueller and Snoke, 1993b; Wright and Snoke, 1993; McGrew and Snee, 1994; Snoke et al., 1997; Howard, 2003).

Stops 1-1 through 1-3 are along or accessed from Nevada Highway 231 (Angel Lake Highway). Take the west Wells exit from I-80, turn south onto Humboldt Avenue, then west on the Angel Lake Highway. Drive ~4.6 mi to Stop 1-1.

Note: All locations are in UTM, NAD27.

Stop 1-1. Overview of the Northern East Humboldt Range and Well-Exposed, Neogene Low-Angle Normal Fault in Roadcut (Figs. 10, 11)

(666240 4547445, Welcome 7.5′ quadrangle)

The following description is modified from Stop 7 of Mueller and Snoke (1993b) and Stop 2-1 of Snoke et al. (1997). Pull off road to the right into large parking space.

From this locality, there is an excellent view westward of the high country of the northern East Humboldt Range as well as the tree-covered forerange and low-lying foothills. The high-country is underlain by amphibolite-facies metamorphic rocks and is part of the high-grade footwall of the East Humboldt metamorphic core complex (McGrew, 1992; McGrew et al., 2000). The forerange is underlain by unmetamorphosed upper Paleozoic sedimentary rocks, and the low foothills expose Tertiary sedimentary and volcanic rocks (Fig. 10). These Paleozoic and Tertiary rocks constitute part of the hanging-wall sequence of the East Humboldt Range core complex. The East Humboldt plastic-to-brittle shear zone/detachment fault system originally separated these disparate crustal levels before being offset by late, high-angle normal faults (Mueller and Snoke, 1993a).

A principal feature of the metamorphic terrane is the basement-cored, southward-closing, Winchell Lake fold-nappe (Lush et al., 1988; McGrew, 1992; Fig. 5A). Chimney Rock, a prominent isolated peak (at about azimuth 235°), is composed of orthogneiss and paragneiss that form the core of this large-scale recumbent fold. The tree-covered forerange consists chiefly of Pennsylvanian and Permian carbonate rocks (Ely Limestone, Pequop Formation, Murdock Mountain Formation), but also includes Pennsylvanian and Mississippian Diamond Peak Formation. A prominent high-angle normal fault separates the Paleozoic rocks from the Tertiary strata. Reddish-brown–weathering siliceous breccia (so-called jasperoid) crops out locally along the contact (e.g., at ~240°). Prominent outcrops in the low-lying Tertiary terrane are lens-like masses of megabreccia derived from middle Paleozoic carbonate rocks (Stop 1-2). Finally, rhyolite porphyry of the Willow Creek complex (Jarbidge Rhyolite type) forms an isolated body along the range front at about azimuth 205°, and a prominent mass of rhyolite is at ~300°.

A low-angle normal fault exposed in the west roadcut (Fig. 5D) immediately north of the pull-out separates steeply dipping Miocene fanglomerate of the hanging wall from a footwall of platy marble representing Ordovician and/or Cambrian strata intruded by pegmatitic leucogranite. Red gouge separates the two units, and the top of the marble is brecciated. As the fault is traced northward along strike, a fault-bounded slice of metadolomite (Silurian and/or Devonian protolith) is present along this tectonic boundary (Fig. 10).

Optional traverse. If the high country is too snow-covered for direct field examination or not accessible, metamorphic rocks are exposed between our parking spot at Stop 1-1 and the ridgeline of Clover Hill. The flank of Clover Hill to the ridgeline is a dip slope consisting chiefly of flaggy, mylonitic quartzite (CZqs) of the footwall. Locally, scattered remnants of mylonitic, impure calcite marble structurally overlie the mylonitic quartzite. Eventually, we will reach kyanite-bearing pelitic schist (Neoproterozoic McCoy Creek Group—probably McCoy Creek G unit of Misch and Hazzard [1962]), which is characterized by a GRAIL metamorphic mineral assemblage: muscovite + biotite + plagioclase + garnet + kyanite + sillimanite + rutile + ilmenite (Hodges et al., 1992; Snoke, 1992). Based on textural relationships, sillimanite (i.e., fibrolite) is a late, minor mineral phase in the metapelitic schists exposed on Clover Hill. Compositionally banded granitic orthogneiss (inferred to be equivalent to the orthogneiss of Angel Lake; Stop 1-3) and associated paragneisses occur in a complexly folded and plastically faulted zone that forms the structurally deepest level exposed on Clover Hill below the ridgeline.

Return to vehicles and continue westward along the Angel Lake Highway for ~1.8 mi.

Stop 1-2. Megabreccia Deposits and Surrounding Tertiary Strata

(665075 4544850, Welcome 7.5′ quadrangle)

Please watch out for rattlesnakes, especially around the megabreccia outcrop. The following description is modified from Stop 8 of Mueller and Snoke (1993b) and Stop 2-2 of Snoke et al. (1997).

In the northern East Humboldt Range, the Humboldt Formation immediately above the middle to late Eocene volcanic and sedimentary rocks consists chiefly of thick-bedded conglomerate and sedimentary breccia (Fig. 11). These coarse-grained deposits disconformably overlie the Eocene rocks, and pebbles of volcanic rock derived from the older Tertiary deposits are a conspicuous component of the detritus near the base of the Humboldt Formation. However, this aspect quickly changes up section, and the Humboldt Formation typically consists nearly

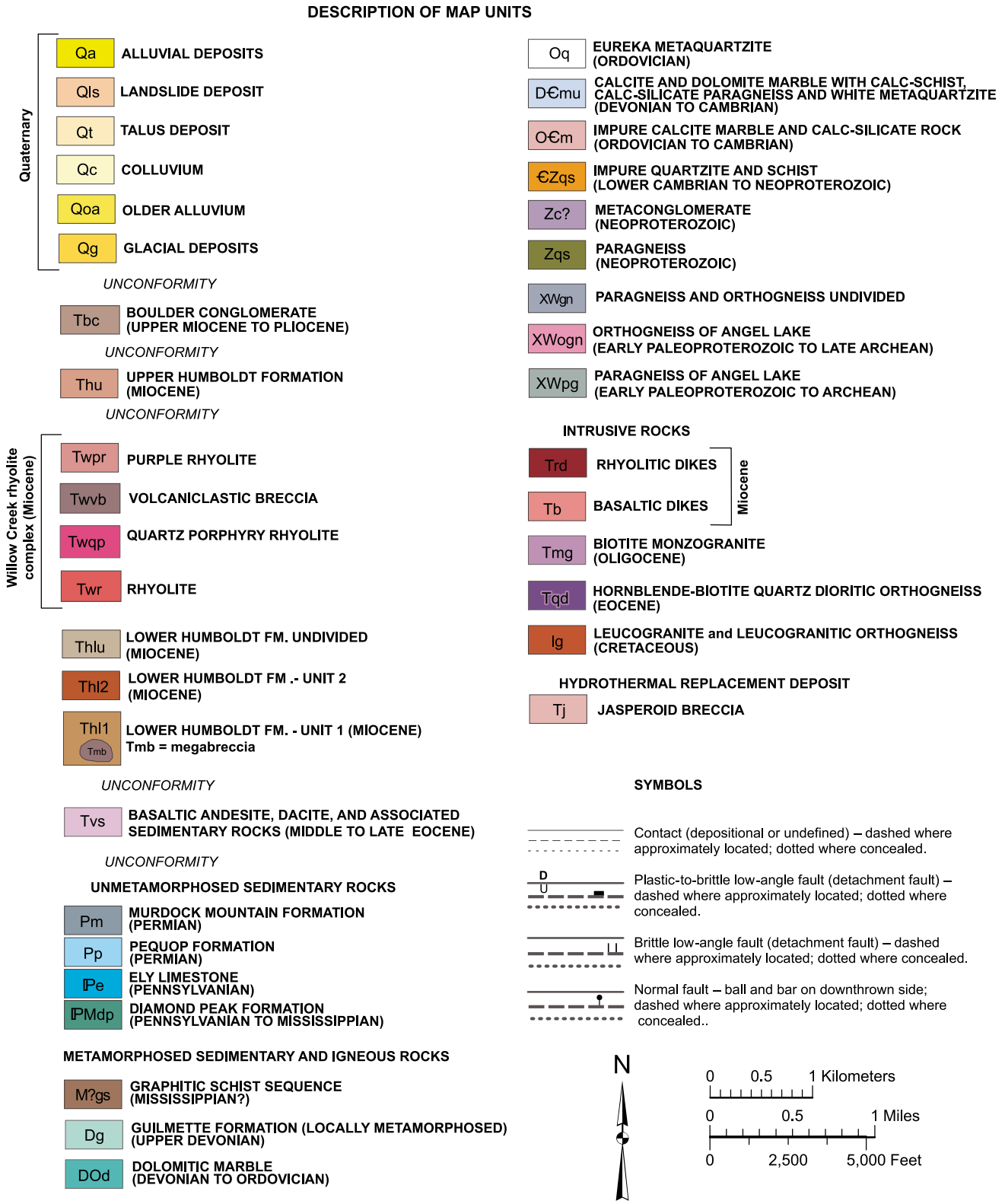

Figure 10. Geologic map of parts of the Welcome and Humboldt Peak 7.5′ quadrangles, East Humboldt Range–Clover Hill area, Elko County, Nevada (A.J. McGrew and A.W. Snoke, unpublished data). (*Continued on following page*.)

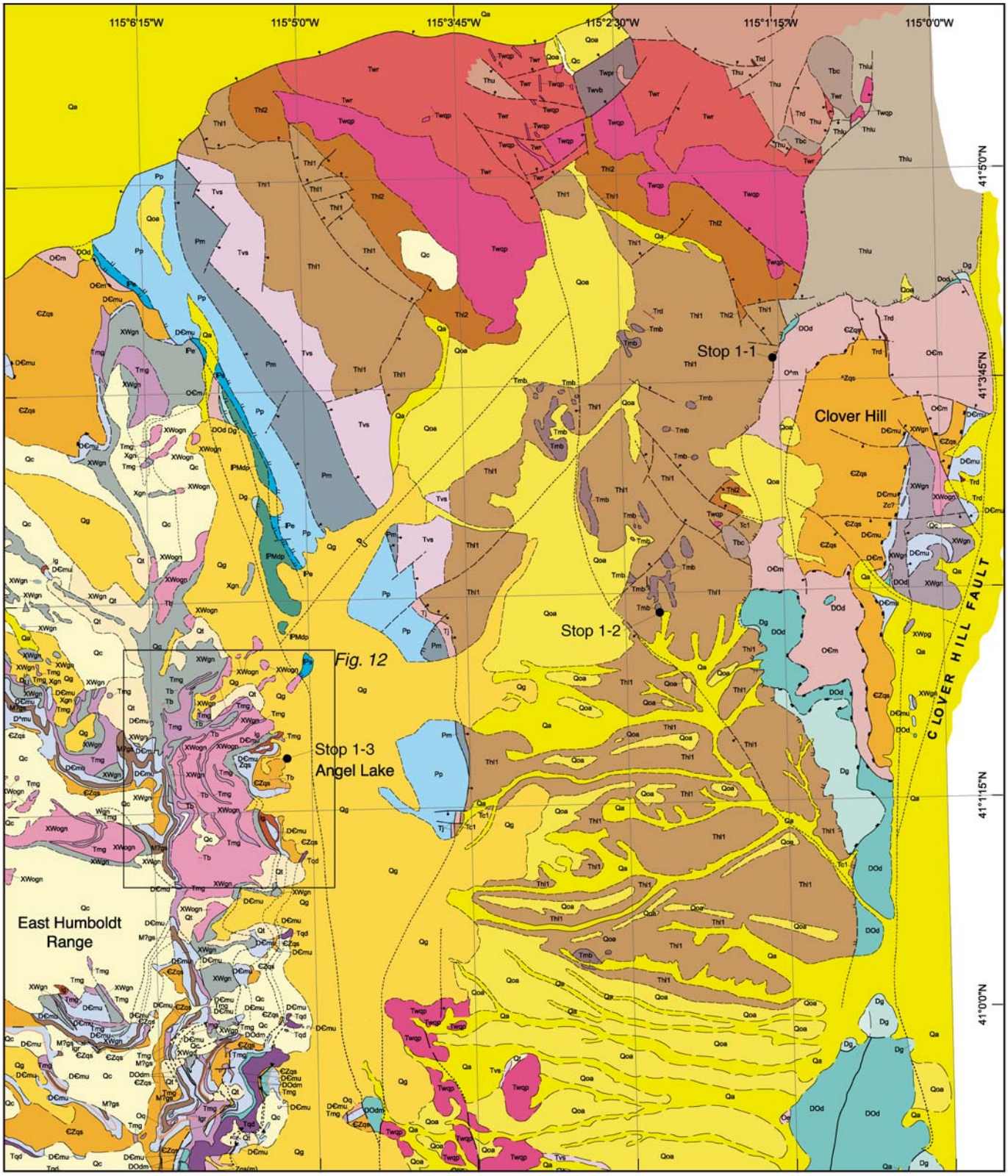

Figure 10 (*continued*).

exclusively of coarse detritus from Paleozoic formations, chiefly the Diamond Peak, Chainman, and Guilmette formations. Megabreccia derived from the Guilmette Formation forms discontinuous lenses in the Humboldt Formation; fine-grained lacustrine limestone, locally cherty, and minor sandstone is intercalated with these coarse deposits.

The roadcut immediately across from the parking place and those to the west provide a useful starting place to examine the megabreccia deposits and encasing beds that are all within what is here termed the lower Humboldt Formation (Thl) (Fig. 11). After briefly examining the roadcut exposing lacustrine limestone and conglomerate, walk west up the road (stratigraphically downward) toward the dark gray roadcuts of megabreccia derived from the Upper Devonian Guilmette Formation. This megabreccia is one of a group of lens-like masses within the Tertiary lower Humboldt Formation, and it both overlies and underlies lacustrine limestone and conglomerate. Therefore, this megabreccia lens, as well as the others, is encased in Tertiary deposits. After examining these roadcut exposures, walk north along the megabreccia lens examining the brecciated internal structure of the deposit. Despite pervasive brecciation, the megabreccia deposits locally display vestiges of relict bedding. If time is available, walk northeastward to another megabreccia lens composed of metadolomite and quartzite derived from Devonian and/or Silurian protoliths. Similar metadolomite and quartzite are exposed as bedrock in place on Clover Hill to the east.

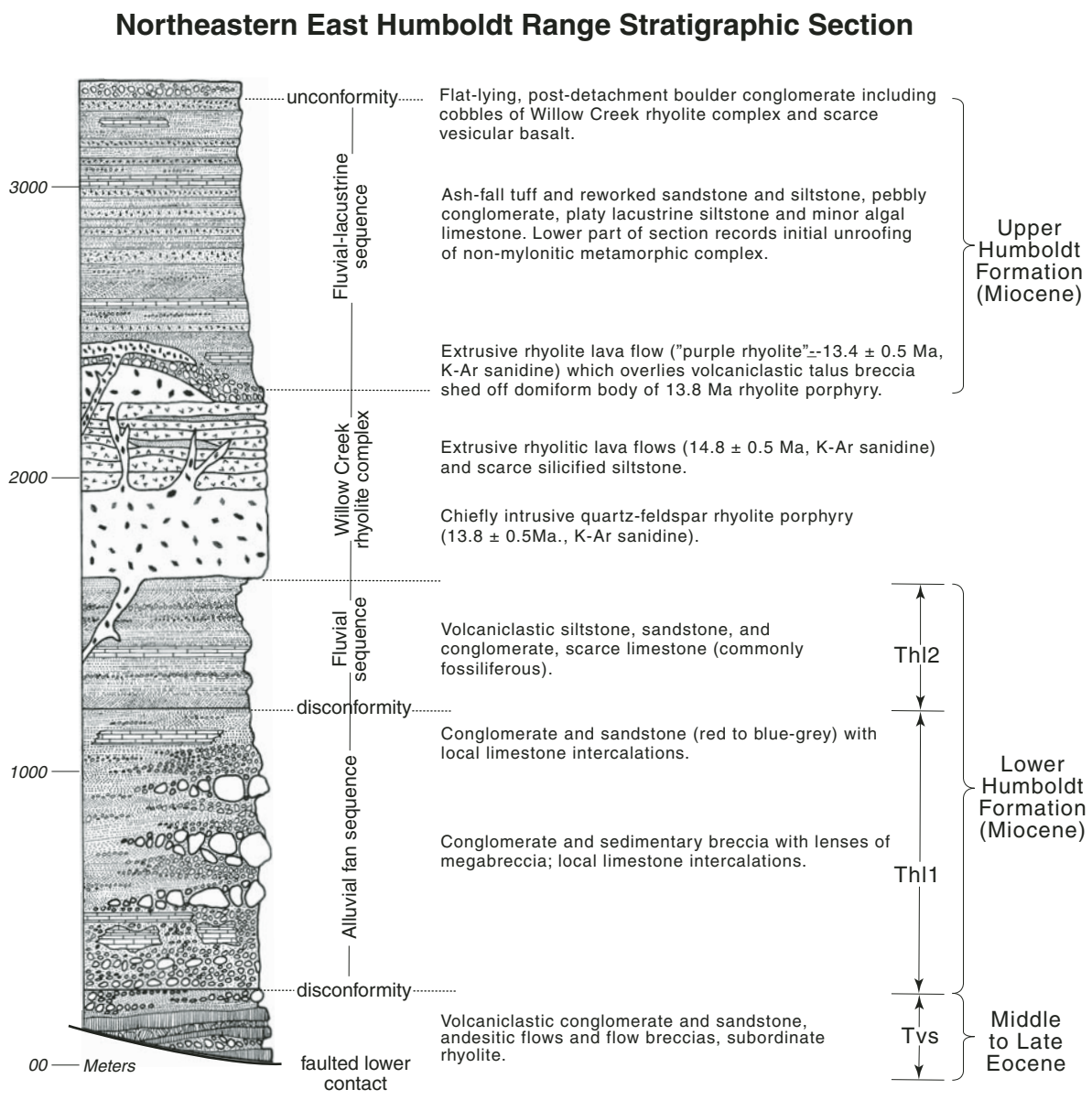

Figure 11. Generalized stratigraphic column of Tertiary rocks in the northeastern East Humboldt Range (modified from Mueller and Snoke, 1993b).

Continue westward on the Angel Lake Highway for ~5.3 mi to Angel Lake, where we hike a steep, 2.0 km traverse west of the lake with an elevation gain of 150 m (~500 ft) to ~2700 m (8860 ft).

Stop 1-3. Angel Lake
(661050 4543196, Welcome 7.5′ quadrangle)

Angel Lake cirque affords an opportunity to appraise the style and conditions of metamorphism and intrusive relationships as well as the deformational character of the high-grade infrastructure of the East Humboldt metamorphic core complex. The large-scale structural architecture of Angel Lake cirque is controlled by the Winchell Lake fold-nappe (Figs. 5A, 10, 12). Although the best exposures of the closure of this fold occur at Winchell Lake cirque ~7 km to the south, a transect from Angel Lake westward to the crest of Greys Peak would take the climber completely through both limbs of the fold. The Greys Peak fold, a map-scale parasitic fold on the upper limb of the Winchell Lake fold-nappe, is visible on the eastward-facing cliff face directly beneath Greys Peak.

Well-developed mylonitic fabrics overprint the fold-nappe in the upper part of the cirque, forming a thick zone of protomylonitic gneiss with WNW-directed kinematic indicators. These rocks represent the northern extent of the Ruby–East Humboldt mylonitic shear zone, which extends over 100 km to the south along the west flanks of both the East Humboldt Range and Ruby Mountains. The mylonitic rocks gradually give way to coarse-grained gneisses with increasing structural depth, and our transect is located entirely within the coarse-grained gneiss domain beneath the mylonitic shear zone. Shear-sense indicators, to the extent that they are observed in this zone, tend to be ESE-directed, antithetical to the overlying mylonitic zone (McGrew, 1992).

The transect climbs through the characteristic stratigraphic sequence on the lower limb of the fold-nappe from bottom to top (Fig. 12): (1) a quartzite and schist sequence of probable Early Cambrian to Neoproterozoic age (CZqs); (2) a thin sequence of calcite marble and calc-silicate gneiss that is probably Upper Cambrian and Ordovician (OCm); (3) a discontinuous, thin orthoquartzite layer (<2 m thick) inferred to correlate with the Ordovician Eureka Quartzite (Oq); (4) a sequence of dolomite marble correlated with Ordovician to Devonian dolomite (DOd); (5) more calcite marble, locally including isolated enclaves of intensely migmatized rusty-weathering graphitic schist (MD?mu); (6) a sequence of highly migmatized quartzofeldspathic to quartzitic paragneiss and schist (Zqs) inferred to correlate with Neoproterozoic (McCoy Creek Group) based on U-Pb SHRIMP analysis of detrital zircons (W.R. Premo, 2010, personal commun.); (7) a thick sequence of distinctively banded biotite monzogranitic orthogneiss of Angel Lake that is probably Archean or near-Archean (XWog; W.R. Premo, 2010, personal commun.; Lush et al., 1988; Premo et al., 2008; McGrew and Snoke, 2010; Premo et al., 2010); and (8) a sequence of strongly migmatitic biotite schist and immature, quartzofeldspathic paragneiss forming the core of the Winchell Lake fold-nappe in this location and probably Paleoproterozoic or latest Archean age (XWpg) based on U-Pb SHRIMP analysis of detrital and metamorphic zircons (W.R. Premo, 2010, personal commun.). The same sequence is present in reverse order on the upper limb of the fold-nappe below Greys Peak. The contact between inferred middle to upper Paleozoic marble (MD?mu) and Neoproterozoic paragneiss (Zqs), must be a pre-folding, pre-metamorphic fault. The contact between Neoproterozoic McCoy Creek Group (Zqs) and Archean orthogneiss (XWog) could be either another pre-metamorphic fault or an unconformity. The contact between Archean orthogneiss and paragneiss (XWpg) could be unconformable, intrusive, or tectonic.

Although the oldest rocks occupy the core of the Winchell Lake fold-nappe, the stratigraphic facing direction of the miogeoclinal sequence is inward, not outward. Therefore it is unclear whether the Winchell Lake fold is anticlinal or synclinal. If synclinal, the Precambrian gneiss complex must have been inverted as it was thrust over the miogeoclinal rocks before folding. If anticlinal, before folding, the miogeoclinal rocks must have been inverted and faulted over the Neoproterozoic McCoy Creek Group, which itself overlays the Archean–Early Paleoproterozoic gneiss. Either reconstruction requires a complex, polydeformational history, although the synclinal interpretation may be easier to envision. Nevertheless, the slightly greater attenuation of the lower limb of the fold and the presence of both south- and north-vergent small-scale folds on the lower limb would seem to argue for an anticline as discussed below.

Small-scale folds occur throughout the transect, with hinge lines parallel to well-developed stretching lineations, showing an average orientation of 5°/295°. Similarly, the axial surfaces of small-scale folds are approximately parallel to foliation, with an average orientation of 270°/15°. Three-dimensional constraints indicate that the map-scale folds (i.e., the Greys Peak fold and Winchell Lake fold-nappe) show the same WNW trend as the smaller scale structures. However, there is considerable dispersion in the small-scale structural data at deep structural levels, and a cryptic, northerly trending lineation of uncertain age can be observed locally. In addition, whereas folds on the upper limb of the Winchell Lake fold-nappe verge systematically southward toward the hinge zone of the first-order structure, folds on the lower limb verge both northward and southward and commonly exhibit "refolded fold" geometries (Ramsey Type 3 interference patterns) (Fig. 5C). The simplest interpretation of these relationships would entail the overprinting of S-folds by Z-folds as they migrate from the upright to the overturned limb of the larger-scale structure as the fold-nappe grows in "tractor tread" fashion. If so, then the fold-nappe would be required to be anticlinal.

The most characteristic pelitic mineral assemblage at all structural levels in Angel Lake cirque is biotite + sillimanite + garnet + quartz + plagioclase ± K-feldspar ± chlorite ± muscovite ± rutile ± ilmenite. However, scarce relict subassemblages of kyanite + staurolite survive on the upper limb of the Winchell

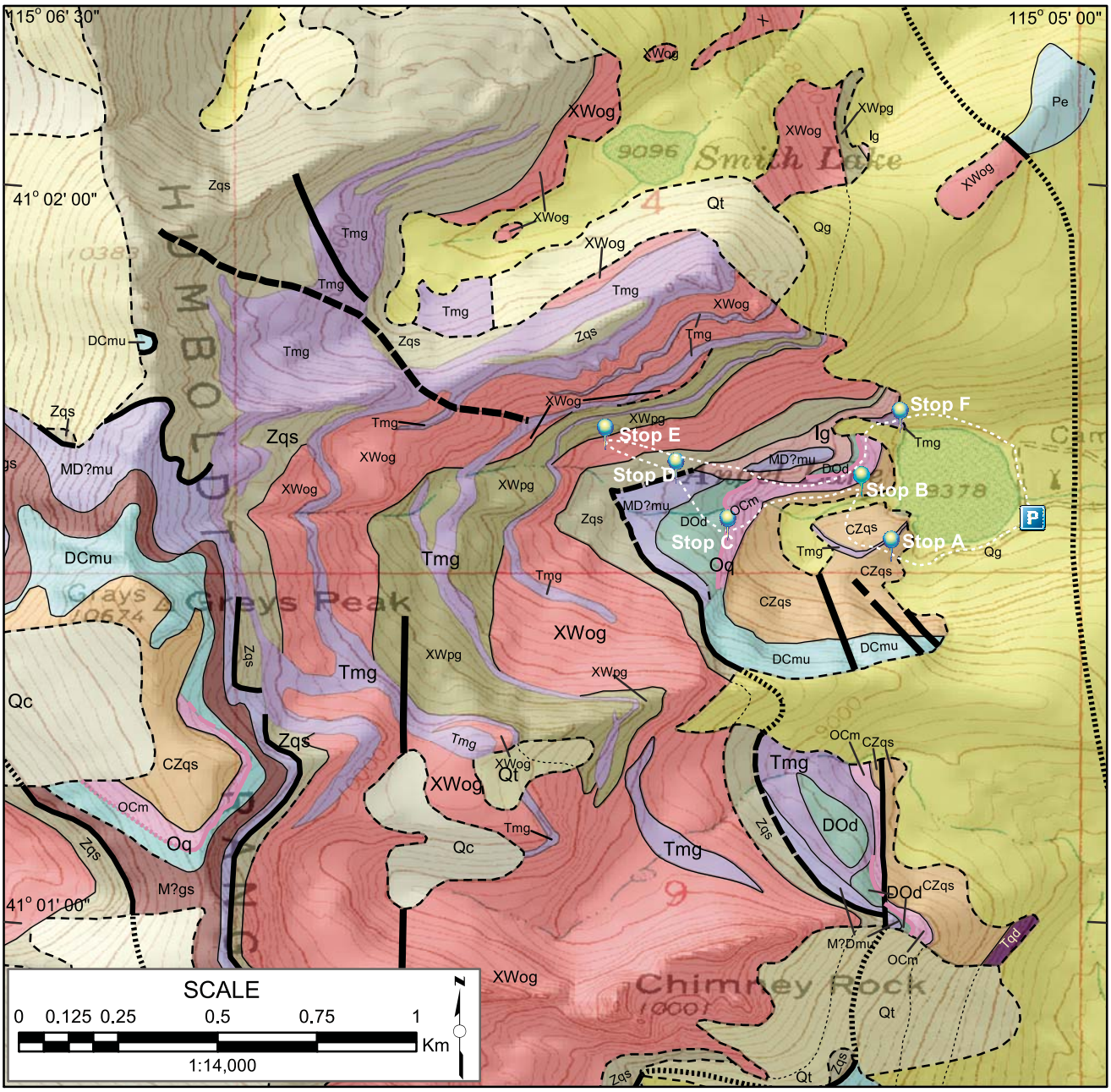

Contacts and Units Mapped as Lines

- Contact, definitely located
- dashed where approximately located
- dotted where buried or inferred
- Fault, definitely located
- dashed where approximately located
- dotted where buried or inferred
- Oq — Eureka Quartzite (Ordovician), dashed where approximately located, dotted where inferred.
- Basalt dike (Miocene), dashed where approximately located or inferred.

Lithologies

Surficial Deposits

- Qc — Colluvium (Holocene)
- Qt — Talus (Holocene)
- Qg — Glacial deposits, (Pleistocene)

Sedimentary Rocks

- Pe — Ely Formation (Pennsylvanian)
- PMdp — Diamond Peak Fm (Pennsylvanian to Mississippian)

Metamorphic and Igneous Rocks

- Tmg — Biotite monzogranitic orthogneiss (29 Ma)
- Tqd — Hbl biot quartz dioritic orthogneiss (40 Ma)
- Ig — Leucogranite (Late Cretaceous to Miocene)
- M?Dmu — Marble and schist, undivided (Miss.? to Devonian).
- M?gs — Graphitic schist, (Mississippian?)
- DCmu — Marble, calc-silicate rock and schist, undivided (Devonian? to Cambrian)
- DOd — Dolomite marble (Devonian to Ordovician)
- OCm — Calcite marble (Ordovician to Cambrian)
- CZqs — Quartzite and schist (Neoproterozoic and Cambrian)
- Zqs — Quartzite and schist (Neoproterozoic)
- XWog — Biotite monzogranitic orthogneiss (Early Paleo-proterozoic to Archean)
- XWpg — Migmatitic paragneiss (Early Paleoproterozoic to Archean)

Figure 12. Detailed geology of the Angel Lake area showing localities A–F (Stops A–F on map) for Stop 1-3 (modified from McGrew, 1992).

Lake fold-nappe. In addition, late stage muscovite and chlorite become increasingly prominent in the well-developed mylonitic rocks at higher structural levels. Five samples of schist from Angel Lake cirque yield internally consistent P-T estimates ranging from 630° ± 105 °C, 5.2 ± 1.2 kbar near the base of the cirque to 700° ± 125 °C, 8.3 ± 1.2 kbar on the ridge line in the northwest corner of the cirque (McGrew et al., 2000). Mark Peters analyzed an amphibolite collected at 2780 m (9120 ft) on the north side of the cirque that yielded the highest P-T estimate reported from the East Humboldt Range, 752° ± 138 °C, 9.3 ± 1.1 kbar. Thus, the Angel Lake area by itself yields much the same P-T trend as has been recognized for the whole East Humboldt Range, and we interpret this trend to represent re-equilibration at various stages along a decompressional P-T trajectory (Fig. 6; McGrew et al., 2000). The higher structural levels in Angel Lake cirque may have cooled and equilibrated at a relatively early stage in the unroofing history as indicated by an $^{40}Ar/^{39}Ar$ hornblende cooling age isochron of 51 ± 2 Ma at an elevation of 2890 m (9480 ft) on the north side of the cirque. On the other hand, samples from deeper structural levels may have experienced a slower cooling history that resulted in equilibration at a later stage because $^{40}Ar/^{39}Ar$ hornblende cooling ages are between ca. 30 and ca. 40 Ma at elevations beneath ~2775 m (9100 ft) (McGrew and Snee, 1994). Cooling of the northern East Humboldt Range through $^{40}Ar/^{39}Ar$ muscovite and biotite closure temperatures (nominally 350 °C and 280 °C, respectively) occurred by ca. 21.5 Ma, presumably due to exhumation along the RMEH mylonitic shear zone (McGrew and Snee, 1994).

Localities A–F below (Fig. 12) mark our planned transect through the lower part of Angel Lake cirque. As snow often lingers deep in the cirque until well into June, we may have to modify this plan depending on conditions.

Locality A. Follow the well-developed path around the south side of the lake to the low bedrock hill labeled "A" on the geologic map (Fig. 12). This locality exposes the inferred Neoproterozoic and Cambrian quartzite and schist (Zqs) at the deepest structural levels on the lower limb of the fold-nappe.

The East Humboldt Range is permeated by intrusive rocks of various ages and compositions, particularly abundant leucogranite at this deep structural level. We interpret at least four generations of leucogranitic intrusion based on cross-cutting relationships. In addition to the leucogranites, sheets of biotite monzogranitic orthogneiss are abundant throughout the RMEH and have yielded U-Pb zircon ages of ca. 29 Ma in many locations, including one at the northwest corner of Angel Lake (locality F) (Wright and Snoke, 1993). Consequently, these monzogranitic sheets are useful gauges for deciphering the structural chronology. The biotite monzogranites cut older generations of leucogranite, but some leucogranite either cuts or intermingles with the monzogranites. At higher structural levels, mylonitic fabrics clearly overprint the monzogranites, providing a crucial constraint on the age of mylonitic deformation. Steeply dipping, amygdaloidal basalt dikes that occupy three deep clefts through the south wall of the cirque were the final phase in the intrusive history of the East Humboldt Range. The end of one of these amygdaloidal basalt dikes can be inspected near this locality. Similar dikes yield approximate ages of 17–14 Ma elsewhere in the Ruby Mountains and East Humboldt Range, providing a younger limit on the age of plastic deformation (Snoke, 1980; Hudec, 1992).

Locality B. Continue over and around the small hill on the southwest side of the lake and cross the stream to point "B" on the map (Fig. 12). The rocks near the base of the slope form a particularly diverse and structurally complex paragneiss sequence. Can you find any amphibolite boudins near here? Normally, amphibolite bodies in the East Humboldt Range are found only in the older Precambrian rocks forming the central part of the cirque, where they probably represent metamorphosed mafic bodies that were presumably intruded before deposition of the upper part of the McCoy Creek Group and the overlying Prospect Mountain Quartzite. However, here one or two amphibolite bodies occur in the inferred Cambrian and/or Neoproterozoic quartzite and schist sequence. The age of the strata at this locality is constrained by anomalously high $\delta^{13}C$ values in the thin marble layers that are interdigitated with the quartzite and schist. As discussed in detail by Peters and Wickham (1992) and Wickham and Peters (1992), the high $\delta^{13}C$ values of these marble layers probably are original protolith values and indicate deposition during one of the Neoproterozoic carbon isotope excursions (e.g., Halverson et al., 2005). Accordingly, these rocks are inferred to correlate with the Neoproterozoic McCoy Creek Group.

Locality C. Contour along the foot of the slope to the base of the waterfall on the west side of the cirque; cross to the south side of the stream. The traverse works upward from the inferred Prospect Mountain Quartzite at the base through the lower calcite marble sequence (OCm) to a distinctive thin, white orthoquartzite approximately halfway up the waterfall. This is the Ordovician Eureka quartzite (Oq), and immediately above it is a relatively thick unit of dolomitic marble (DOd). Marble and calc-silicate assemblages here typically consist of calcite + diopside + quartz ± dolomite ± phlogopite ± plagioclase ± grossular ± scapolite ± K-feldspar ± sphene ± amphibole ± epidote. Peters and Wickham (1994) report that the diopside-bearing primary assemblages probably equilibrated at ≥6 kbar, 550–750 °C and likely record conditions during Late Cretaceous or early Cenozoic metamorphism. They also report a secondary subassemblage, amphibole + grossular + epidote, that records infiltration of water-rich fluids under a metamorphic regime that proceeded from high temperature (600–750 °C) to lower temperature (<525 °C) conditions. This event was probably related to Tertiary extension and associated magmatism. Above the dolomitic marble is more calcite marble, presumably of Devonian to Lower Mississippian age (MD?mu). At the top of the waterfall are a series of steep, ~1-m-thick, cross-cutting aplitic leucogranite dikes, probably the latest intrusive phase exposed in the East Humboldt Range other than the middle Miocene basaltic dikes.

Locality D. From the top of the waterfall, regroup at a ledge on the north side of the stream marking the contact with the overlying quartzite and schist sequence (Zqs). Detrital

zircon data show a well-developed spike of Grenville-aged zircons, with the youngest zircons being ca. 900 Ma (W.R. Premo, unpublished data). Accordingly, this paragneiss probably correlates with the Neoproterozoic McCoy Creek Group but contrasts with the quartzite and schist sequence at the base of the cirque in that it is dominated by impure, feldspathic and/or micaceous metapsammite with little "clean" quartzite and almost no marble, except for probable infolds of middle to upper Paleozoic marble directly adjacent to the contact. In addition, volumetrically small but relatively common and widespread, inferred originally mafic intrusions now form sheets and boudins of orthoamphibolite. Since these orthoamphibolite bodies are absent from the inferred Paleozoic metasedimentary rocks and rare in the inferred upper McCoy Creek Group rocks such as those described at Stop B, we infer that these rocks represent an older part of the McCoy Creek Group that may not be exposed elsewhere in the Great Basin.

The contact here between the McCoy Creek Group paragneiss and the underlying, inferred middle to upper Paleozoic marble sequence must be a pre-metamorphic, pre–Winchell Lake fold tectonic contact, and may be one of the major structures that buried the Paleozoic rocks to such great depth. Could the rocks at the contact be annealed mylonite? Can you recognize any possible vestiges of this inferred pre–Late Cretaceous shearing event?

Locality E. The traverse from locality D works through sporadic outcrops of lower McCoy Creek paragneiss to locality E on the north side of the cirque, where the contact with the banded biotite monzogranitic orthogneiss of Angel Lake (XWog) is exposed (Fig. 5B). Generally pale gray, this coarse-grained rock locally displays feldspar augen and is easily recognized by its distinctive striped appearance due to biotite segregation. As discussed in detail in the section on Precambrian, this unit was dated as Late Archean by Lush et al. (1988), but U-Pb SHRIMP analysis of zircons from a newly collected, more homogeneous and far less migmatized sample near the top of the orthogneiss complex west of Chimney Rock yielded an earliest Paleoproterozoic age (2450 ± 5 Ma; W.R. Premo, 2010, personal commun.). In addition, renewed field investigation of the gneiss complex of Angel Lake led to the delineation of a previously unmapped unit of impure, micaceous, feldspathic paragneiss and intensely migmatized biotite schist occupying the core of the Winchell Lake fold (XWpg; Fig. 12). Newly acquired U-Pb SHRIMP data on detrital zircons from this unit constrain it to be younger than ca. 2550 Ma (the age of the youngest detrital zircons) and older than a previously unrecognized ca. 1.8 Ga metamorphic event recorded by a few metamorphic zircons (W.R. Premo, 2010, personal commun.). So far we have not been able to decipher the original contact relationships between this newly recognized late Archean or Paleoproterozoic paragneiss and the orthogneiss that is folded around it, but if time and snow conditions permit, ambitious climbers may be able to climb to inspect this newly recognized map unit for themselves. Many important questions remain to be resolved about the only Archean or near-Archean rocks exposed in Nevada, and the collaboration with Wayne Premo is continuing to improve understanding of the history of these complicated exposures.

Locality F. From locality E we will work our way down the north side of the cirque to locality F at the northwest corner of Angel Lake. As you walk, try to decipher the relative age relationships between leucogranitic intrusions, and note the variation in leucogranite abundance depending on the host rock type. Some leucogranites are fully involved in folding whereas others cut folds. Outcrops at locality F consist predominantly of biotite monzogranitic and leucogranitic orthogneiss. The biotite monzogranite at this locality has yielded a U-Pb zircon age of 29 ± 0.5 Ma (Wright and Snoke, 1993). Is this sheet of monzogranite folded? Walk around the corner of the outcrop before you decide. Some monzogranitic sheets are clearly involved in folding, but others cut folds, and at map scale a number of monzogranitic bodies cut the Winchell Lake fold-nappe itself, lending credence to the interpretation that the Winchell Lake fold predates Oligocene deformation. However, the monzogranitic orthogneisses bear the same WNW-trending stretching lineations as the country rock, and at higher structural levels they are overprinted by mylonitic microstructures, thus documenting a post–29 Ma age for extensional deformation. It seems highly likely that older structures were profoundly transposed during Tertiary deformation, including the Winchell Lake fold-nappe itself.

From locality F, follow the trail around the north and east sides of Angel Lake to the parking lot. Return to Wells and drive ~28 mi south on U.S. Highway 93 from the east Wells exit off I-80. Turn west on Nevada Highway 229, which turns north after ~14 mi. Drive ~1 mi north to Stop 1-4.

Stop 1-4. Secret Creek Gorge, Northern Ruby Mountains
(647160 4525050, Soldier Peak 7.5' quadrangle)

Pull left into large parking space. From here we walk back up the road to Stop 1-4. The following description is modified from Stop 12 of Snoke et al. (1984) and Stop 3-1 of Snoke et al. (1997). *Please watch out for rattlesnakes in this area.*

This stop consists of a guided traverse through an anastomosing system of distinctive lithologic slices bounded by low-angle normal faults (perhaps best referred to as an extensional duplex structure; Fig. 13). The purpose of this traverse is to demonstrate the complex structural style characteristic of the low-angle fault complex, but also to develop the structural chronology between mylonitic deformation, low-angle normal faulting, and high-angle normal faulting. To facilitate the use of this guide, specific localities are designated A–F on Figure 13.

Locality A (roadcut along Nevada 229). Mylonitic, interlayered migmatitic schist and impure quartzite with subordinate orthogneiss, cut by numerous westward-dipping normal faults. Many of the normal faults are planar, but a few are clearly curviplanar. Associated with the westward-dipping normal faults are spectacular drag features as well as crushed zones and thin ultramylonitic to cataclastic layers along the fault planes. In addition, flaggy micaceous quartzites with conspicuous mica porphyroclasts ("mica fish") are useful indicators of the sense-of-shear in the mylonite zone. Other mesoscopic criteria useful

in the determination of sense-of-shear include asymmetric feldspar porphyroclasts, composite planar surfaces in pelitic schists (S-C-C′ fabric), and mesoscopic folds that deform the mylonitic foliation. Well-developed microstructural fabrics are also common in these mylonitic rocks (e.g., the mylonitic impure quartzites are classic examples of Type II S-C mylonites of Lister and Snoke, 1984). All of these criteria taken together indicate a top to the west-northwest sense-of-shear throughout the quartzite and schist unit in the northern Ruby Mountains and southwestern East Humboldt Range.

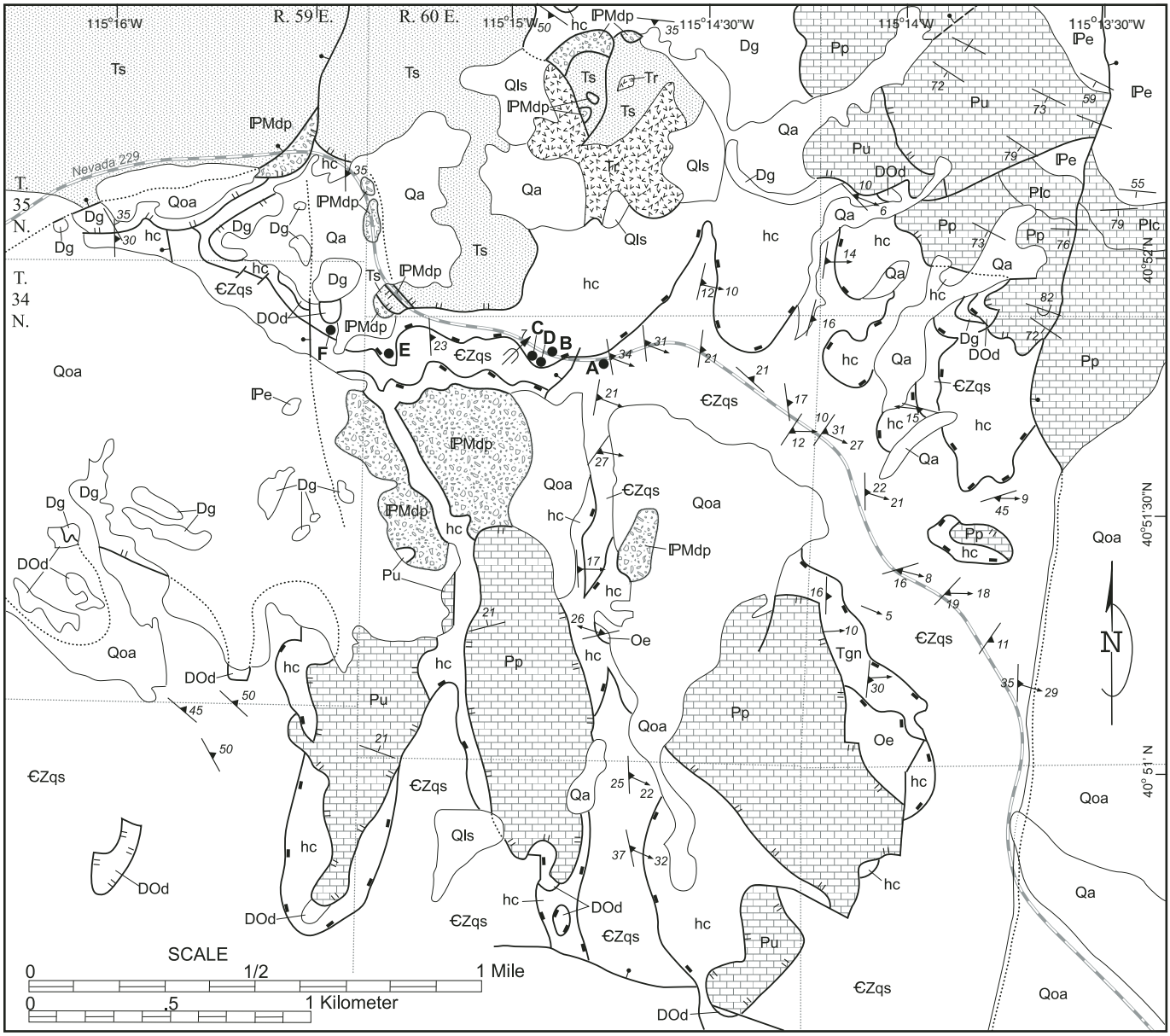

Figure 13. Geologic map of the Secret Creek gorge area, northern Ruby Mountains, Nevada (modified from Snoke et al., 1997). Qa—alluvium (Quaternary); Qoa—older alluvium (Quaternary); Qls—landslide deposits (Quaternary); Ts—sedimentary rocks (Miocene); Tr—rhyolite (middle Miocene); Tgn—granitic orthogneiss (Tertiary); Pp—Pequop Formation (Permian); Plc—limestone and conglomerate (Permian); Pu—Permian rocks undivided; Pe—Ely Limestone (Pennsylvanian); PMdp—Diamond Peak Formation (Pennsylvanian and Mississippian); Dg—Guilmette Formation (Devonian); DOd—metadolomite (Devonian to Ordovician); Oe—Eureka metaquartzite (Ordovician); hc—Horse Creek assemblage (metasedimentary and granitic rocks); CZqs—impure metaquartzite and schist (Cambrian and Neoproterozoic). Standard symbols for attitude of bedding or foliation, trend and plunge of lineation, hinge line of mesoscopic fold, geologic contacts, and normal faults (except double tick marks on the upper plate of brittle low-angle normal fault except double tick marks on the upper plate of brittle low-angle normal fault [detachment fault] and filled squares on upper plate of plastic-to-brittle low-angle normal fault). Faults are dotted where concealed. Localities A–F are field trip stops.

The mylonitic quartzites at this locality as well as other rock types in the Secret Creek gorge area were the subject of a stable isotope study by Fricke et al. (1992), which demonstrated the importance of meteoric water infiltration during mylonitization.

Locality B (roadcut exposure along Nevada 229, west of Locality A). We have crossed a low-angle normal fault that separates the overlying Horse Creek assemblage from the underlying quartzite and schist unit. The Horse Creek assemblage is diverse and includes impure calcite marble and calc-silicate gneiss and schist (inferred Ordovician and Cambrian protoliths), and mafic to felsic orthogneisses including a distinctive deformed biotite-hornblende mafic quartz diorite. Mylonitic rocks are ubiquitous and include spectacular calc-mylonite containing competent mineral grains and rock clasts. Many of the obvious folds deform the mylonitic foliation and display westward vergence. Folded boudins and dismembered folds are other manifestations of a complex strain history (inferred as progressive, non-coaxial deformation). Scarce sheath folds also occur in the Horse Creek assemblage.

Locality C (slope above old road bed). Folded mylonitic white quartzite in the Horse Creek assemblage. This west-vergent fold displays rotation of an earlier mylonitic lineation during late folding in the mylonitic shear zone.

Locality D (along the old road). Disharmonic west-vergent folds in the Horse Creek assemblage. Rock types include impure calcite marble with mafic pelitic layers, granodioritic augen gneiss, and white quartzite. Note how layer thickness controlled the amplitude and wavelength of the folds.

The traverse between localities D and E along the old road crosses the low-angle fault contact between the overlying Horse Creek assemblage and the underlying quartzite and schist unit several times. A secondary black ultramylonite is common along this contact (i.e., a ductile-brittle low-angle fault) where the mylonitic foliation in both the upper and lower plates is roughly subparallel. In other cases, where foliation in the upper plate is highly discordant to foliation in the lower plate, the contact appears to be a brittle low-angle normal fault that has perhaps soled into (i.e., reworked) the earlier ductile-brittle low-angle fault. Furthermore, steeper normal faults cut the Horse Creek plate.

Locality E. We are presently situated on the Horse Creek assemblage. The contact between the Horse Creek assemblage and underlying quartzite and schist unit can be seen in fine detail up canyon. The mapped low-angle fault contact is probably composite; parts of the contact are a low-angle, ductile-brittle fault and parts are younger, low-angle brittle normal faults that have soled into the older ductile-brittle fault.

Locality F. The slope above the old road crosses two low-angle normal faults. The lower fault (the main break in metamorphic grade and here the top of the mylonitic zone) separates the Horse Creek assemblage from a higher slice of low-grade metadolomite; the upper fault separates the metadolomite from a structurally higher slice of low-grade but fossiliferous Upper Devonian Guilmette Formation. At this locality, the Guilmette Formation is a medium gray, highly calcite-veined, low-grade metalimestone. A similar tectonic slice of Guilmette Formation exposed south of Secret Creek gorge yielded Late Devonian conodonts with color alteration index (CAI) = 5½, suggesting that the host rock reached 300–350 °C (A. Harris, 1982, written commun.).

At the top of the hill (i.e., the resistant gray exposures of Guilmette Formation), part of a roadcut that exposes dismembered Diamond Peak Formation can be seen to the east-southeast, across from where the vehicles are parked. This roadcut is topographically and structurally above your present position. Therefore, another low-angle fault must separate the Upper Devonian Guilmette Formation from the Mississippian and Pennsylvanian Diamond Peak Formation. Structurally above the roadcut, Miocene Humboldt Formation is also in low-angle fault contact with the underlying rocks of the Diamond Peak Formation as well as Horse Creek assemblage (Fig. 13). Haines and van der Pluijm (2010) used X-ray diffraction to characterize clay minerals in gouges related to low-angle and high-angle faults exposed along Nevada 229 and $^{40}Ar/^{39}Ar$ to date the clay minerals. A key locality in their study was the roadcut across from where the vehicles are parked (their locality Secret-2). Authigenic illite-rich illite/smectite in the gouges, including this locality, yielded ages of 11.6 ± 0.1 Ma, 12.3 ± 0.1 Ma, and <13.8 ± 0.2 Ma. Based on these ages, Haines and van der Pluijm (2010) concluded the last major period of activity along the low-angle faults (part of the detachment system) and a kinematically related high-angle fault was 13–11 Ma.

Upon completion of the traverse, please congregate in the parking area and examine the roadcut across from the vehicles. Return to Wells by continuing westward to the Halleck interchange and then eastward on I-80. Stop 1-4 can also be accessed by this return route.

Day 2. North Paleovalley and Copper Basin

In dry conditions, Copper Basin can be reached by taking Elko County Road 747 (the Charleston-Deeth Road) 42.7 mi north from I-80 at the Deeth exit (Nevada Highway 230) to the intersection with Elko County Road 746 at Charleston Reservoir (Stop 2-3 is in the low hills northwest of this junction). In poorer weather, take Nevada Highway 225 (the Mountain City Highway) ~53.6 mi north from Elko to Elko County Road 746. Take ECR 746 ~20.8 mi east to the intersection with ECR 747 at Charleston Reservoir. By either route, head north on the road to Jarbidge (Jarbidge-Charleston County Road; National Forest Development Road 062). Drive ~13.1 mi north to an unmarked track to west (626756 4622232), the start of an ~6 km traverse (round-trip; Fig. 14).

Stop 2-1. Copper Basin

The traverse leads westward along the south ridgeline of Copper Basin, which provides an excellent perspective of the geology of Copper Basin. Copper Basin is an ~25 km^2 area of Eocene ash-flow tuff and tuffaceous, partly lacustrine sedimentary rocks (the Dead Horse Formation) and Oligocene conglomerate (the Meadow Fork Formation) in the hanging wall of the

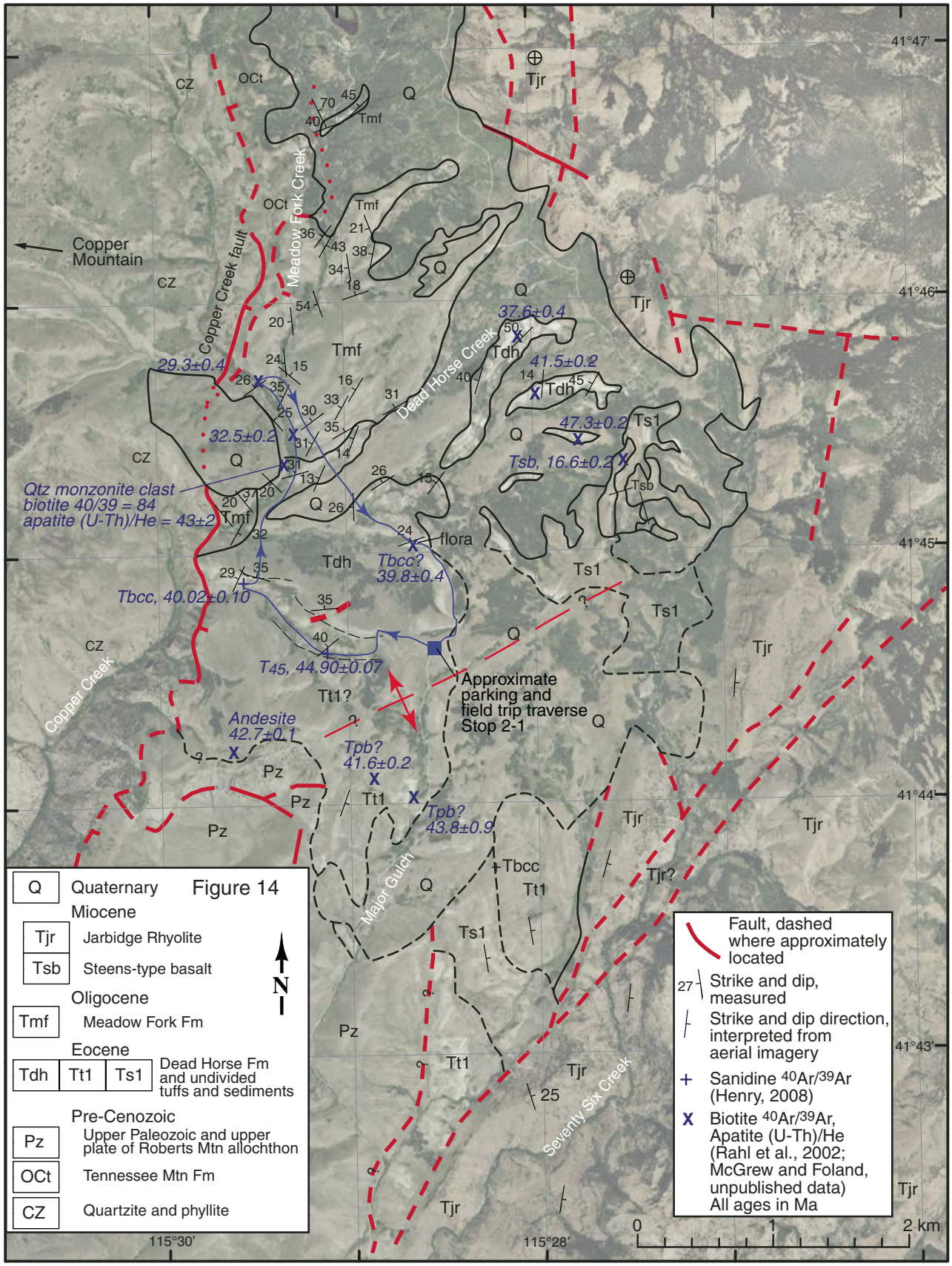

Figure 14. Simplified geologic map of Copper Basin (from Coats, 1964, 1987; Rahl et al., 2002; and this study). T45—45 Ma tuff; Tpb—plagioclase-biotite tuff; Tbcc—tuff of Big Cottonwood Canyon. See text for discussion and Figure 2 for location.

Copper Creek fault, a major east-dipping normal fault (Figs. 9, 14; Table 1; Coats, 1964; Axelrod, 1966a, 1966b; Rahl et al., 2002). In the northeastern part of the basin, coarsely plagioclase-phyric basalt dated at 16.5 ± 0.2 Ma intrudes the Dead Horse Formation, and middle Miocene Jarbidge Rhyolite overlies the Eocene-Oligocene rocks in what appears to be an angular unconformity (Fig. 9; Coats, 1964; Rahl et al., 2002).

The Dead Horse Formation is at least 800 m thick and consists of ash-flow tuff overlain by and interbedded with tuffaceous, lacustrine sedimentary rocks and lesser basal conglomerate and andesite. At least four ash-flow tuffs are exposed in the southern part of the Dead Horse Formation along the traverse: the 45 Ma tuff (625926 4622238), a plagioclase-biotite-hornblende tuff (626292 4622357), the ca. 41 Ma tuff of Coal Mine Canyon, and the 40 Ma tuff of Big Cottonwood Canyon (625304 4622726; Fig. 14; Henry, 2008). A channel along the ridgeline (625436 4622741) cuts into the tuff of Big Cottonwood Canyon and contains pebbles up to 4 cm in diameter of Paleozoic quartzite and chert and Tertiary volcanic rocks, mostly the tuff of Big Cottonwood Canyon. Paleozoic clasts are mostly well rounded, whereas Tertiary clasts are subrounded to subangular.

From the channel fill proceed west along the ridge to the Copper Creek fault (625010 4622587) and follow the fault northward to Copper Creek. Neoproterozoic to Lower Cambrian Prospect Mountain Quartzite crops out in the footwall. The hanging wall of the fault consists of Dead Horse Formation on the ridgeline, but a fault slice of Meadow Fork Formation overlies the fault in the valley. The Copper Creek fault has an average attitude of 025°/35°; average slickenlineations plunge 34° toward 123°, indicating nearly ideal dip-slip. The overlying strata are oriented on average 220°/24°, with both the Dead Horse and Meadow Fork Formations showing statistically identical dips. Restoring the Cenozoic strata to horizontal rotates the Copper Creek fault to 030°/58° (Fig. 8; Rahl et al., 2002). Based on this restoration, Rahl et al. (2002) estimated 8–12 km of displacement on the Copper Creek fault system, exhuming the Copper Mountains from a paleodepth of 11 ± 3 km as the net result of Eocene and Oligocene extension.

Good exposures of the contact between the Dead Horse Formation and the overlying Meadow Fork Formation are along Copper Creek at the mouth of Dead Horse Creek (625738 4623476) and of the lower Meadow Fork Formation for a few hundred meters north along Copper Creek from there. The Meadow Fork Formation is at least 600 m thick and consists of tuffaceous sedimentary rocks and coarse arkosic sandstone and conglomerate containing clasts of quartzite, marble, phyllite, and granitoids up to 1 m in diameter. Biotite $^{40}Ar/^{39}Ar$ dates on rare, interbedded pyroclastic-fall tuffs are 32.5 ± 0.2 Ma near the base and 29.3 ± 0.4 Ma in the upper middle part of the section (Fig. 14; Table 1).

Climb uphill toward the east and southeast to the Copper Basin Flora locality (626590 4622994), a mixed deciduous-coniferous flora discovered by Axelrod (1966a, 1966b) and deposited in a marginal lacustrine facies of the Copper Basin (Rigby et al., 2006). Paleoelevation estimates from the flora range from 1.1 km (Axelrod, 1966a, 1966b), to 2.0 ± 0.2 km (Wolfe et al., 1998), and to 2.8 ± 1.8 km (Chase et al., 1998). Current elevation of Copper Basin is ~2.1 km. The flora are in a thin (~1 m) horizon of light brown, organic-rich shale. Approximately 7–10 m beneath the shale are interbedded tuffaceous siltstone, sandstone (commonly in graded beds), and clast-supported conglomerate, consisting mostly of angular, 2–10-mm diameter volcanic clasts with subsidiary quartzite and phyllite in an ashy matrix. Less than 2 m below the base of the conglomerate is an ~6-m-thick, massive, white, fine-grained tuff with sparse small phenocrysts of biotite and feldspar. The tuff yields an $^{40}Ar/^{39}Ar$ age of 39.8 ± 0.2 Ma (Table 1), suggesting a possible correlation with the tuff of Big Cottonwood Canyon. If so, the massively bedded, cobble conglomerate filling a channel above that tuff is missing here, replaced by a few graded beds of tuffaceous pebble conglomerate.

This location provides a good view of the northern part of the Dead Horse Formation, which consists of lacustrine deposits containing a series of white, fine-grained pyroclastic-fall deposits. Although Rahl et al. (2002) reported that these pyroclastic-fall deposits overlay the ash-flow tuffs of the southern part of the basin, new $^{40}Ar/^{39}Ar$ dates indicate that the fall deposits overlap in age with the ash-flow tuffs (Fig. 14; Table 1). Moreover, the fall deposits appear to be along strike with the dated locations of the 45 Ma tuff and tuff of Big Cottonwood Canyon. A fall deposit near the base of the section yields a biotite plateau age of 47.3 ± 0.2 Ma that would make it the oldest known Eocene tuff in northeastern Nevada. An overlying tuff dated at 41.5 ± 0.2 Ma probably correlates with the plagioclase-biotite tuff, and the tuff just below the Copper Basin flora may correlate with the 40 Ma tuff of Big Cottonwood Canyon. The top of the Dead Horse Formation is marked by a pyroclastic-fall tuff dated at 37.6 ± 0.4 Ma (Rahl et al., 2002). Based on these data, A.J. McGrew interprets the fall deposits to have accumulated in a lake mostly contemporaneously with deposition of the terrestrial ash-flow tuffs.

In this better studied, northern part of the basin, the Dead Horse and Meadow Fork Formations mostly strike northeast and dip moderately northwest, although attitudes vary widely, indicating an angular unconformity with overlying Jarbidge Rhyolite (Fig. 14). Based only on examination of air photos and Google Earth images, the Eocene-Oligocene(?) rocks strike north and dip moderately to the east in the southeastern part of the basin. The Jarbidge Rhyolite appears to strike and dip the same way. We infer that steep, west-dipping Miocene faults cut and tilt all the rocks in the eastern part, resulting in a northeast-striking, extensional-accommodation anticline between the two differently dipping parts of the basin. This eastern tilt domain may be visible from the flora locality or from the parking area.

Climb back uphill to the vehicles and drive ~12 mi south toward Charleston Reservoir along the Jarbidge-Charleston Road.

Stop 2-2 (Optional). Jarbidge Rhyolite Lava Flow Margin

Please watch for rattlesnakes.

Drive south ~12 mi toward Charleston Reservoir along the Jarbidge-Charleston road. The hills to the east are the 45 Ma

tuff (0623727 4609661) and Jarbidge Rhyolite, while most of the sedimentary deposits to the west are tuffaceous sedimentary rocks (Humboldt Formation?; Coats, 1987). Approximately 1.5 mi north of the junction with Elko County Road 746 (at Charleston Reservoir), stop and park (0624540 4606261). The outcrops immediately east of the road provide an outstanding example of a rhyolite lava flow-top (carapace) breccia (Fig. 15A).

Jarbidge Rhyolite lavas typically contain 15%–40% smoky quartz and feldspar phenocrysts and are meta-to-peraluminous (~72–78 wt% SiO_2 and average TiO_2/MgO = 8.2). These and other chemical characteristics identify Jarbidge magmas as "A-type." The rhyolite breccia consists of abundant pebble to boulder-sized clasts of rhyolite vitrophyre, flow-banded stony rhyolite, and massive stony rhyolite. Vitrophyre boulders weather out from beneath the breccia in places; this is consistent with the breccia being the upper carapace of the flow. Callicoat (2010) interpreted this exposure to be the western margin of a Jarbidge Rhyolite lava flow.

The total volume of Jarbidge Rhyolite exposures in this region is estimated to be ~500 km^3, which is similar to the Central Plateau rhyolites in Yellowstone (Callicoat et al., 2010). However, unlike Yellowstone, no caldera-source appears present. Instead, Callicoat (2010) suggested that the Jarbidge magmatic system, although very large (total magma volumes equal or greater than 1500 km^3), was characterized by primarily effusive eruptions similar to other large volume silicic systems dominated by effusive volcanism (e.g., the Taylor Creek Rhyolite, New Mexico; the Badlands lava flow, Idaho). Jarbidge rhyolite lava flows between this location and Copper Basin, as well as flows farther north along the road, yield ages between ca. 16 and 15.5 Ma (Callicoat, 2010; Brueseke, unpublished data).

Stop 2-3. Charleston Reservoir Fluvial Megabreccia and Ash-Flow Tuff Relationships

Please watch for rattlesnakes.

Drive south to the Elko County Road 746–Jarbidge-Charleston Road junction and park in the open area east of the junction. Sagebrush-covered flats and low hills south, north, and west of the parking area are underlain by Cenozoic sedimentary strata and ash-flow tuffs (Fig. 15B). Coats (1987) mapped the ash-flow tuffs as part of a regionally widespread Eocene unit (Tt_1). The sediments are likely part of the younger Humboldt Formation. Massive outcrops adjacent to and east of the reservoir are Jarbidge Rhyolite lava flows (Callicoat, 2010).

Walk across the road(s) and head northwest toward the megabreccia outcrops on the small hill (Fig. 15B). Outcrops in the vicinity of Charleston Reservoir provide an outstanding view of a "dam-burst flood" megabreccia deposit, as well as overlying ash-flow tuff, and sedimentary deposits. Cook and Brueseke (2010) presented more detailed descriptions of the Charleston Reservoir deposits and used major and trace element geochemistry, in conjunction with published data, to correlate the tuffs to other Eocene tuffs in the region. Vitrophyric ash-flow tuff float (Tcm; Fig. 15B) may be apparent in the flat and slopes leading up to the megabreccia outcrop that forms the ridgeline. Geochemical analyses of the vitrophyre indicates that it is the Tuff of Coal Mine Canyon (Cook and Brueseke; 2010), which had not previously been identified in this region. Its presence here and to the north in Copper Basin provides evidence of a paleovalley intersecting the north paleovalley of Henry (2008) and is consistent with a source caldera located to the southwest.

The megabreccia exposure is ~4.5 m high (Fig. 15C). This deposit forms a resistant topographic high of semi-continuous outcrop between the two roads (Fig. 15B). Breccia clasts are angular to subrounded, pebble to boulder-sized, plagioclase-biotite tuff (Cook and Brueseke, 2010; Fig. 15D; 0624776 4604533). The matrix consists of medium to coarse tuffaceous sand and gravel and sparse, <1 cm fragments of Paleozoic limestone. Although this breccia resembles caldera mesobreccia, its location and contact relationships to adjacent units suggest that its origin was via dam-burst type flood events, like other paleovally megabreccias studied by Henry (2008). These occur after ash-flow tuff deposition blocks a drainage and the tuff "dam" catastrophically fails (Henry, 2008; see also Stop 3-1). Walk/scramble up through the exposure and continue in a northwest direction. For the next ~1/3 mi, plagioclase-biotite tuff boulders are sporadically exposed along the upper surface of the megabreccia.

After walking up and over a small rise, look for tuff of Coal Mine Canyon vitrophyre float in the topographic low (Cook and Brueseke, 2010; Fig. 15B; 0624468 4604778). This vitrophyre is chemically identical (thus stratigraphically equivalent), to the tuff of Coal Mine Canyon vitrophyre that crops out between the well-exposed megabreccia outcrops and the parking area (Cook and Brueseke, 2010). Cook and Brueseke (2010) suggest that this ash-flow tuff flowed down the same paleovalley as the plagioclase-biotite tuff that forms the megabreccia but flowed around and over the megabreccia. This paleovalley is interpreted to have extended to the north to Copper Basin, on the basis of a newly identified outcrop of the tuff of Coal Mine Canyon in Copper Basin (Cook and Brueseke, 2010). The tuff of Coal Mine Canyon that overlies the megabreccia dips ≤10° NW. Walk another 20–30 ft northwest and move out of the basal vitrophyre into non-vitrophyric ash-flow tuff (0624371 4604789). Continue walking northwest to the small ridge directly ahead and encounter a new clastic unit (Tbx; Fig. 15B; 0624228 4604821). This unit contains angular to subrounded clasts of limestone, ash-flow tuff (including vitrophyre), and other lithics and is silicified in places. Based on mapping and aerial image interpretation, it overlies the tuff of Coal Mine Canyon (also exposed to the SE, adjacent to tan silt deposits; 0624012 4604639). The age of the silt deposits is unclear; however this unit overlies the Eocene deposits and is likely part of the younger package of sediments that fill the basin to the north and south (Humboldt Formation?; Coats, 1987).

Stop 2-4 (Optional). Eocene Ash-Flow Tuff Stratigraphy

Please watch for rattlesnakes.

This stop is along Elko County Road 746 ~9.1 mi west of Charleston Reservoir (11.7 mi east of NV 225 [Mountain City

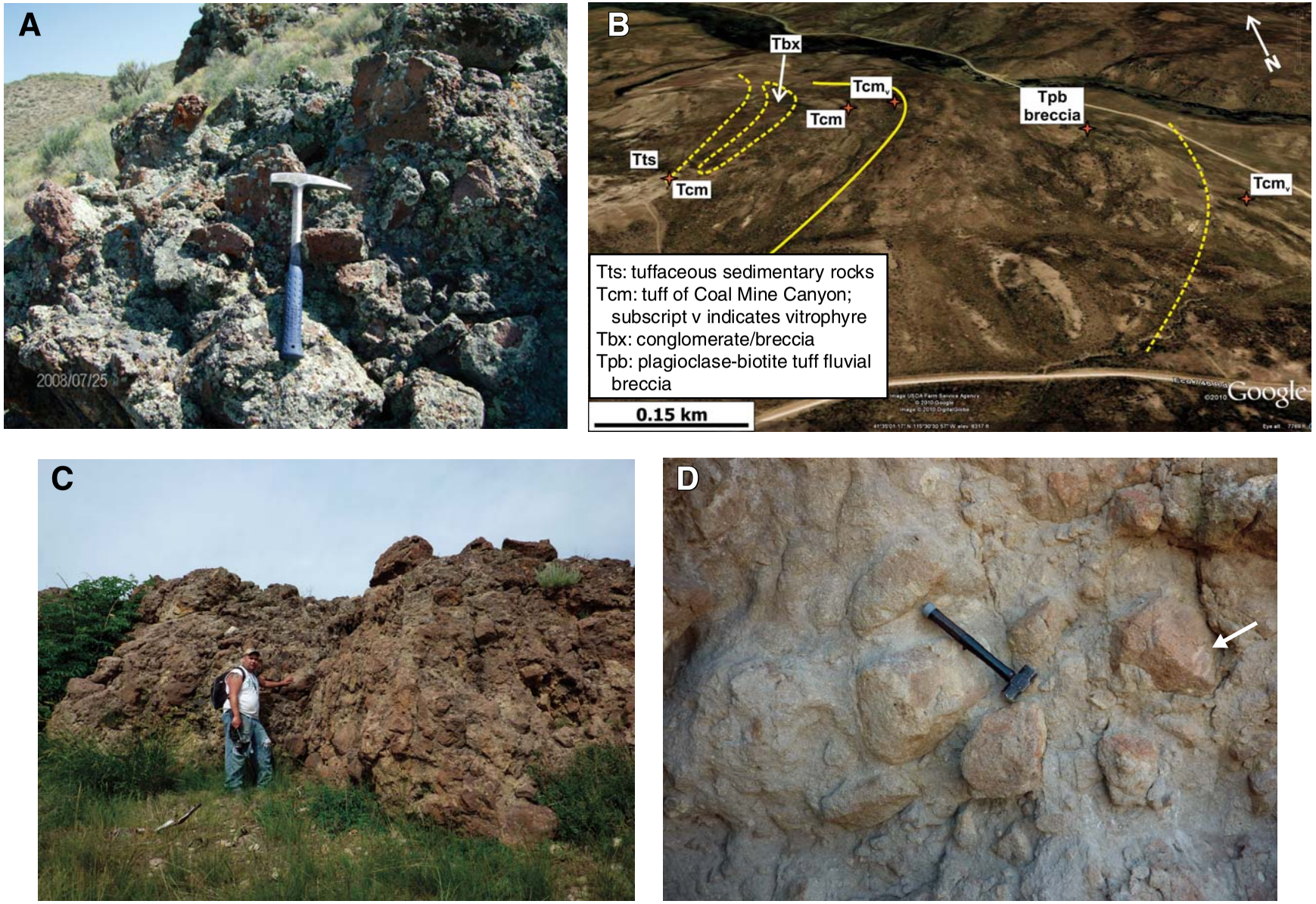

Figure 15. (A) Oxidized breccia on Jarbidge Rhyolite flow-top, north of Charleston Reservoir. Hammer is 55 cm long. (B) Complex relationships between fluvial megabreccia and overlying ash-flow tuff and sediments at Charleston Reservoir. Tcm lies above (and dips to the NW) a topographic high of Tpb. Tcm$_v$ exposed SE of the Tpb megabreccia is chemically identical (thus stratigraphically equivalent) to Tcm exposed NW of megabreccia. Dashed lines are inferred contacts and solid line is contact. Oblique Google Earth view simplified from Cook and Brueseke (2010). (C) Tpb fluvial megabreccia at Charleston Reservoir. Person is ~1.7 m tall. View to west. (D) Close-up of Tpb fluvial megabreccia. Notice the wide range in clast size and clast with tan fiamme (arrow) to the right of the hammer (~50 cm long).

Highway]) where a dirt track leads to the southeast (612380 4602076). This stop provides an overview of ash-flow tuff stratigraphy (Tt_1; Coats, 1987) and subsequent faulting that characterizes the region between Charleston Reservoir and NV 225. The cliffs just south of the road east of this point are plagioclase-biotite tuff, while the parking area sits on the dipslope of the southeast-dipping 45 Ma tuff, which underlies the plagioclase biotite tuff (Cook and Brueseke, 2010). If time allows, walk northwest to observe excellent exposures of 45 Ma tuff (0612183 4602201). North-northeast–trending normal faults in this region cut the ash-flow tuffs, leading to complex stratigraphic relationships between Eocene eruptive units and the paleovalley inferred by Cook and Brueseke (2010) that goes through the Charleston Reservoir region toward Copper Basin. Detailed mapping is needed to further refine these relationships.

Day 3. Eastern Continuation of Central Paleovalley

Take the Nevada Highway 233 (Oasis) exit off I-80, turn south on the good gravel road and drive ~1.5 mi south to a side road to the northwest. Take this road ~1.9 mi to a junction and take the right-hand fork about another 0.8 mi to whatever convenient parking can be found (Fig. 16). The road continues and can be driven to some of the initial points on the traverse below.

Stop 3-1. Nanny Creek Paleovalley, Ash-flow Tuffs, and Fluvial Megabreccia

Nanny Creek, one of the best-exposed and most informative paleovalleys in northeastern Nevada, illustrates paleovalley geometry, enclosed sedimentary deposits, distal ash-flow tuffs, and fluvial megabreccia consisting of reworked ash-flow tuff (Fig. 16; Henry, 2008; Brooks et al., 1995a, 1995b). The stratigraphic section is exposed along an ~5 km, nonstrenuous traverse.

The exposed width of the Nanny Creek paleovalley is ~6 km, but it is faulted against Paleozoic rocks on the south side and the original width is thus unknown. Mississippian and Permian sedimentary rocks make up the paleovalley wall (Thorman, 1970; Brooks et al., 1995a, 1995b; Camilleri, 2010).

A 20–30-m-thick, basal Tertiary conglomerate consists of a lag of rounded boulders commonly up to 1.5 m in diameter, and with one 6 m across (706009, 4544578). Most clasts, including the largest ones, are chert ± quartzite-pebble conglomerate similar to rocks of the Chainman, Diamond Peak, or Dale Canyon Formations, which crop out in immediately adjacent paleovalley walls (Thorman, 1970; Camilleri, 2010). So the largest clasts need not have been transported far. However, numerous clasts of coarse-grained granite up to 1.7 m in diameter, andesite, and silicified, finely laminated lake-bed sediments are present, rock types that do not crop out locally (Brooks et al., 1995a). A granite boulder that we will see (706045, 4544464) has a U-Pb zircon rumor-chron date of ca. 158 Ma (Top Secret Data, 2010). Unfortunately, bedding to determine dip in the conglomerate is not exposed.

Conglomerate is overlain by a plagioclase-biotite tuff, dated at 40.7 Ma (706115, 4544488), which is in turn overlain by the 40.0 Ma tuff of Big Cottonwood Canyon (706329, 4544541; Fig. 16). The plagioclase-biotite tuff is petrographically and compositionally similar to, but possibly younger than, a plagioclase-biotite tuff in Copper Basin. Tuff thicknesses are uncertain because of uncertainty in their dip. Foliation in the tuffs dips 30–60° eastward, but dips are probably partly primary, resulting from compaction of the tuffs against paleovalley walls (Henry, 2008; Henry and Faulds, 2010). Using the 30–60° range, the plagioclase-biotite tuff and tuff of Big Cottonwood Canyon could be 60–140 m and 90–190 m thick, respectively. Both values are significantly greater than the thicknesses of 25 m and 55 m, respectively, reported by Brooks et al. (1995a) from this same locality. The tuff of Big Cottonwood Canyon here is 150 km from its source in the Tuscarora volcanic field, yet it is at least 55 m thick and restricted to a paleovalley within which it wedges out against the sides. Andesite and andesite flow breccia dated at 39.5 ± 1.0 Ma (Brooks et al., 1995a, 1995b) overlie the tuff of Big Cottonwood Canyon.

The uppermost unit in Nanny Creek is a breccia (Tx, Fig. 16) composed of blocks, mostly of silicified tuff of Big Cottonwood Canyon with lesser plagioclase-biotite tuff and andesite (from 706799, 4544865 through 708236, 4544944). Pre-Cenozoic clasts are rare (708016, 4544946). Clasts of tuff of Big Cottonwood Canyon are up to 12 m across (707463, 4545044), plagioclase-biotite tuff is up to 8 m long (707459, 4545061), and andesite is as much as 2 m across (708137, 4544789). Blocks range from angular to rounded, and many are internally broken but not disaggregated (707975, 4544954). Rarely exposed matrix consists of coarse sand and variably rounded pebbles and cobbles. Brooks et al. (1995a) recognized the hummocky character of this unit and the possibility that the hummocks might be landslide blocks. Chemical analysis and dating of one clast confirm that it is tuff of Big Cottonwood Canyon (Henry, 2008). Furthermore, highly discordant compaction foliations and scattered magnetization directions from several breccia clasts (M.R. Hudson, *in* Brooks et al., 1995a; Palmer and MacDonald, 2002, their sites W02, W15, and W18) confirm that these blocks are not in place. We interpret these breccia deposits as resulting from "dam-burst floods," in which the tuff of Big Cottonwood Canyon initially blocked a drainage, then the tuff "dam" collapsed once a lake backed up behind and overtopped the dam. Blockage of drainages and dam-burst floods are common even in historic times (Costa and Schuster, 1988; Waythomas, 2001; the Thistle landslide that blocked the Spanish Fork River in Utah in 1982).

ACKNOWLEDGMENTS

We greatly appreciate discussions with David John, Keith Howard, Chuck Thorman, Alan Wallace, Chuck Chapin, Dave Boden, Jim Faulds, Patrick Goldstrand, John Muntean, Fred Zoerner, Ken Hickey, Dick Tosdal, and Mike Ressel, and very helpful reviews by Keith Howard and Jeffrey Lee.

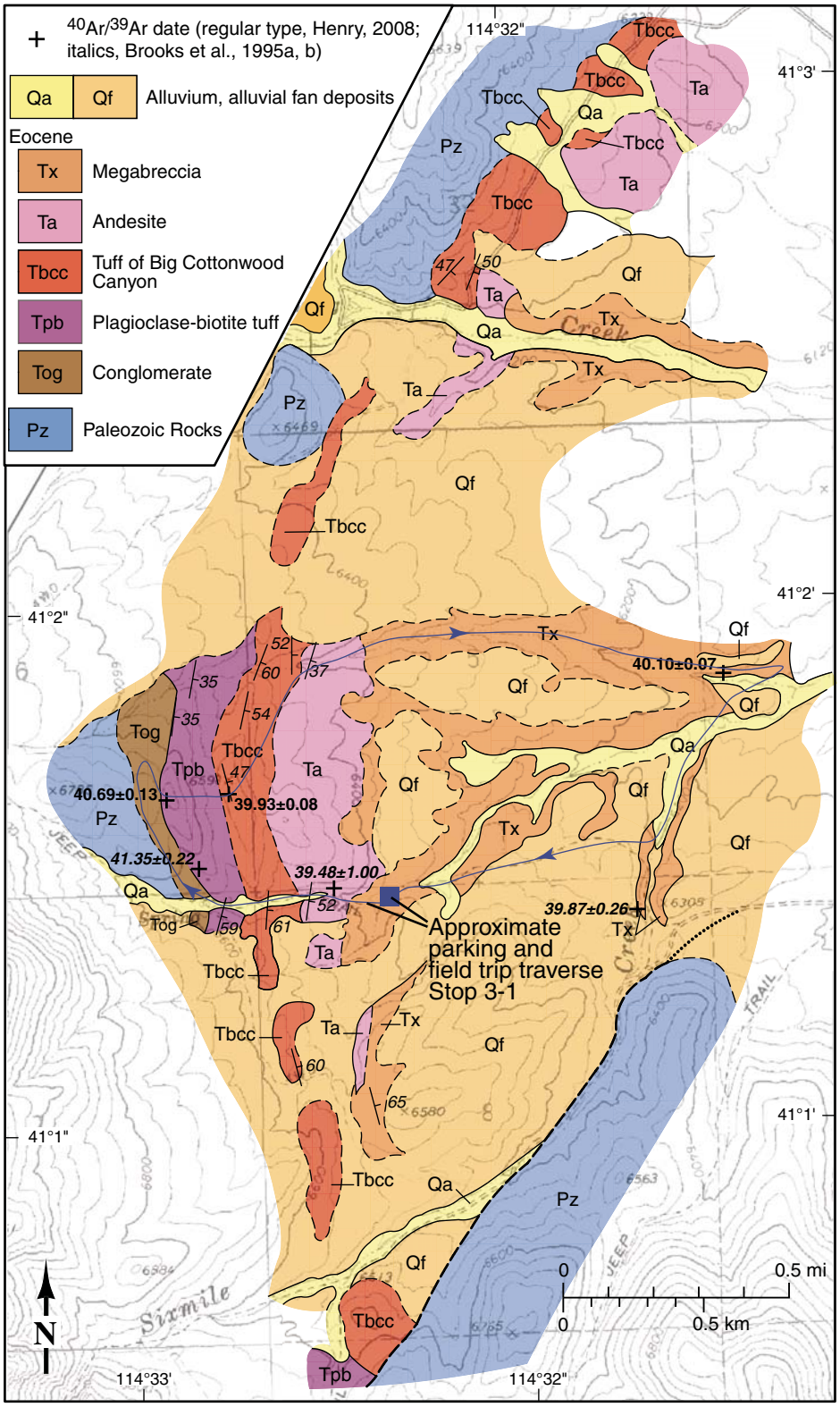

Figure 16. Geologic map of the paleovalley at Nanny Creek, eastern Pequop Mountains, showing traverse for Stop 3-1. The paleovalley, which was at least 6 km wide and possibly 1.6 km deep, has basal conglomerate containing rounded boulders up to 6 m in diameter, overlain by a plagioclase-biotite tuff and tuff of Big Cottonwood Canyon, andesite lavas, and a thick fluvial megabreccia consisting of angular blocks mostly of the tuff of Big Cottonwood Canyon.

REFERENCES CITED

Armstrong, R.L., 1968, Sevier orogenic belt in Nevada and Utah: Geological Society of America Bulletin, v. 79, p. 429–458, doi:10.1130/0016-7606(1968)79[429:SOBINA]2.0.CO;2.

Armstrong, R.L., and Hansen, E., 1966, Cordilleran infrastructure in the eastern Great Basin: American Journal of Science, v. 264, p. 112–127, doi:10.2475/ajs.264.2.112.

Axelrod, D.I., 1966a, Potassium-Argon ages of some western Tertiary floras: American Journal of Science, v. 264, p. 497–506, doi:10.2475/ajs.264.7.497.

Axelrod, D.I., 1966b, The Eocene Copper Basin flora of northeastern Nevada: University of California Publications in Geological Sciences, v. 59, 124 p.

Baars, D.L., Bartleson, B.L., Chapin, C.E., Curtis, B.F., De Voto, R.H., Everett, J.R., Johnson, R.C., Molenaar, C.M., Peterson, F., Schenk, C.J., Love, J.D., Merin, I.S., Rose, P.R., Ryder, R.T., Waechter, N.B., and Woodward, L.A., 1988, Basins of the Rocky Mountain region, *in* Sloss, L.L., ed., Sedimentary Cover—North American Craton: U.S.: Geological Society of America, Geology of North America, v. D-2, p. 109–220.

Barton, M.D., 1996, Granitic magmatism and metallogeny of southwestern North America, *in* Brown, M., Candela, P.A., Peck, D.L., Stephens, W.E., Walker, R.J., and Zen, E-An, eds., Origin of Granites and Related Rocks: Geological Society of America Special Paper 315, p. 261–280.

Best, M.G., and Christiansen, E.H., 1991, Limited extension during peak Tertiary volcanism, Great Basin of Nevada and Utah: Journal of Geophysical Research, v. 96, p. 13,509–13,528, doi:10.1029/91JB00244.

Best, M.G., Barr, D.L., Christiansen, E.H., Gromme, S., Deino, A.L., and Tingey, D.G., 2009, The Great Basin Altiplano during the middle Cenozoic ignimbrite flareup: insights from volcanic rocks: International Geology Review, v. 51, p. 589–633, doi:10.1080/00206810902867690.

Bohlen, S.R., Montana, A., and Kerrick, D.M., 1991, Precise determination of the equilibria kyanite-sillimanite and kyanite-andalusite and revised triple point for Al_2SiO_5 polymorphs: The American Mineralogist, v. 76, p. 677–680.

Brooks, W.E., Thorman, W.E., and Snee, L.W., 1995a, The $^{40}Ar/^{39}Ar$ ages and tectonic setting of the middle Eocene northeast Nevada volcanic field: Journal of Geophysical Research, v. 100, p. 10,403–10,416, doi:10.1029/94JB03389.

Brooks, W.E., Thorman, W.E., Snee, L.W., Nutt, C.W., Potter, C.J., and Dubiel, R.F., 1995b, Summary of chemical analyses and $^{40}Ar/^{39}Ar$-spectra data for Eocene volcanic rocks from the central part of the northeast Nevada volcanic field: U.S. Geological Survey Bulletin 1988-K, p. K1–K33.

Bryant, B., Naeser, C.W., Marvin, R.F., and Mehnert, H.H., 1989, Upper Cretaceous and Paleogene sedimentary rocks and isotopic ages of Paleogene tuffs, Uinta Basin, Utah: U.S. Geological Survey Bulletin 1787-J, 22 p.

Bushnell, K., 1967, Geology of the Rowland Quadrangle, Elko County, Nevada: Nevada Bureau of Mines Bulletin 67, 38 p.

Callicoat, J.S., 2010, Significance of mid-Miocene volcanism in northeast Nevada: petrographic, chemical, isotopic, and temporal importance of the Jarbidge Rhyolite [M.S. thesis]: Manhattan, Kansas, Kansas State University, p. 1–108.

Callicoat, J., Brueseke, M., and Larson, P.B., 2010, Oxygen isotope constraints on voluminous mid-Miocene effusive silicic magmatism in north-central Nevada: Geological Society of America Abstracts with Programs, v. 42, no. 5, p. 101.

Camilleri, P., 2010, Geologic map of the Wood Hills, Elko County, Nevada: Nevada Bureau of Mines and Geology Map 172, 1:48,000.

Camilleri, P., and Chamberlain, K.R., 1997, Mesozoic tectonics and metamorphism in the Pequop Mountains and Wood Hills, northeast Nevada: Implications for the architecture and evolution of the Sevier orogen: Geological Society of America Bulletin, v. 109, p. 74–94, doi:10.1130/0016-7606(1997)109<0074:MTAMIT>2.3.CO;2.

Camilleri, P., Yonkee, W.A., Coogan, J.C., DeCelles, P.G., McGrew, A., and Wells, M., 1997, Hinterland to foreland transect through the Sevier orogen, NE Nevada to SW Wyoming: structural style, metamorphism, and kinematic history of a large contractional orogenic wedge, *in* Link, P.K., and Kowallis, B.J., eds., Proterozoic to Recent Stratigraphy, Tectonics, and Volcanology, Utah, Nevada, Southern Idaho and Central Mexico: Brigham Young University Geology Studies, v. 42, part 1, p. 297–309.

Cassel, E.J., Henry, C.D., Graham, S.A., and Chamberlain, P.C., 2010, Determining Oligocene topography and tectonism across the northern Sierra Nevada and western Basin and Range using stable isotope paleoaltimetry in volcanic glass: Geological Society of America Abstracts with Programs, v. 42, no. 5, p. 184.

Chase, C.G., Gregory, K.M., Parrish, J.T., and DeCelles, P.G., 1998, Topographic history of the western Cordilleran of North America and the etiology of climate, *in* Crowley, T.J., and Burke, K., eds., Tectonic boundary conditions for climate reconstructions: Oxford Monographs on Geology and Geophysics, no. 39, p. 73–99.

Christiansen, R.L., and Yeats, R.S., 1992, Post-Laramide geology of the U.S. Cordilleran region, *in* Burchfiel, B.C., Lipman, P.W., and Zoback, M.L., eds., The Cordilleran Orogen: Conterminous U.S.: Geological Society of America, Geology of North America, v. G-3, p. 261–406.

Cline, J.S., Hofstra, A.H., Muntean, J.L., Tosdal, R.M., and Hickey, K.A., 2005, Carlin-type gold deposits in Nevada: Critical geologic characteristics and viable models, *in* Hedenquist, J.W., Thompson, J.F.H., Goldfard, R.J., and Richards, J.P., eds., 100th Anniversary Volume, Economic Geology, p. 451–484.

Coash, J.R., 1967, Geology of the Mount Velma Quadrangle, Elko County, Nevada: Nevada Bureau of Mines Bulletin 68, 20 p.

Coats, R.R., 1964, Geology of the Jarbidge Quadrangle, Nevada–Idaho: U.S. Geological Survey Bulletin 1141-M, 24 p.

Coats, R.R., 1987, Geology of Elko County, Nevada: Nevada Bureau of Mines and Geology Bulletin 101, 112 p.

Coats, R.R., and Riva, J.F., 1983, Overlapping thrust belts of late Paleozoic and Mesozoic ages, northern Elko County, Nevada, *in*, Miller, D.M., Todd, V.R., and Howard, K.A., eds., Tectonic and Stratigraphic Studies in the eastern Great Basin: Geological Society of America Memoir 157, p. 305–327.

Colgan, J.P., and Henry, C.D., 2009, Rapid middle Miocene collapse of the Sevier orogenic plateau in north-central Nevada: International Geology Review, v. 51, p. 920–961, doi:10.1080/00206810903056731.

Colgan, J.P., John, D.A., Henry, C.D., and Fleck, R.J., 2008, Large-magnitude Miocene extension of the Caetano caldera, Shoshone and Toiyabe Ranges, Nevada: Geosphere, v. 4, p. 107–131, doi:10.1130/GES00115.1.

Colgan, J.P., Howard, K.A., Fleck, R.J., and Wooden, J.L., 2010, Rapid middle Miocene extension and unroofing of the southern Ruby Mountains, Nevada: Tectonics, v. 29, p. TC6022, doi:10.1029/2009TC002655.

Coney, P.J., and Harms, T.A., 1984, Cordilleran metamorphic core complexes: Cenozoic extensional relics of Mesozoic compression: Geology, v. 12, p. 550–554, doi:10.1130/0091-7613(1984)12<550:CMCCCE>2.0.CO;2.

Cook, C.C., and Brueseke, M.E., 2010, Petrography and identification of Eocene ash-flow tuffs in the vicinity of the Jarbidge Mountains, Nevada: Geological Society of America Abstracts with Programs, v. 42, no. 5, p. 285.

Costa, J.E., and Schuster, R.L., 1988, The formation and failure of natural dams: Geological Society of America Bulletin, v. 100, p. 1054–1068, doi:10.1130/0016-7606(1988)100<1054:TFAFON>2.3.CO;2.

Crafford, A.E.J., 2007, Geologic map of Nevada: U.S. Geological Survey Data Series 249, 46 p.

Dallmeyer, R.D., Snoke, A.W., and McKee, E.H., 1986, The Mesozoic-Cenozoic tectonothermal evolution of the Ruby Mountains, East Humboldt Range, Nevada: a Cordilleran metamorphic core complex: Tectonics, v. 5, p. 931–954, doi:10.1029/TC005i006p00931.

Davis, S.J., Mulch, A., Carroll, A.R., Horton, T.W., and Chamberlain, C.P., 2009, Paleogene landscape evolution of the central North American Cordillera: Developing topography and hydrology in the Laramide foreland: Geological Society of America Bulletin, v. 121, p. 100–116, doi:10.1130/B26308.1.

DeCelles, P.G., 2004, Late Jurassic to Eocene evolution of the Cordilleran thrust belt and foreland basin system, western U.S.A: American Journal of Science, v. 304, p. 105–168, doi:10.2475/ajs.304.2.105.

DeCelles, P.G., and Coogan, J.C., 2006, Regional structure and kinematic history of the Sevier fold and-thrust belt, central Utah: Geological Society of America Bulletin, v. 118, p. 841–864, doi:10.1130/B25759.1.

dePolo, C.M., Smith, K.D., and Henry, C.D., 2011, Summary of the 2008 Wells, Nevada earthquake documentation volume, *in* dePolo, C.M., and LaPointe, D.D., eds., A compendium of earthquake-related investigations prepared by the University of Nevada, Reno: Nevada Bureau of Mines and Geology Special Publication 36, p. 7–14.

Dickinson, W.R., 2002, The Basin and Range Province as a composite extensional domain: International Geology Review, v. 44, p. 1–38, doi:10.2747/0020-6814.44.1.1.

Dickinson, W.R., 2006, Geotectonic evolution of the Great Basin: Geosphere, v. 2, p. 353–368, doi:10.1130/GES00054.1.

Dilek, Y., and Moores, E.M., 1999, A Tibetan model for the early Tertiary western United States: Journal of the Geological Society, v. 156, p. 929–941, doi:10.1144/gsjgs.156.5.0929.

Dokka, R.K., Mahaffie, M.J., and Snoke, A.W., 1986, Thermochronologic evidence of major tectonic denudation associated with detachment faulting,

northern Ruby Mountains–East Humboldt Range, Nevada: Tectonics, v. 5, p. 995–1006, doi:10.1029/TC005i007p00995.

Druschke, P., Hanson, A.D., and Wells, M.L., 2008, Detrital zircon provenance of Cretaceous to Eocene strata in the Sevier hinterland, central Nevada; implications for tectonics and paleogeography: Geological Society of America Abstracts with Programs, v. 40, no. 1, p. 78.

Druschke, P., Hanson, A.D., and Wells, M.L., 2009a, Structural, stratigraphic, and geochronologic evidence for extension predating Palaeogene volcanism in the Sevier hinterland, east-central Nevada: International Geology Review, v. 51, p. 743–775, doi:10.1080/00206810902917941.

Druschke, P., Hanson, A.D., Wells, M.L., Rasbury, T., Stockli, D.F., and Gehrels, G., 2009b, Synconvergent surface-breaking normal faults of Late Cretaceous age within the Sevier hinterland, east-central Nevada: Geology, v. 37, p. 447–450, doi:10.1130/G25546A.1.

Farmer, G.L., and DePaolo, D.J., 1983, Origin of Mesozoic and Tertiary granite in the western United States and implications for pre-Mesozoic crustal structure; 1, Nd and Sr isotopic studies in the geocline of the northern Great Basin: Journal of Geophysical Research, v. 88, p. 3379–3401, doi:10.1029/JB088iB04p03379.

Faulds, J.E., Henry, C.D., and Hinz, N.H., 2005, Kinematics of the northern Walker Lane: An incipient transform fault along the Pacific–North American plate boundary: Geology, v. 33, p. 505–508, doi:10.1130/G21274.1.

Fouch, T.D., Hanley, J.H., and Forester, R.M., 1979, Preliminary correlation of Cretaceous and Paleogene lacustrine and related nonmarine sedimentary and volcanic rocks in parts of the eastern Great Basin of Nevada and Utah, *in* Newman, G.W., and Goode, H.D., eds., Basin and Range symposium and Great Basin field conference: Rocky Mountain Association of Petroleum Geologists and Utah Geological Association, p. 305–312.

Fricke, H.C., Wickham, S.M., and O'Neil, J.R., 1992, Oxygen and hydrogen isotope evidence for meteoric water infiltration during mylonitization and uplift in the Ruby Mountains–East Humboldt Range core complex, Nevada: Contributions to Mineralogy and Petrology, v. 111, p. 203–221, doi:10.1007/BF00348952.

Gans, P.B., 1987, An open-system, two-layer crustal stretching model for the eastern Great Basin: Tectonics, v. 6, p. 1–12, doi:10.1029/TC006i001p00001.

Garside, L.J., Henry, C.D., Faulds, J.E., and Hinz, N.H., 2005, The upper reaches of the Sierra Nevada auriferous gold channels, *in* Rhoden, H.N., et al., eds., Window to the World: Geological Society of Nevada Symposium Proceedings, 14–18 May 2005.

Goldstrand, P.M., 1994, Tectonic development of Upper Cretaceous to Eocene strata of southwestern Utah: Geological Society of America Bulletin, v. 106, p. 145–154, doi:10.1130/0016-7606(1994)106<0145:TDOUCT>2.3.CO;2.

Hacker, B.R., Yin, A., Christie, J.M., and Snoke, A.W., 1990, Differential stress, strain rate, and temperatures of mylonitization in the Ruby Mountains, Nevada; implications for the rate and duration of uplift: Journal of Geophysical Research, v. 95, p. 8569–8580, doi:10.1029/JB095iB06p08569.

Haines, S.H., and van der Pluijm, B., 2010, Dating the detachment fault system of the Ruby Mountains, Nevada: Significance for the kinematics of low-angle normal faults: Tectonics, v. 29, p. TC4028, doi:10.1029/2009TC002552.

Hallett, B.W., and Spear, F.S., 2010, The tectonic record preserved in growth and diffusion zoning patterns in garnet from migmatitic pelites of the East Humboldt Range, Nevada: Geological Society of America Abstracts with Programs, v. 42, no. 5, p. 629.

Halverson, G.P., Hoffman, P.F., Schrag, D.P., Maloof, A.C., and Rice, A.H.N., 2005, Toward a Neoproterozoic composite carbon-isotope record: Geological Society of America Bulletin, v. 117, p. 1181–1207, doi:10.1130/B25630.1.

Haynes, S.R., 2003, Development of the Eocene Elko basin, northeastern Nevada: Implications for paleogeography and regional tectonism [M.S. thesis]: The University of British Columbia, 159 p.

Haynes, S.R., Hickey, K.A., Mortensen, J.K., and Tosdal, R.M., 2002, Onset of extension in the Basin and Range: Basin analysis of the Eocene Elko Formation, NE Nevada: Geological Society of America Abstracts with Programs, v. 34, no. 6, p. 83.

Henry, C.D., 2008, Ash-flow tuffs and paleovalleys in northeastern Nevada: Implications for Eocene paleogeography and extension in the Sevier hinterland, northern Great Basin: Geosphere, v. 4, p. 1–35, doi:10.1130/GES00122.1.

Henry, C.D., and Faulds, J.E., 1999, Geologic map of the Emigrant Pass Quadrangle, Lander County, Nevada: Nevada Bureau of Mines and Geology Open-file Report 99-9.

Henry, C.D., and Faulds, J.E., 2010, Ash-flow tuffs in the Nine Hill, Nevada, paleovalley and implications for tectonism and volcanism of the western Great Basin, USA: Geosphere, v. 6, p. 339–369, doi:10.1130/GES00548.1.

Henry, C.D., and Ressel, M.W., 2000, Eocene magmatism of northeastern Nevada: The smoking gun for Carlin-type gold deposits, *in* Cluer, J.K., Price, J.G., Struhsacker, E.M., Hardyman, R.F., and Morris, C.L., eds., Geology and Ore Deposits 2000: The Great Basin and Beyond: Geological Society of Nevada Symposium Proceedings, 15–18 May 2000, p. 365–388.

Henry, C.D., Boden, D.R., and Castor, S.C., 1999, Geologic map of the Tuscarora Quadrangle, Nevada: Nevada Bureau of Mines and Geology Map 116, scale 1:24,000, 20 p. text.

Hickey, K., Tosdal, R., Haynes, S., and Moore, S., 2005, Tectonics, paleogeography, volcanic succession, and the depth of formation of Eocene sediment-hosted gold deposits of the northern Carlin trend, Nevada: Geological Society of Nevada Field Trip Guidebook, v. 3, p. 97–105.

Hintze, L.F., 1993, Geologic history of Utah: Brigham Young University Geology Studies Special Publication 7, 202 p.

Hodges, K.V., 2006, A synthesis of the channel flow-extrusion hypothesis as developed for the Himalayan-Tibetan orogenic system, *in* Law, R.D., Searle, M.P., and Godin, L., eds., Channel flow, ductile extrusion and exhumation in continental collision zones: Geological Society, London, Special Publication 268, p. 71–90.

Hodges, K.V., and Walker, J.D., 1992, Extension in the Cretaceous Sevier orogen, North American Cordillera: Geological Society of America Bulletin, v. 104, p. 560–569, doi:10.1130/0016-7606(1992)104<0560:EITCSO>2.3.CO;2.

Hodges, K.V., Snoke, A.W., and Hurlow, H.A., 1992, Thermal evolution of a portion of the Sevier hinterland: The northern Ruby Mountains–East Humboldt Range and Wood Hills, northeastern Nevada: Tectonics, v. 11, p. 154–164, doi:10.1029/91TC01879.

Howard, K.A., 1980, Metamorphic infrastructure in the northern Ruby Mountains, Nevada, *in* Crittenden, M.D., Jr., Coney, P.J., and Davis, G.H., eds., Cordilleran metamorphic core complexes: Geological Society of America Memoir 153, p. 335–347.

Howard, K.A., 2000, Geologic map of the Lamoille Quadrangle, Elko County, Nevada: Nevada Bureau of Mines and Geology Map 125, 1:24,000.

Howard, K.A., 2003, Crustal structure in the Elko-Carlin region, Nevada, during Eocene gold mineralization: Ruby–East Humboldt metamorphic core complex as a guide to the deep crust: Economic Geology, v. 98, p. 249–268, doi: 10.2113/gsecongeo.98.2.249.

Hudec, M.R., 1992, Mesozoic structural and metamorphic history of the central Ruby Mountains metamorphic core complex, Nevada, with Supplementary Data item 92-27: Geological Society of America Bulletin, v. 104, p. 1086–1100, doi:10.1130/0016-7606(1992)104<1086:MSAMHO>2.3.CO;2.

Humphreys, E.D., 1995, Post-Laramide removal of the Farallon slab, western United States: Geology, v. 23, p. 987–990, doi:10.1130/0091-7613(1995)023<0987:PLROTF>2.3.CO;2.

Hurlow, H.A., Snoke, A.W., and Hodges, K.V., 1991, Temperature and pressure of mylonitization in a Tertiary extensional shear zone, Ruby Mountains–East Humboldt Range, Nevada: Tectonic implications: Geology, v. 19, p. 82–86, doi:10.1130/0091-7613(1991)019<0082:TAPOMI>2.3.CO;2.

John, D.A., Wallace, A.R., Ponce, D.A., Fleck, R.B., and Conrad, J.E., 2000, New perspectives on the geology and origin of the northern Nevada rift, *in* Cluer, J.K., Price, J.G., Struhsacker, E.M., Hardyman, R.F., and Morris, C.L., eds., Geology and Ore Deposits 2000: The Great Basin and Beyond: Geological Society of Nevada Symposium Proceedings, 15–18 May 2000, p. 127–154.

Ketner, K.B., and Alpha, A.G., 1992, Mesozoic and Tertiary rocks near Elko Nevada—Evidence for Jurassic to Eocene folding and low-angle faulting: U.S. Geological Survey Bulletin 1988-C, 13 p.

Ketner, K.B., Murchey, B.L., Stamm, R.G., and Wardlaw, B.R., 1993, Paleozoic and Mesozoic rocks of Mount Ichabod and Dorsey Canyon, Elko County, Nevada; evidence for post–Early Triassic emplacement of the Roberts Mountains and Golconda allochthons: U.S. Geological Survey Bulletin 1988, p. D1–D12.

Ketner, K.B., Repetski, J.E., Wardlaw, B.R., and Stamm, R.G., 1995, Geologic map of the Rowland-Bearpaw Mountain area, Elko County, Nevada: U.S. Geological Survey Miscellaneous Investigations Series I-2356, 1:24,000.

Kistler, R.W., Ghent, E.D., and O'Neil, J.R., 1981, Petrogenesis of garnet two-mica granites in the Ruby Mountains, Nevada: Journal of Geophysical Research, v. 86, p. 10591–10606, doi:10.1029/JB086iB11p10591.

Law, R.D., Searle, M.P., and Simpson, R.L., 2004, Strain, deformation temperatures and vorticity of flow at the top of the Greater Himalayan Slab, Everest Massif, Tibet: Journal of the Geological Society, v. 161, p. 305–320, doi:10.1144/0016-764903-047.

Lee, S.Y., Barnes, C.G., Snoke, A.W., Howard, K.A., and Frost, C.D., 2003, Petrogenesis of Mesozoic, peraluminous granites in the Lamoille Canyon

area, Ruby Mountains, Nevada, USA: Journal of Petrology, v. 44, p. 713–732, doi:10.1093/petrology/44.4.713.

Lindgren, W., 1911, The Tertiary gravels of the Sierra Nevada of California: U.S. Geological Survey Professional Paper 73, 226 p.

Lister, G.S., and Snoke, A.W., 1984, S-C mylonites: Journal of Structural Geology, v. 6, p. 617–638, doi:10.1016/0191-8141(84)90001-4.

Lush, A.P., McGrew, A.J., Snoke, A.W., and Wright, J.E., 1988, Allochthonous Archean basement in the northern East Humboldt Range, Nevada: Geology, v. 16, p. 349–353, doi:10.1130/0091-7613(1988)016<0349:AABITN>2.3.CO;2.

MacCready, T., 1996, Misalignment of quartz c-axis fabrics and lineations due to oblique final strain increments in the Ruby Mountains core complex, Nevada: Journal of Structural Geology, v. 18, p. 765–776, doi:10.1016/S0191-8141(96)80010-1.

MacCready, T., Snoke, A.W., Wright, J.E., and Howard, K.A., 1997, Mid-crustal flow during Tertiary extension in the Ruby Mountains core complex, Nevada: Geological Society of America Bulletin, v. 109, p. 1576–1594, doi:10.1130/0016-7606(1997)109<1576:MCFDTE>2.3.CO;2.

McGrew, A.J., 1992, Tectonic evolution of the northern East Humboldt Range, Elko County, Nevada [Ph.D. dissertation]: Laramie, University of Wyoming, 191 p.

McGrew, A.J., 2002, Spreading the welt or melting to spread? Late Cretaceous to Eocene tectonothermal evolution of the hinterland of the Sevier orogenic belt, western USA (abst.): Abstracts, Geological Society of Australia, v. 67, p. 181.

McGrew, A.J., and Casey, M., 1993, *in* Brandmayr, M., and Wallbrecher, E., eds., Transition to deep-crustal flow in the East Humboldt Range metamorphic core complex, Nevada, USA: Terra Abstracts, v. 5, Suppl. 2, p. 22.

McGrew, A.J., and Foland, K.A., 2004, Age and significance of the Copper Basin fault system, Elko County, Nevada: Geological Society of America Abstracts with Programs, v. 36, no. 5, p. 23.

McGrew, A.J., and Snee, L.W., 1994, $^{40}Ar/^{39}Ar$ thermochronologic constraints on the tectonothermal evolution of the northern East Humboldt Range metamorphic core complex, Nevada: Tectonophysics, v. 238, p. 425–450, doi:10.1016/0040-1951(94)90067-1.

McGrew, A.J., and Snoke, A.W., 2010, SHRIMP-RG U-Pb isotopic systematics of zircon from the Angel Lake orthogneiss, East Humboldt Range, Nevada: Is this really Archean crust?: Comment: Geosphere, v. 6, no. 6, doi:10.1130/GES0056.1, 2 figures.

McGrew, A., and Vance, J., 2008, Buried canyons: End-Laramide paleotopography of northeastern Nevada preserved beneath Eocene to Miocene volcanic sequences: Geological Society of America Abstracts with Programs, v. 40, no. 1, p. 48.

McGrew, A.J., Peters, M.T., and Wright, J.E., 2000, Thermobarometric constraints on the tectonothermal evolution of the East Humboldt Range metamorphic core complex, Nevada: Geological Society of America Bulletin, v. 112, p. 45–60, doi:10.1130/0016-7606(2000)112<45:TCOTTE>2.0.CO;2.

McGrew, A.J., Foland, K.A., and Stockli, D., 2007, Evolution of Cenozoic volcanism and extension in the Copper Mountains, northeastern Nevada: Geological Society of America Abstracts with Programs, v. 39, no. 6, p. 226.

McGrew, A.J., Premo, W.R., Snoke, A.W., and Asher, A., 2009, The Angel Lake Gneiss Complex revisited; Precambrian geology of the northern East Humboldt Range, Elko County, Nevada: Geological Society of America Abstracts with Programs, v. 41, no. 7, p. 271.

Miller, D.M., 1985, Geologic map of the Lucin quadrangle, Box Elder County, Utah: Utah Geological and Mineral Survey Map 78, 1:24,000.

Miller, D.M., Nakata, J.K., and Glick, L.J., 1990, K-Ar ages of Jurassic to Tertiary plutonic and metamorphic rocks, northwestern Utah and northeastern Nevada: U.S. Geological Survey Bulletin 1906, 18 p.

Miller, D.M., Lush, A.P., and Schneyer, J.D., 1993, Geologic map of the Patterson Pass quadrangle, Box Elder County, Utah, and Elko County, Nevada: Utah Geological Survey Map 144, 1:24,000.

Miller, E.L., and Gans, P.B., 1989, Cretaceous structure and metamorphism in the hinterland of the Sevier thrust belt, western U.S. Cordillera: Geology, v. 17, p. 59–62, doi:10.1130/0091-7613(1989)017<0059:CCSAMI>2.3.CO;2.

Miller, E.L., Miller, M.M., Stevens, C.H., Wright, J.E., and Madrid, R., 1992, Late Paleozoic paleogeographic and tectonic evolution of the Western U.S. Cordillera, *in* Burchfield, B.C., Lipman, P.W., and Zoback, M.L., eds., The Cordilleran Orogen: Conterminous U.S.: Geological Society of America, Geology of North America, v. G-3, p. 57–106.

Miller, E.L., Dumitru, T.A., Brown, R.W., and Gans, P.B., 1999, Rapid Miocene slip on the Snake Range–Deep Creek Range fault system, east-central Nevada: Geological Society of America Bulletin, v. 111, p. 886–905, doi:10.1130/0016-7606(1999)111<0886:RMSOTS>2.3.CO;2.

Miller, R.B., and Snoke, A.W., 2009, The utility of crustal cross sections in the analysis of orogenic processes in contrasting tectonic settings, *in* Miller, R.B., and Snoke, A.W., eds., Crustal Cross Sections from the Western North American Cordillera and Elsewhere: Implications for Tectonic and Petrologic Processes: Geological Society of America Special Paper 456, p. 1–38, doi: 10.1130/2009.2456(01).

Misch, P., and Hazzard, J.C., 1962, Stratigraphy and metamorphism of late Precambrian rocks in central northeastern Nevada and adjacent Utah: Bulletin of the American Association of Petroleum Geologists, v. 46, p. 289–343.

Mix, H.T., Mulch, A., Kent-Corson, M.L., and Chamberlain, C.P., 2011, Cenozoic migration of topography in the North American Cordillera: Geology, v. 39, p. 87–90, doi:10.1130/G31450.1.

Mortensen, J.K., Thompson, J.F.H., and Tosdal, R.M., 2000, U-Pb age constraints on magmatism and mineralization in the northern Great Basin, Nevada, *in* Cluer, J.K., Price, J.G., Struhsacker, E.M., Hardyman, R.F., and Morris, C.L., eds., Geology and Ore Deposits 2000: The Great Basin and Beyond: Geological Society of Nevada Symposium Proceedings, 15–18 May 2000, p. 419–438.

Mueller, K.J., 1992, Tertiary basin development and exhumation of the northern East Humboldt –Wood Hills metamorphic complex, Elko County, Nevada [Ph.D. dissertation]: Laramie, University of Wyoming, 205 p.

Mueller, K.J., 1993, Geologic map of the Windermere Hills, northeastern Nevada: Nevada Bureau of Mines and Geology Field Studies Map 4, 1:48,000.

Mueller, K.J., and Snoke, A.W., 1993a, Progressive overprinting of normal fault systems and their role in Tertiary exhumation of the East Humboldt–Wood Hills metamorphic complex, northeast Nevada: Tectonics, v. 12, p. 361–371, doi:10.1029/92TC01967.

Mueller, K.J., and Snoke, A.W., 1993b, Cenozoic basin development and normal fault systems associated with the exhumation of metamorphic complexes in northeast Nevada, *in* Lahren, M.M., Trexler, J.H., Jr., and Spinosa, C., eds., Crustal evolution of the Great Basin and Sierra Nevada: Department of Geological Sciences, University of Nevada, Reno, Cordilleran–Rocky Mountain Section, Geological Society of America Guidebook, p. 1–34.

Mueller, K.J., Cerveny, P.K., Perkins, M.E., and Snee, L.W., 1999, Chronology of polyphase extension in the Windermere Hills, northeast Nevada: Geological Society of America Bulletin, v. 111, p. 11–27, doi:10.1130/0016-7606(1999)111<0011:COPEIT>2.3.CO;2.

Muntean, J.L., Cline, J., Johnston, M.R., Ressel, M.W., Seedorff, E., and Barton, M.D., 2004, Controversies on the origin of world-class gold deposits; Part I, Carlin-type gold deposits in Nevada: Society of Economic Geologists Newsletter, v. 59, p. 1–18.

Muntean, J.L., and Henry, C.D., 2007, Preliminary geologic map of the Jerritt Canyon mining district, Elko County, Nevada: Nevada Bureau of Mines and Geology Open-File Report 07-3, 1:24,000.

Palmer, H.C., and MacDonald, W.D., 2002, The northeast Nevada volcanic field: Magnetic properties and source implications: Journal of Geophysical Research, v. 107, doi: 1029/2001JB000690.

Peters, M.T., and Wickham, S.M., 1992, High $\delta^{13}C$ marbles from the East Humboldt Range, Nevada: Eos (Transactions, American Geophysical Union), v. 73, p. 326.

Peters, M.T., and Wickham, S.M., 1994, Petrology of upper amphibolite facies marbles from the East Humboldt Range, Nevada, USA; evidence for high-temperature, retrograde, hydrous volatile fluxes at mid-crustal levels: Journal of Petrology, v. 35, p. 205–238.

Poole, F.G., Stewart, J.H., Palmer, A.R., Sandberg, C.A., Madrid, R.J., Ross, R.J., Hintze, L.F., Miller, M.M., and Wrucke, C.T., 1992, Latest Precambrian to latest Devonian time; development of a continental margin, *in* Burchfiel, B.C., Lipman, P.W., and Zoback, M.L., eds., The Cordilleran Orogen: Conterminous U.S.: Geological Society of America, Geology of North America, v. G-3, p. 9–56.

Premo, W.R., Castiñeiras, P., and Wooden, J.L., 2008, SHRIMP-RG U-Pb isotopic systematics of zircon from the Angel Lake orthogneiss, East Humboldt Range, Nevada: Is this really Archean crust?: Geosphere, v. 4, p. 963–975, doi:10.1130/GES00164.1.

Premo, W.R., Castiñeiras, P., and Wooden, J.L., 2010, SHRIMP-RG U-Pb isotopic systematics of zircon from the Angel Lake orthogneiss, East Humboldt Range, Nevada: Is this really Archean crust?: Reply: Geosphere, v. 6, p. 966–972, doi:10.1130/GES00592.1.

Rahl, J.M., McGrew, A.J., and Foland, K.A., 2002, Transition from contraction to extension in the northeastern Basin and Range: New evidence for the Copper Mountains, Nevada: The Journal of Geology, v. 110, p. 179–194, doi:10.1086/338413.

Ressel, M.W., and Henry, C.D., 2006, Igneous geology of the Carlin trend, Nevada: Development of the Eocene plutonic complex and significance for Carlin-type Gold deposits: Economic Geology, v. 101, p. 347–383, doi:10.2113/gsecongeo.101.2.347.

Rigby, M.T., McGrew, A.J., and Foland, K.A., 2006, Onset of Cenozoic volcanism and regional extension in northeast Nevada: Geological Society of America Abstracts with Programs, v. 38, no. 4, p. 65–66.

Roberts, R.J., 1964, Stratigraphy and structure of the Antler Peak quadrangle, Humboldt and Lander Counties, Nevada: U.S. Geological Survey Professional Paper 459-A, 93 p.

Roberts, R.J., Hotz, P.E., Gilluly, J., and Ferguson, H.G., 1958, Paleozoic rocks of north-central Nevada: The American Association of Petroleum Geologists Bulletin, v. 42, p. 2813–2857.

Satarugsa, P., and Johnson, R.A., 2000, Cenozoic tectonic evolution of the Ruby Mountains metamorphic core complex and adjacent valleys, northeastern Nevada: Rocky Mountain Geology, v. 35, p. 205–230, doi:10.2113/35.2.205.

Scholz, C.H., 1990, The mechanics of earthquakes and faulting: New York, Cambridge University Press, 439 p.

Seedorff, E., 1991, Magmatism, extension, and ore deposits of Eocene to Holocene age in the Great Basin—mutual effects and preliminary proposed genetic relationships, *in* Raines, G.L., Lisle, R.E., Schafer, R.W., and Wilkinson, W.H., eds., Geology and Ore Deposits of the Great Basin: Geologic Society of Nevada Symposium Proceedings, p. 133–178.

Sharp, R.P., 1939, The Miocene Humboldt Formation in northeastern Nevada: The Journal of Geology, v. 47, p. 133–160, doi:10.1086/624749.

Shoemaker, K.A., 2004, The tectonomagmatic evolution of the late Cenozoic Owyhee Plateau, northwestern United States [dissertation]: Oxford, Ohio, Miami University, 288 p.

Smith, J.F., Jr., and Ketner, K.B., 1976, Stratigraphy of post-Paleozoic rocks and summary of resources in the Carlin–Piñon Range area, Nevada: U.S. Geological Survey Professional Paper 867-B, 48 p.

Smith, J.F., Jr., and Ketner, K.B., 1977, Tectonic events since early Paleozoic in the Carlin–Piñon Range area, Nevada: U.S. Geological Survey Professional Paper 867-C, 18 p.

Smith, J.F., Jr., and Ketner, K.B., 1978, Geologic map of the Carlin–Piñon Range area, Elko and Eureka counties, Nevada: U.S. Geological Survey Miscellaneous Investigations Map I-1028, scale 1:62,500.

Snoke, A.W., 1980, Transition from infrastructure to suprastructure in the northern Ruby Mountains, Nevada, *in* Crittenden, M.D., Jr., Coney, P.J., and Davis, G.H., eds., Cordilleran Metamorphic Core Complexes, Geological Society of America Memoir 153, p. 287–333.

Snoke, A.W., 1992, Clover Hill, Nevada: Structural link between the Wood Hills and East Humboldt Range, *in* Wilson, J.R., ed., Field guide to geologic excursions in Utah and adjacent areas of Nevada, Idaho, and Wyoming: Utah Geological Survey, Miscellaneous Publication 92-3, p. 107–122.

Snoke, A.W., Howard, K., and Lush, A.P., 1984, Polyphase Mesozoic-Cenozoic deformational history of the northern Ruby Mountain–East Humboldt Range, Nevada: Field trip 9, *in* Lintz, J., ed., Western geological excursions; v. 4: University of Nevada at Reno, Department of Geological Sciences, p. 232–303.

Snoke, A.W., Howard, K.A., McGrew, A.J., Burton, B.R., Barnes, C.G., Peters, M.T., and Wright, J.E., 1997, The grand tour of the Ruby–East Humboldt metamorphic core complex, northeastern Nevada: Brigham Young University Geological Studies, v. 42, p. 1, p. 225–269.

Snoke, A.W., Barnes, C.G., Howard, K.A., Wright, J.E., and Copeland, P., 2004, Late Eocene and Oligocene intrusions in the Ruby–East Humboldt core complex, Nevada: magmatic processes in the middle crust in relation to tectonic extension: Geological Society of America Abstracts with Programs, v. 36, no. 4, p. 71.

Solomon, B.J., McKee, E.H., and Andersen, D.W., 1979, Stratigraphy and depositional environments of Paleogene rocks near Elko, Nevada, *in* Cenozoic paleogeography of the western United States: Society of Economic Paleontologists and Mineralogists, Pacific Section, Pacific Coast Paleogeography Symposium 3, p. 75–88.

Sonder, L.J., and Jones, C.H., 1999, Western United States extension: How the West was widened: Annual Review of Earth and Planetary Sciences, v. 27, p. 417–462, doi:10.1146/annurev.earth.27.1.417.

Sullivan, W.A., and Snoke, A.W., 2007, Comparative anatomy of core-complex development in the northeastern Great Basin, U.S.A: Rocky Mountain Geology, v. 42, p. 1–29, doi:10.2113/gsrocky.42.1.1.

Taylor, W.J., Bartley, J.M., Martin, M.W., Geissman, J.W., Walker, J.D., Armstrong, P.A., and Fryxell, J.E., 2000, Relations between hinterland and foreland shortening: Sevier orogeny, central North American Cordillera: Tectonics, v. 19, p. 1124–1143, doi:10.1029/1999TC001141.

Thorman, C.H., 1970, Metamorphosed and nonmetamorphosed Paleozoic rocks in the Wood Hills and Pequop Mountains, northeast Nevada: Geological Society of America Bulletin, v. 81, p. 2417–2448, doi:10.1130/0016-7606(1970)81[2417:MANPRI]2.0.CO;2.

Thorman, C.H., Ketner, K.B., Brooks, W.E., Snee, L.W., and Zimmerman, R.A., 1991, Late Mesozoic–Cenozoic tectonics in northeastern Nevada, *in* Raines, G.L., Lisle, R.E., Schafer, R.W., and Wilkinson, W.H., eds., Geology and Ore Deposits of the Great Basin Symposium: Geological Society of Nevada, Reno, Proceedings, v. 1, p. 25–45.

Vanderhaeghe, O., Teyssier, C., and Ord, A., eds., 2001, Crustal-scale rheological transitions during late-orogenic collapse: Tectonophysics, v. 335, p. 211–228, doi:10.1016/S0040-1951(01)00053-1.

Vandervoort, D.S., and Schmitt, J.G., 1990, Cretaceous to early Tertiary paleogeography in the hinterland of the Sevier thrust belt, east-central Nevada: Geology, v. 18, p. 567–570, doi:10.1130/0091-7613(1990)018<0567:CTETPI>2.3.CO;2.

Wallace, A.R., Perkins, M.E., and Fleck, R.J., 2008, Late Cenozoic paleogeographic evolution of northeastern Nevada: Evidence from the sedimentary basins: Geosphere, v. 4, p. 36–74, doi:10.1130/GES00114.1.

Waythomas, C.F., 2001, Formation and failure of volcanic debris dams in the Chakachatna River valley associated with eruptions of the Spurr volcanic complex, Alaska: Geomorphology, v. 39, p. 111–129, doi:10.1016/S0169-555X(00)00097-0.

Wells, M.L., and Hoisch, T.D., 2008, The role of mantle delamination in widespread Late Cretaceous extension and magmatism in the Cordilleran Orogen, western United States: Geological Society of America Bulletin, v. 120, p. 515–530, doi:10.1130/B26006.1.

Wernicke, B., 1992, Cenozoic extensional tectonics of the U.S. Cordillera, *in* Burchfiel, B.C., Lipman, P.W., and Zoback, M.L., eds., The Cordilleran Orogen: Conterminous U.S.: Geological Society of America, Geology of North America, v. G-3, p. 553–581.

Wernicke, B.P., and Getty, S.R., 1997, Intracrustal subduction and gravity currents in the deep crust: Sm-Nd, Ar-Ar, and thermobarometric constraints from the Skagit Gneiss Complex, Washington: Geological Society of America Bulletin, v. 109, p. 1149–1166, doi:10.1130/0016-7606(1997)109<1149:ISAGCI>2.3.CO;2.

Wickham, S.M., and Peters, M.T., 1992, Oxygen and carbon isotope profiles in metasediments from Lizzies Basin, East Humboldt Range, Nevada; constraints on mid-crustal metamorphic and magmatic volatile fluxes: Contributions to Mineralogy and Petrology, v. 112, p. 46–65, doi:10.1007/BF00310955.

Wolfe, J.A., Forest, C.E., and Molnar, P., 1998, Paleobotanical evidence of Eocene and Oligocene paleoaltitudes in midlatitude western North America: Geological Society of America Bulletin, v. 110, p. 664–678, doi:10.1130/0016-7606(1998)110<0664:PEOEAO>2.3.CO;2.

Wooden, J.L., Kistler, R.W., Tosdal, R.M., Robinson, A., and Wright, J.E., 1997, Pb vs. Sr isotopic mapping of crustal structure in the northern Great Basin: Geological Society of America Abstracts with Programs, v. 29, p. 70.

Woods, A.W., Bursik, M.I., and Kurbatov, A.V., 1998, The interaction of ash flows with ridges: Bulletin of Volcanology, v. 60, p. 38–51, doi:10.1007/s004450050215.

Wright, J.E., and Snoke, A.W., 1993, Tertiary magmatism and mylonitization in the Ruby–East Humboldt metamorphic core complex, northeastern Nevada: U-Pb geochronology and Sr, Nd, and Pb isotope geochemistry: Geological Society of America Bulletin, v. 105, p. 935–952, doi:10.1130/0016-7606(1993)105<0935:TMAMIT>2.3.CO;2.

Wright, J.E., and Wooden, J.L., 1991, New Sr, Nd, and Pb isotopic data from plutons in the northern Great Basin: Implications for crustal structure and granite petrogenesis in the hinterland of the Sevier thrust belt: Geology, v. 19, p. 457–460, doi:10.1130/0091-7613(1991)019<0457:NSNAPI>2.3.CO;2.

Zoback, M.L., McKee, E.H., Blakely, R.J., and Thompson, G.A., 1994, The northern Nevada rift: Regional tectonomagmatic relations and middle Miocene stress direction: Geological Society of America Bulletin, v. 106, p. 371–382, doi:10.1130/0016-7606(1994)106<0371:TNNRRT>2.3.CO;2.

Manuscript Accepted by the Society 4 March 2011

Printed in the USA